Faculty of Science and Technology

MASTER'S THESIS

Study program/Specialization: Petroleum Engineering/ Natural Gas Engineering	Spring semester, 2016 Open
Writer: Emil Gazizullin	…… (Writer's signature)
Faculty supervisor: Rune W. Time Co-supervisor: Hermonja A. Rabenjafimanantsoa	
Thesis title: Gas lift simulation and experiments in conjunction with the Lyapkov P. D. methodic	
Credits (ECTS): 30	
Key words: Nodal analysis Multiphase flow Gas lift optimization PVT properties Pressure distribution curve	Pages: 130 + enclosure: including Stavanger, 15.06.2016 Date/year

Acknowledgements

This Master's Project was a great final of my study at the University of Stavanger. A lot of new skills and knowledge were gained here.

I consider it an honor to work with the Professor Rune Wiggo Time, who have helped me despite his busyness. I am pleased to acknowledge his helpful comments and suggestions without which my work would not go further.

I owe my deepest gratitude to the Senior Engineer Hermonja A. Rabenjafimanantsoa also known as Benja for encouragement in various ways, valuable guidance and time spent for me.

I also thank the UiS engineer Svein Myhren, who spent his valuable time helping me to deal with the hardware and software for the experiments.

I express many thanks to the lab assistant Nikita Potokin for his assistance, without whom my work would significantly slow down.

I would like to thank Rinat Khabibullin, Gazprom research center worker who gave me a solid foundation and understanding of programming skills that formed a basis for my current work.

Finally, all my gratitude to my mother for her encouragement, without her support I would have never achieved my goals.

Abstract

The present Master's thesis reports the study of continuous gas lift for a production oil well.

The objective of the present work is a better understanding of processes occurring in a gas lift well, as well as optimization of the gas lift system. Numerical simulation for a gas lift well was carried out by means of Matlab. The program and a step-by-step guide were developed on the basis on nodal analysis, with implementation of the Lyapkov's methodic; the program calculates pressure distribution curves along with local mixture properties along the wellbore in tubing and annulus space for steady state flow of multiphase mixture. The gas lift simulation has been performed for different gas injection rates to see how the liquid production will increase.

For experimental purposes, a 5 m experimental loop was used. All experiments were carried out with tap water as reservoir fluid and compressed treated air from the atmosphere as injection gas. A range (from 0,01 to 5 standard liters per minute) of different gas injection rates were chosen to observe a shape of the liquid production curve.

Finally, experimental results are to be confirmed by calculations, based on Bernoulli's equation for the experimental setup.

During the experiments it was a great luck to install and use a new gas flowmeter provided by Alicat Company and a Sensirion SQT-QL500 liquid flowmeter.

Contents

List of tables

List of figures

1 Introduction

The author (myself) has created a program for an electrical submersible pump (ESP) selection for a vertical inclined onshore well. This program is based on the Lyapkov's method, which was developed in 1987 and was widely used in the USSR. The method has been reconsidered and implemented in terms of the nodal analysis. It means that the system "well-near wellbore area-reservoir" is considered as a sum of pressure gradients that are easy determined, when the following parameters are known: well inflow, depression and PVT properties of the fluid. The program was implemented on the basis of VBA in MS Office Excel.

Project work

The objective of the following master thesis is to create a program, which is able to calculate a pressure profile along the well in case of a gaslift well as well as its optimization. The program was realized in Matlab workspace. In optimization section it was necessary to simulate an oil well with certain input parameters. It was also assumed that gas lift was installed into the well and different gas injection rates were simulated. The optimization consisted in defining the optimal gas injection rate based on the production curve. Later an experiment has to be carried out in order to prove the gas lifted well's behavior for a certain range of gas injection rates, namely for linear section of the production curves at low gas rates.

Motivation for oil production

Gas lift takes a large share in oil production. Many oilfield wells are equipped with gas lift injecting systems. The optimal gas lift design guarantees lower operational exchanges along with high oil production rates.

Due to time limits it is not always possible to test gas lifted wells in order to determine their optimal regimes. Another question is an oil well is a sophisticated system with many variables that

affect pressure drops along the well. Taking into account the fact, that in most cases reservoir fluid is presented by multiphase flow, the necessity of a program that allows to simulate a well with a continuous gas lift is a task of high importance. The program must simulate multiphase flow occurring in the well.

Many attempts have been made by researchers (Vazquez&Hernandez, 2005), (Chia&Hussain, 1999), (Bahadori, Ayatollahi & Shirazz, 2001) to develop such simulators. The main similarity is that they were developed based on the same principle, which is pressure drops calculations based on nodal analysis. The main difference is various correlations, which vary depending on fluid properties for different oil fields.

The program must be relatively simple with a user friendly interface and could be used by a regular engineer.

Similar programs that were previously developed give only pressure curves. The author [myself] has not met any program that can give a characteristic of the multiphase flow at any point along the well from the bottomhole to the surface. For studying purposes it would be interesting to implement such option, that will be represented in plots, showing well fluids' PVT data or dynamic parameters, such as fraction velocity or flow patterns.

2 Theory

2.1 Gas Lift Operational Principle

When the reservoir energy is not sufficient for the well's fluids to flow, or an engineer has desired the production rate to be greater than the reservoir energy can deliver, it becomes vital to install artificial lift into the well to provide the energy to bring the flow to the well surface («Schlumberger Well Completions and Productivity», 1999) .

In gas lifting natural gas that is compressed at the surface is injected in the well stream at some downhole point. Gas is injected at a certain depth from the tubing string into the flow string or casing-tubing annulus. As a sequence, the gas significantly reduces the density of the well stream and the flowing pressure losses at the point above the injection point since the major part of the pressure drop is due to potential energy change. Hence, total pressure gradient along the tubing will decrease as well, allowing the bottomhole pressure to overcome the weight of the liquid column and lift the fluid to the surface. For dead wells gas lift installation makes it possible to renew exploitation and wells with low production rates are able to produce greater liquid volumes than before. So, continuous gas lift may be implemented as the continuation of the production period (Takacs, 2005).

2.2 Multiphase flow

Multiphase flow can be observed throughout the entire production system from oil and gas reservoirs to processing facilities at the surface. The production system term in this context refers to the reservoir; the well completion; the annulus and tubing strings that connect the reservoir to the surface ; all surface facilities on land, seabed, or offshore platform; and any pipelines that deliver produced fluids to other processing facilities. The multiphase flow can be any combination of a water phase, a hydrocarbon liquid phase, and a natural gas phase (Brill,1987).

Therefore, for petroleum engineers it is important to have understanding about multiphase phenomena. The basis of any optimization problem is then pressure distribution curves with which the main parameters of fluid flow can be calculated. The precise calculation of multiphase flow parameters not only improves the engineering work, but plays a significant economic role (Takacs, 2005).

Scientists, researchers and engineers in the petroleum industry are faced with the requirement to predict the relationships for the fluids produced from a reservoir between pressure drops, flow rates, and geometry of pipes (diameter, length, angle, etc.) over the entire life of the field (Brill,1987).

2.3 Basic principles

According to Szilas (Szilas, 1985):

- For any multiphase flow problems pressure drop along the well can be affected by a great amount of variables as well as by thermodynamic parameters for each phase, parameters, describing the interaction between the phases (interfacial tension, etc.) and other factors. In correlations scientists try to reduce the number of variables by introducing non dimensional parameter groups.
- Density of the multiphase flow depends on local thermodynamic conditions. Since pressure and temperature vary in a wide range, the respective effect must be accounted for.
- Frictional pressure losses for multiphase flow are more difficult to describe compared to one phase flow, as more than one phase is in contact with well walls. Also velocity distributing in a cross-sectional area differs from a single phase laminar or turbulent flow, that adds difficulty in pressure drop calculations.
- Pressure drop significantly varies with the spatial arrangement in the pipe for different flow patterns or flow regimes. So, different correlations and procedures must be considered when calculating the pressure drop.

Before flow patterns will be discussed in details, some assumptions must be listed:

- Only steady-state flow is investigated. Most horizontal and vertical well problems involve steady-state flow,- only special cases (slugging in long offshore flowlines, etc.) necessitate the more complex treatment required for transient two-phase flow.
- The temperature distribution along the flow path is known. Although simultaneous calculation of the pressure and temperature distribution is possible, it requires additional data on

the thermal properties of the flowing fluids and the pipe's environment, and these are seldom available.

- Reservoir fluid has behavior of the black oil type, i.e. the composition of the liquid phase remains constant. In case compositional changes occur in the liquid phase along the well, black oil model cannot be applied; however, in most engineering calculations this model can be used (Szilas, 1985).

2.4 Flow regimes

Pressure gradient and the holdup of the dense phase are the important properties of two-phase flow as depend strongly on the distribution of the phases in the pipe. Thus, a great number of scientists have tried to identify the various flow regimes or flow patterns that take place in a well. One extreme case is observed when dense liquid with low content of dispersed gas flowing in the pipe. The other extreme case is occurs with a small quantity of the liquid phase dispersed in a continuous light phase. Starting from the first extreme with introduction of an increasing amount of the light phase (gas), all possible flow patterns will be considered. Here only vertical flow patterns will be considered (Zavareh, Hill & Podia, 1988).

Depending on phase velocities and local fluid parameters, the main flow parameters had been investigated by Takacs (Takacs, 2005). These are bubble, slug, transition and mist flows. They are given in the sequence of increasing velocity. It reminds conditions in a producing oil well as the fluid goes up, higher velocities are reached. Near the bottomhole single phase fluid is present (in case bottomhole pressure is greater that saturation pressure). Going upward, more and more gas evolves from oil resulting in increased gas velocity. It increases even more due to reduction of the pressure. The continuous gas velocity increase provides all the possible flow patterns in a well.

Here is a classification proposed by Barnea (Barnea, 1987), given for a vertical well from the bottom upwards to the surface. Later, in the experimental part, frames of the flow regimes for different gas rates will be shown.

Bubble Flow

When the gas velocity is low, gas phase forms bubbles distributed discretely in the continuous liquid phase. Gas bubbles due to their lower density tend to pass the liquid, which is called gas slippage. When calculating gas density, one must include gas slippage effects. Friction loss calculations are in this case relatively simple due to contact of liquid with the walls.

The previously discussed case is valid for low liquid and gas velocities. It is usually observed in pipes with large diameter. When gas velocity is increased without changing liquid velocity, the

individual small bubbles coalesce into so-called *Taylor bubbles*. The flow regime increasingly changes into the slug flow. The transition may be observed at gas fractions $\varepsilon_g > 0.25$. But if liquid velocity is also increased, the process of turbulence will break bigger bubbles and will stop the coalescence of smaller ones. So even at gas fractions, higher than $\varepsilon_g > 0.25$, slug flow cannot be fully developed, however transition from bubble flow into dispersed bubble will occur.

Dispersed Bubble Flow

When liquid velocity is even higher at low gas velocities, the gas bubbles have a very small size and they are uniformly distributed in the continuous liquid phase. Gas bubbles are evenly taken by the continuous liquid phase, so the two phases rise at the same velocity without slippage. The two-phase mixture act as a homogeneous phase. Thus, for the dispersed bubble flow regime mixture density can be easily found from the no-slip liquid holdup, since $\varepsilon_g = 0.52$.

This case is close to real single phase liquid flow as before (there is a strong contact between the wall and the liquid phase). For higher gas velocities small gas bubbles are packed so tightly that they coalesce even at high liquid velocities. The flow regime changes into the churn flow at gas volume fractions of $\varepsilon_g > 0{,}52$.

Slug Flow

When the continuous liquid phase is present in bubbles and dispersed bubble flow starts to decrease, slugs of gas and liquid flow arise consequently. The large Taylor gas bubbles having a shape of a bullet contain most of the gas phase and occupy the whole cross-sectional area. They are surrounded by a liquid film, falling down at the walls. Liquid slug also occupy the whole cross-sectional area and separate Taylor bubbles one from another. They contain small dispersed bubbles inside. A different approach is required to calculate the mixture density. For pressure drop calculations a unit of a Taylor bubble and a water slug must be considered.

When gas rate is increased, Taylor bubbles become larger in size and liquid contains more dispersed gas inside. If the critical value (which is about $\varepsilon_g = 0.52$) is reached, the liquid slug stars to break and transition or churn flow is observed.

Transition (Churn) Row

At higher gas rates neither liquid slugs nor Taylor bubbles exist any longer, neither of the phases is continuous. Liquid now is lifted by the smaller Taylor bubbles of distorted shape. Hence, the liquid phase makes an up and down motion in vertically alternating directions.

When the gas rates increase even more, churn flow is transformed into mist or annular pattern. Liquid film stability and bridging are two mechanisms that govern the transition.

Annular (Mist) Row

At extremely high gas velocities, gas phase becomes continuous along the pipe. Liquid is presented as a wavy film on the pipe walls and as small droplets in the gas flow. The last ones are transported at the same velocity as the gas phase velocity. No slippage occurs between the phases. Density, therefore, can be calculated from the non-slip holdup. Determination of film thickness on the pipe walls is of high importance because of friction losses occurring on the gas-liquid interface (Barnea, 1987).

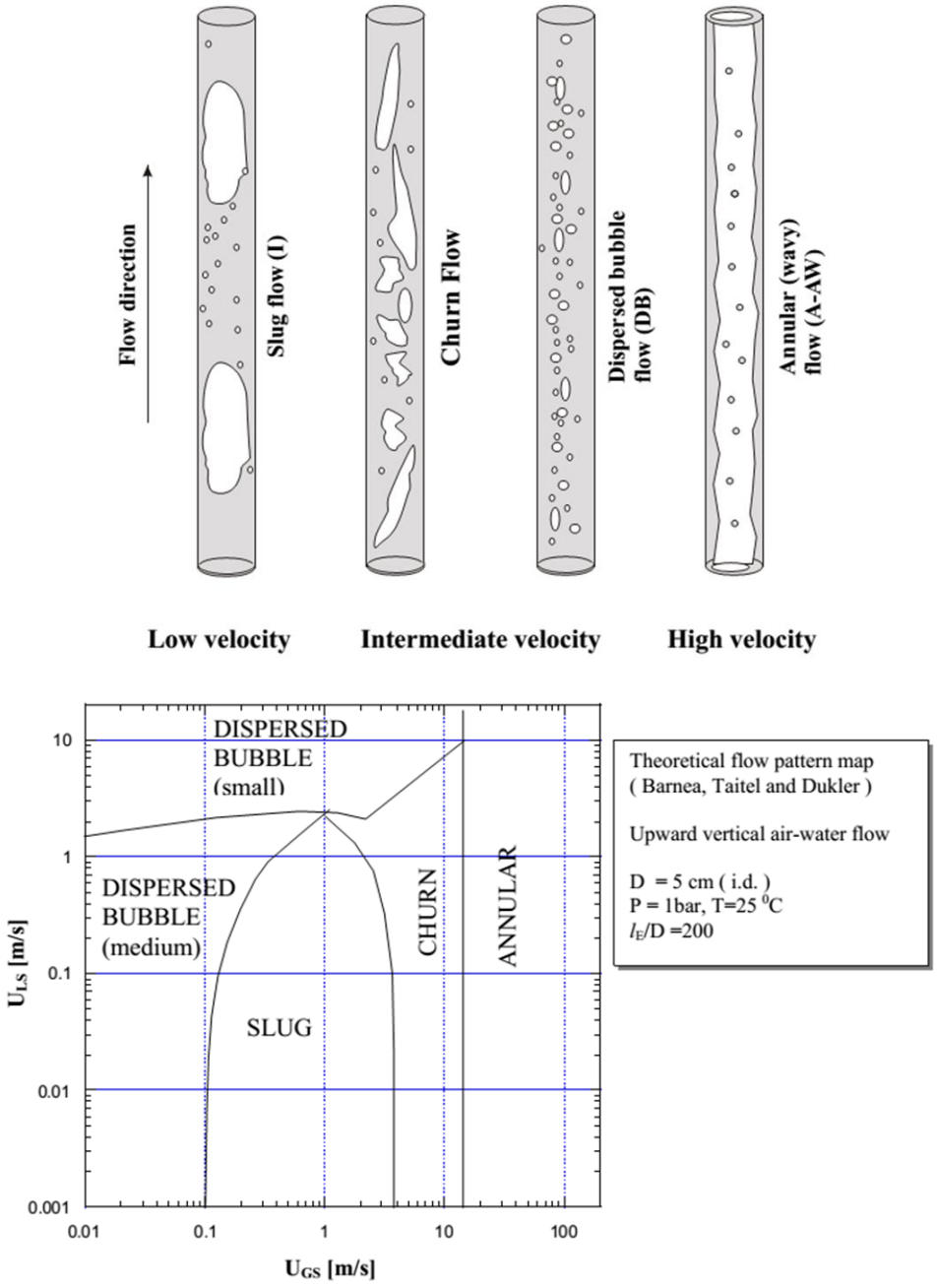

Figure 1- Flow regimes and flow regime map in vertical two-phase flow. (Time, 2009)

2.5 Nodal analysis principle

"Nodal analysis is an approach for applying systems analysis to the complete well system from the outer boundary of the reservoir to the sand face, across the perforations and completion section, up the tubing string, the flow line and separator". A producing well can be considered as a series of hydraulic connected systems that are bordered by certain points, called nodes (in connection with Figure 2). The node can be classified as a functional node in case there is a pressure differential across it and the pressure or flow rate can be represented by a physical or mathematical function (Stoisits, 1992).

System's performance evaluation can be done by meeting the following requirements:

- Mass flow rate throughout the system is constant, although with changes in pressure and temperature phase conditions change too.
- Pressure decreases in the direction of flow because of the energy losses occurring in the various system components.
- At node points, input pressure to the next component must equal the output pressure of the previous component.
- System parameters being constant for considerable periods of time are:
    - the endpoint pressures at the separator and in the reservoir
    - the wellbore and surface geometry data (pipe diameters, lengths, etc.)
    - the composition of the fluid entering the well bottom

Flow rate can be determined, taking into account above mentioned features of the production system. It can be described by a procedure in which the system is divided into two subsystems at a node that is called the solution node. Starting from the points with known constant pressures (well boundaries-bottomhole and separator pressures), local pressures in the different hydraulic elements of the production system are calculated.

The system analysis principles can be applied to the gas lift well analysis. This is made possible by the fact that multiphase flow is present in the tubing string. A gas lift well scheme is given in Figure 2 (Takacs, 2005).

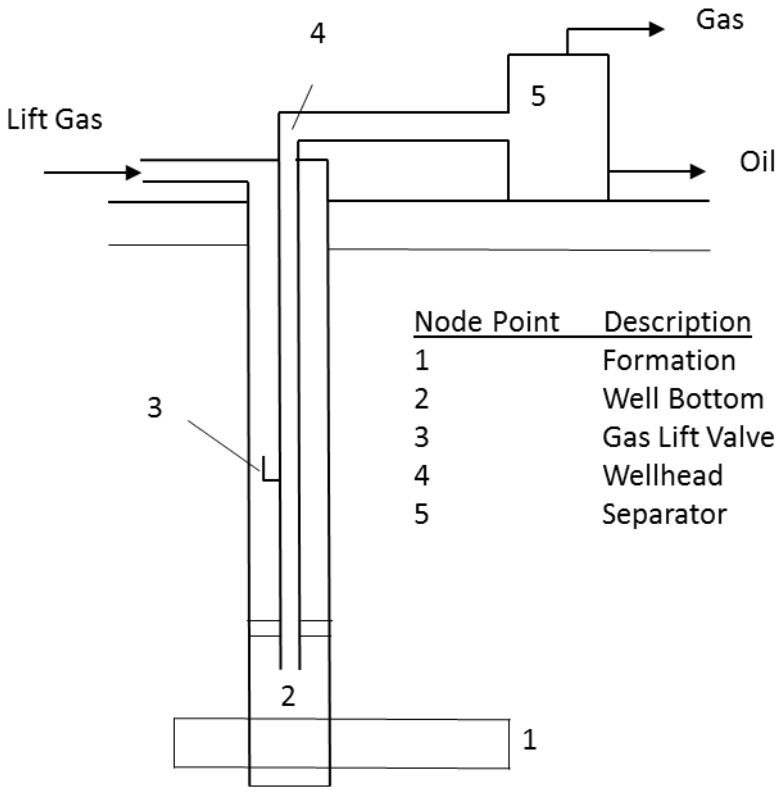

Figure 2- The production system of a continuous flow gas lift well (reproduction) (Takacs, 2005)

2.6 Gas lift installation type

In the considered case in the following master thesis an assumption has been made that gas injected in the gas lift well comes to the lower part of the tubing string. It means that gas lift installation type is open.

In the open gas lift installation the production oil system consists of the tubing, hanging inside the casing string without packer installed (Figure 3).

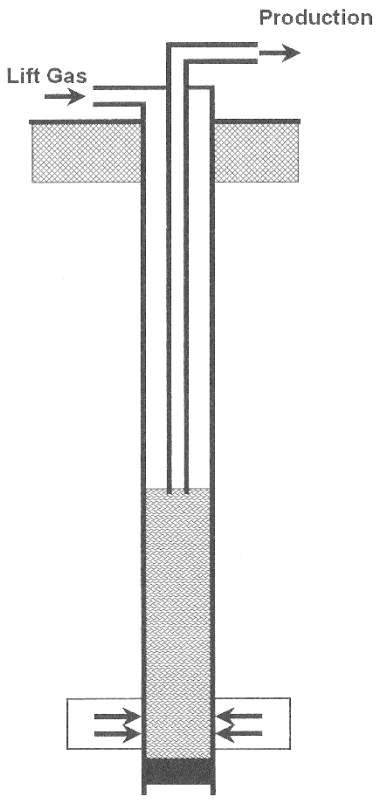

Figure 3- Open tubing flow installation with gas injection at the tubing shoe (Takacs, 2005)

This type was used in the begging of the gas lift era, when no gas lift valves were installed and gas was injected at the tubing shoe. It leads to enormous gas consumption and hence low effectivity. The proper setting depth selection is a difficult task. It is a function of the surface injection pressure. Any changes in the surface pressure after the system is run may lead to wide range of fluctuations in the injected gas rate. Liquid rate fluctuates accordingly. The requirement of continuous flow of gas at a constant gas injection volume cannot be achieved (Takacs, 2005).

2.7 Pressure gradients calculation

In multi-phase flow pressure drop is probably the quantity that researchers deal with most often. Large number of dimensionless variables is a big problem. For example, the friction factor is identified as a function of the Reynolds number, Froude number, the Weber number, the flow-rate ratio, density ratio, and the viscosity ratio (Griffith, 1984).

One may consider the total pressure gradient in the pipe as a function of 3 different terms:

Frictional pressure gradient $\left(\frac{dp}{dx}\right)_f$, hydrostatic pressure gradient $\left(\frac{dp}{dx}\right)_h$ and acceleration pressure gradient $\left(\frac{dp}{dx}\right)_a$.

Thus $\left(\frac{dp}{dx}\right) = \left(\frac{dp}{dx}\right)_f + \left(\frac{dp}{dx}\right)_h + \left(\frac{dp}{dx}\right)_a$ (2.1)

Each of these terms contribute in a different way in single phase and two phase flow.

For two-phase flow calculations one starts with the assumption that the fluids mixture properties are given by the mixing rules. This approach is called *the homogeneous two-phase pressure drop model.* In order to obtain appropriate fluid fractions calculation may be done by assuming either no-slip (S = 1) or by specifying a certain slip ratio. The Beggs and Brill pressure drop model applies a homogeneous model for friction and hydrostatic pressure, some parts calculated with the no-slip assumption, and some taking into account the real slip.

Frictional pressure drop

As in single phase, the following expression is used:

$$\left(\frac{dp}{dx}\right)_f = \frac{4}{D} \cdot C\left(\mathrm{Re}_m\right)^{-n} \cdot \frac{1}{2} \rho_m U_{mix}{}^2 \quad (2.2)$$

Where index “m” means “mixture”. The homogeneous model is realistic essentially in turbulent well mixed flow, which means the selection C=0.046, n=0.2 should be used.

The mixture Reynolds number is calculated as:

$$\mathrm{Re}_m = \frac{\rho_m U_{mix} D}{\mu_m} \quad (2.3)$$

Hydrostatic pressure gradient

The hydrostatic pressure gradient can be calculated as follows:

$$\left(\frac{dp}{dx}\right)_h = \rho_m g \cos\beta \quad (2.4)$$

(Angle β relative to *vertical* direction)

Where the mixture density is different from the single phase flow.

Acceleration pressure drop

The two most important contributions come from:

- Change in gas density

- Change in velocity change and pipe cross sectional area

The acceleration pressure gradient is similar to the single phase flow:

$$\left(\frac{dp}{dx}\right)_a = -\rho_m U_{mix} \cdot \frac{dU_{mix}}{dx} \tag{2.5}$$

modifying only the density and using the mixture velocity (Time, 2009).

3 Simulation part

3.1 Previous works review

A number of papers and articles on experimental studies were researched in order to obtain a theoretical basis for planned simulation work.

A great work has been done by the authors of (Vazquez & Hernandez, 2005), where a continuous gas lift model has been developed based on nodal analysis. Three cases of study were considered to check if the developed model resembled experimental data. Problems solved included gas lift optimization, namely determination of appropriate amount of gas required to lift reservoir fluid, provided that outlet pressure at surface manifold matched actual pressure. Researchers used computational approach and concluded, that proposed model had produces appropriate results and could be applied in simulation of optimization of gas lift systems.

Paper (Chia & Hussain, 1999) by Y. C. Chia and Sies Hussain gives an insight of challenges that are encountered during gas lift optimization in Malaysian oil fields. It is mentioned that to meet the challenges, the GOAL model (Gas Lift Optimization Allocation Model) is applied, which is a developed PC based production system model. It is also based on nodal analysis in order to generate well performance curves for a system of wells. Optimization is also possible by defining an objective (maximizing liquid production, oil etc.) Model considers emulsion and sand production and is able to simulate dual completion gas lift design.

Paper (Wang & Litvak, 2004) describes a method for gas lift optimization problem for multiple objects and applies certain algorithms that reduce calculation time because of less CPU is required, which is vital in real oilfields, where the amount of wells is significant. The method is named “GLINC”, and generates results for long-term simulation studies.

Similarly to the present work, a work has been done by the authors of paper (Bahadori, Ayatollahi & Shirazz, 2001) for the Ayatollahi oilfield, where it is mentioned that the choice of appropriate PVT and fluid correlations play an important role. After the author have selected the correlations, performance curves was calculated. An optimum production rate was then found from

the well performance curve and finally valve installation depth was designed. All calculations were performed in a numerical simulator, developed by the authors.

Paper (Pablano, Camacho & Fairuzov, 2005) develops a concept of stability maps for continuous gas lift flow, when transition from stable to unstable flow occurs. It allows to compare different gas lift stability criteria (injection rate, the injector port size, tubing diameter) and quantify the effects of these criteria. The authors mention that well-stabilizing methods may be developed on the basis of the concepts, that provides minimum CAPEX and OPEX.

3.2 Introduction to the program

The software package developed by the author [myself] in the following thesis consists of separate calculation blocks- calculation of PVT properties section, the calculation of pressure gradients section and gaslift parameters calculation section. In its turn, each section consists of separate functions. Some of the functions refer to other ones, which are more elementary. Thus, every function that is used in the program will be described. The description of every function is comprised of the following elements:

1. “Name”-name of the function;
2. “Variables”- variables of the function;
3. “Subfunctions”- called functions that are used in the body of the function;
4. “Function’s body”- a set of formulae, that is used to obtain the results of the function;
5. “Calculated parameters”- function’s output.

Here is a summary flowchart of the program:

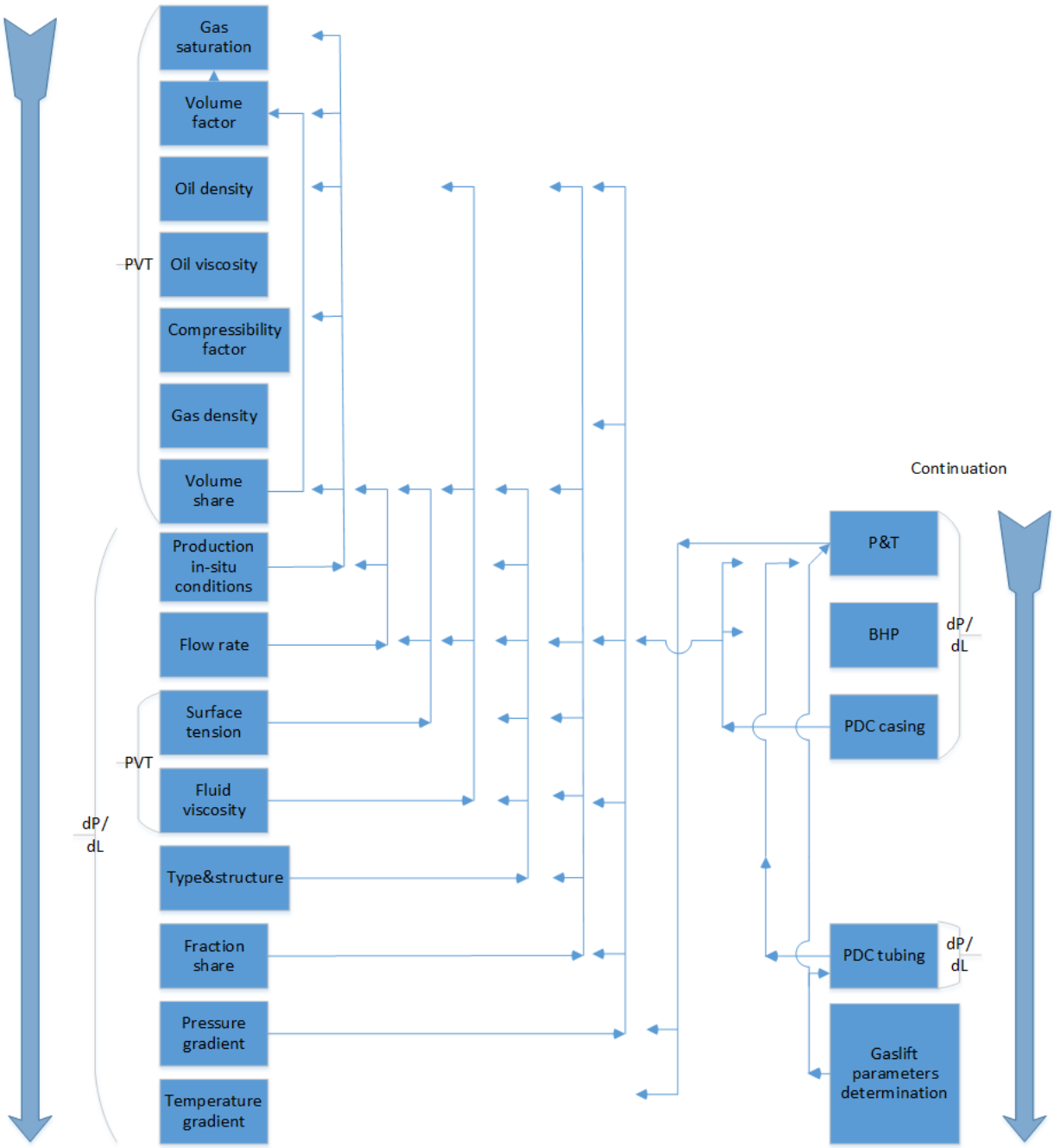

Figure 4- Summary flowchart of the program

Methodology of a gaslift well optimization consists of execution of the following basic steps:

- Preparation of input data describing the necessary parameters of the drained reservoir, production casing of the well, steady-state flow, as well as the properties and fractions of produced oil, water and gas at different thermodynamic conditions;

- Calculation and making a plot of pressure distribution curves (PDC) along the length of the production casing and tubing in the interval from the well's bottomhole to the surface for a given production oil rate at standard conditions.

- Calculation of oil and liquid production depending on amount of gas injected in a gaslift well
- Optimization of gaslift, calculation of optimal gas injection rate.

Input data that is necessary and sufficient if shown below:

Table 1- Well input data

Parameter	*Value*	*Units*
Reservoir pressure	17,4	MPa
Productivity	22	m3/(d*MPa)
Reservoir temperature	103	C
Geotharmal gradient	0,02	deg/m
Wellbore flowline pressure	0,84	MPa
Annulus pressure	1	MPa
Wellbore length	1607	m
Inclination	0,2	deg
Annulus diameter	157	mm
Tubing duameter	68	mm
Oil density at SC	819,9	kg/m3
Water density at SC	1120	kg/m3
Associated gas density	1,333	kg/m3
Gas injection rate	0,7	m3/s
Watercut	60	%
Saturation pressure	8,5	MPa
Gas injection rates range	0-2	m3/s

3.3 Calculation steps

At first, a pressure distribution curve (PDC) along the casing has to be built. It is performed stepwise. The well length is divided into n=100 segments upwards from bottom to top. PDC is an array of pressures and positions in the well, so the goal is to determine local pressures along the well, namely at the ends of each segment. However, it is more convenient to determine pressure gradients instead.

In general, pressure gradient is defined from Bernoulli's equation:

$$\frac{\partial P}{\partial L} = g \cdot (\varphi_o \cdot \rho_o + \varphi_w \cdot \rho_{w.sc} + \varphi_g \cdot \rho_g) \cos\theta + \frac{\lambda}{2D}\left(\frac{\rho_o \omega_o^2}{\varphi_o} + \frac{\rho_w \omega_w^2}{\varphi_w} + \frac{\rho_g \omega_g^2}{\varphi_g}\right) \quad (3.1)$$

Where:

$\varphi_o, \varphi_w, \varphi_g$ is oil, water and gas fractions respectively;

ρ_o, ρ_w, ρ_g is oil, water and gas densities respectively;

$\omega_o, \omega_w, \omega_g$ is oil, water and gas flowrates respectively;

θ is average inclination;

D is annulus (tubing) diameter;

λ - hydraulic friction coefficient.

Since liquid and gas conditions are determined not only at a certain pressure but at a temperature as well, it is important to obtain the temperature gradient:

$$\frac{\partial T}{\partial L} = \frac{(0,0034 + 0,79G)}{10^{\frac{Q_{l.sc}}{20D^{2,67}}}} \tag{3.2}$$

Where;

$Q_{l.sc}$ - well inflow at SC;

G - Geothermal gradient.

The starting point is bottomhole of the well. However, bottomhole pressure has not been found yet. Here an iteration procedure has to be applied. The idea of the procedure is that pressure at the bottomhole is assumed to be known. Knowing the reservoir pressure, well flow can now be determined. Then further calculations are carried out (they are described below in more details), the final result of which is calculated (not real) wellhead pressure. Comparing this pressure and the factual one, assumed bottomhole pressure is “calibrated” until the real wellhead pressure is equal to the calculated wellhead pressure, or more precisely the difference between them is less than a certain tolerance value. When the equality has been reached, such parameters as the well flow and the bottomhole pressure now become determined.

When bottomhole pressure is determined, the three fundamental values which are bottomhole pressure, temperature and position are established. Using empirical correlations and theoretical calculations presented in the Matlab program it is easy to obtain fluid properties at bottomhole conditions that in its turn makes it simple to obtain local pressure and temperature gradients, according to the formulas above.

Pressure at the second end of the first interval can be calculated as follows:

$$P_{out} = P_{in} - \frac{\partial P}{\partial L}\Delta L \tag{3.3}$$

Where:

P_{in} -pressure at the inlet of I stage;

P_{out} - pressure on the next stage.

So, the pressure and the temperature at the both ends of the first interval are know now. Pressure at the end of the first section is equal to the one at the beginning of the second section. Hence the same operation is proceeded for the whole range of length intervals, giving us the pressure-temperature-local position array.

The same procedure is performed to obtain an array of pressures for tubing space. Calculations are done upwards from the lower position of the tubing to the wellhead.

It is worth mentioning that during the calculation one obtains arrays for the oil mixture properties, as local densities, volumetric fractions, oil viscosities and so one. By knowing critical values that are not to be exceeded, one may analyze and optimize the oil flow.

After all, pressure distribution curves for annulus and tubing for a given well are obtained.

To get a better understanding of the program the following figure is given:

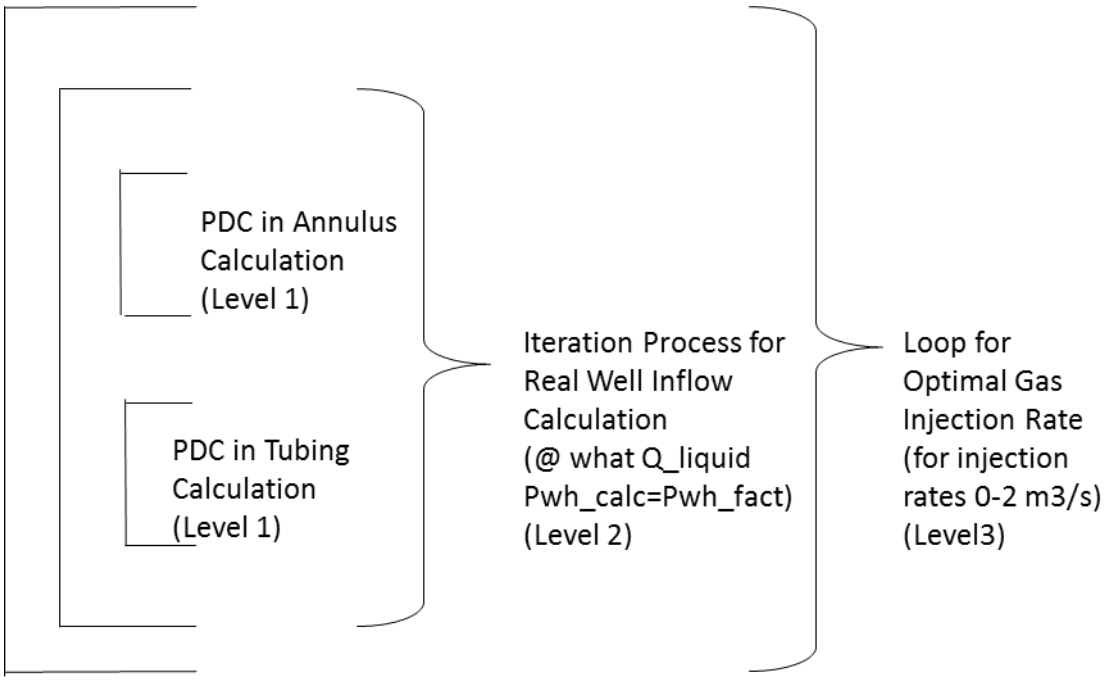

Figure 5- Structure of the program

In this figure the structure of the program is shown. The two main block calculate pressure distribution curves (PDC) for casing and tubing space for given well parameters. However, at that step the factual well flow rate at bottomhole conditions is unknown. The iteration process then is required, which calculates a series of PDC for the same well with changing well inflow, unless the

wellhead pressure (which is the resulting parameter of PDC) coincides with the real wellhead pressure given as the initial datum.

Then, when gas lift is simulated, a range of gas injection rates is tested, which requires an additional loop, containing all previous loops. Then based on results of the previous loop, the *production curve* is built (it represents liquid production and gas lift operating pressure vs. gas injection rate), from where the optimum injection range of rates at which maximum liquid production can be reached is found.

More precisely the program description is given in the next subchapter. For the program code, see Appendix A. There are comments, describing steps that may be challenging, so it is highly recommended to look through the code.

3.4. Program description

3.4.1 Calculation of PVT

For calculation of physical and chemical properties of the reservoir fluids a technique, suggested by (Lyapkov, 1987), (Dunushkin & Mishenko, 1982), (Mishenko, 2003) is used.

3.4.1.1 Calculation of gas saturation

Function- gas_saturation

Here and after the correlations, that are used in the PVT properties calculations, dynamic parameters calculations and other calculations are based on the following handbooks: (Gimatudinov, 1983), (Gimatudinov, 1974), (Buhalenko et al., 1983), (Trebin et al., 1980), (Shtof, 1974).

Table 2- Input data

Parameter	Symbol	Unit
Pressure	P	MPa
Saturation pressure	P_{sat}	MPa
Gas to oil ratio at saturation pressure	GOR_{sat}	m3/m3
GOR coeff.-s	m_{GOR}	-
	n_{GOR}	-

$$GOR = \begin{cases} m_{GOR} \cdot P^{n_{GOR}}, P < P_{sat} \\ GOR_{sat}, P \geq P_{sat} \end{cases} \quad (3.4)$$

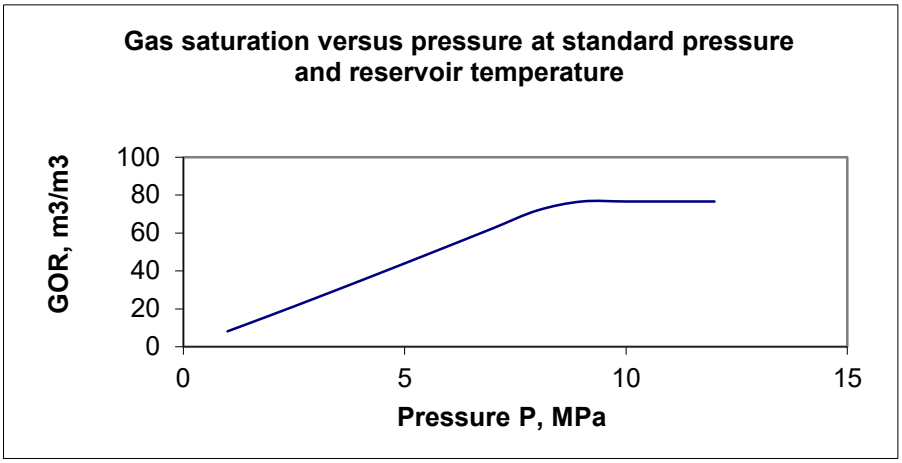

Figure 6- Gas saturation versus pressure at standard pressure and reservoir temperature for Karakuduk oilfield (reservoir J-1/2)

Table 3- Output data

Parameter	Symbol	Unit
Gas to oil ratio	GOR	m3/m3

3.4.1.2 Calculation of oil volume factor

Function- volume_factor

Table 4- Input data

Parameter	Symbol	Unit
Pressure	P	MPa
Saturation pressure	P_{sat}	MPa
Volume factor coeff.-s	m_b	-
	n_b	-

$$b_o = \begin{cases} m_b \cdot P^{n_b}, P < P_{sat} \\ m_b \cdot P_{sat}{}^{n_b}, P \geq P_{sat} \end{cases} \quad (3.5)$$

As can be seen from Figure 7:

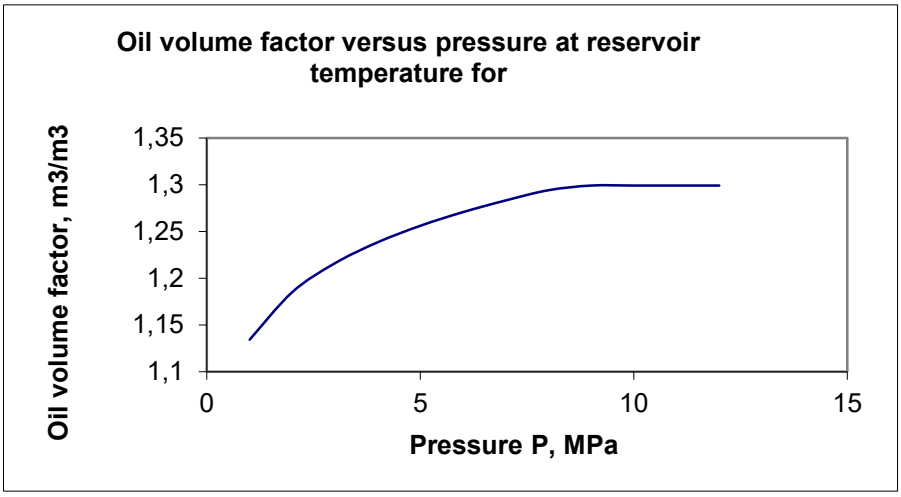

Figure 7– Oil volume factor versus pressure at reservoir temperature for Karakuduk oilfield (reservoir J-1/2)

Table 5- Output data

Parameter	Symbol	Unit
Oil volume factor	b_o	m3/m3

3.4.1.3 Calculation of oil density

Function- oil_density

Table 6- Input data

Parameter	Symbol	Unit
Pressure	P	MPa
Saturation pressure	P_{sat}	MPa
Oil density coeff.-s	m_ρ	-
	n_ρ	-

$$\rho_o = \begin{cases} m_\rho / P^{n_\rho}, P < P_{sat} \\ m_\rho / {P_{sat}}^{n_\rho}, P \geq P_{sat} \end{cases} \quad (3.6)$$

As can be seen from Figure 8:

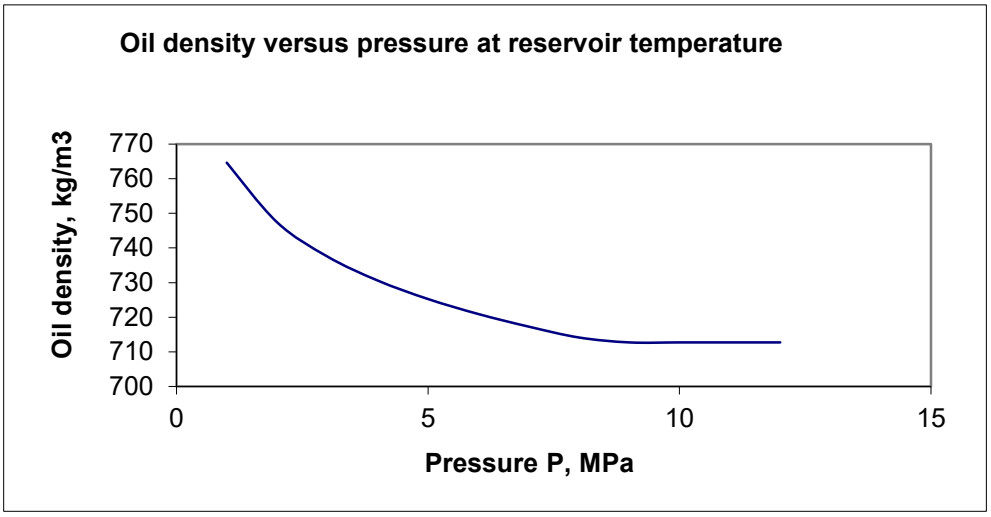

Figure 8–Oil density versus pressure at reservoir temperature for Karakuduk oilfield (reservoir J-1/2)

Table 7- Output data

Parameter	Symbol	Unit
Oil density	ρ_o	kg/m3

3.4.1.4 Calculation of oil viscosity

Function- oil_viscosity

Table 8- Input data

Parameter	Symbol	Unit
Pressure	P	MPa
Temperature	T	K
Saturation pressure	P_{sat}	MPa
Oil viscosity coeff.-s	m_μ	-
	n_μ	-

Oil viscosity is related to pressure by the following equation:

$$\mu_o = \begin{cases} m_\mu / P^{n_\mu}, P < P_{sat} \\ m_\mu / P_{sat}{}^{n_\mu}, P \geq P_{sat} \end{cases} \quad (3.7)$$

As can be seen from Figure 9:

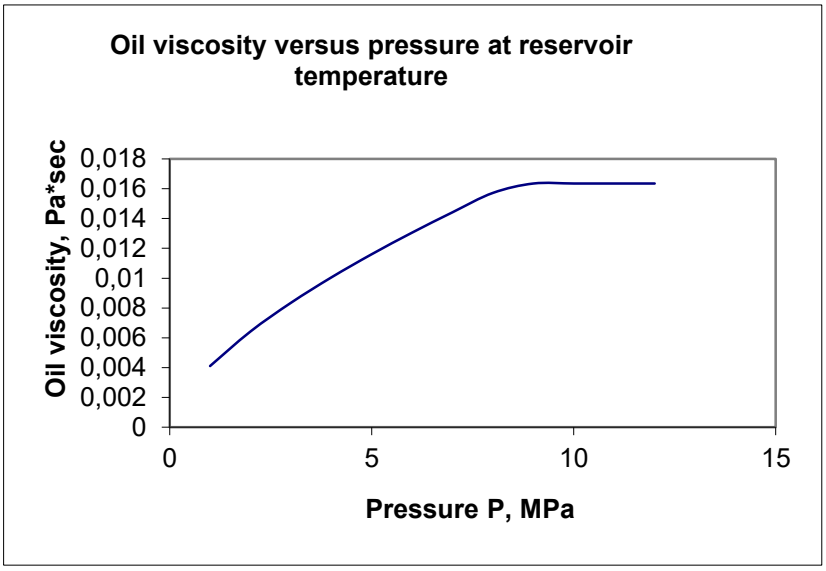

Figure 9– Oil viscosity versus pressure at reservoir temperature for Karakuduk oilfield (reservoir J-1/2)

However it is known that oil viscosity is strongly dependent on the temperature. Lewis- Squires correction, which considers it, needs to be introduced:

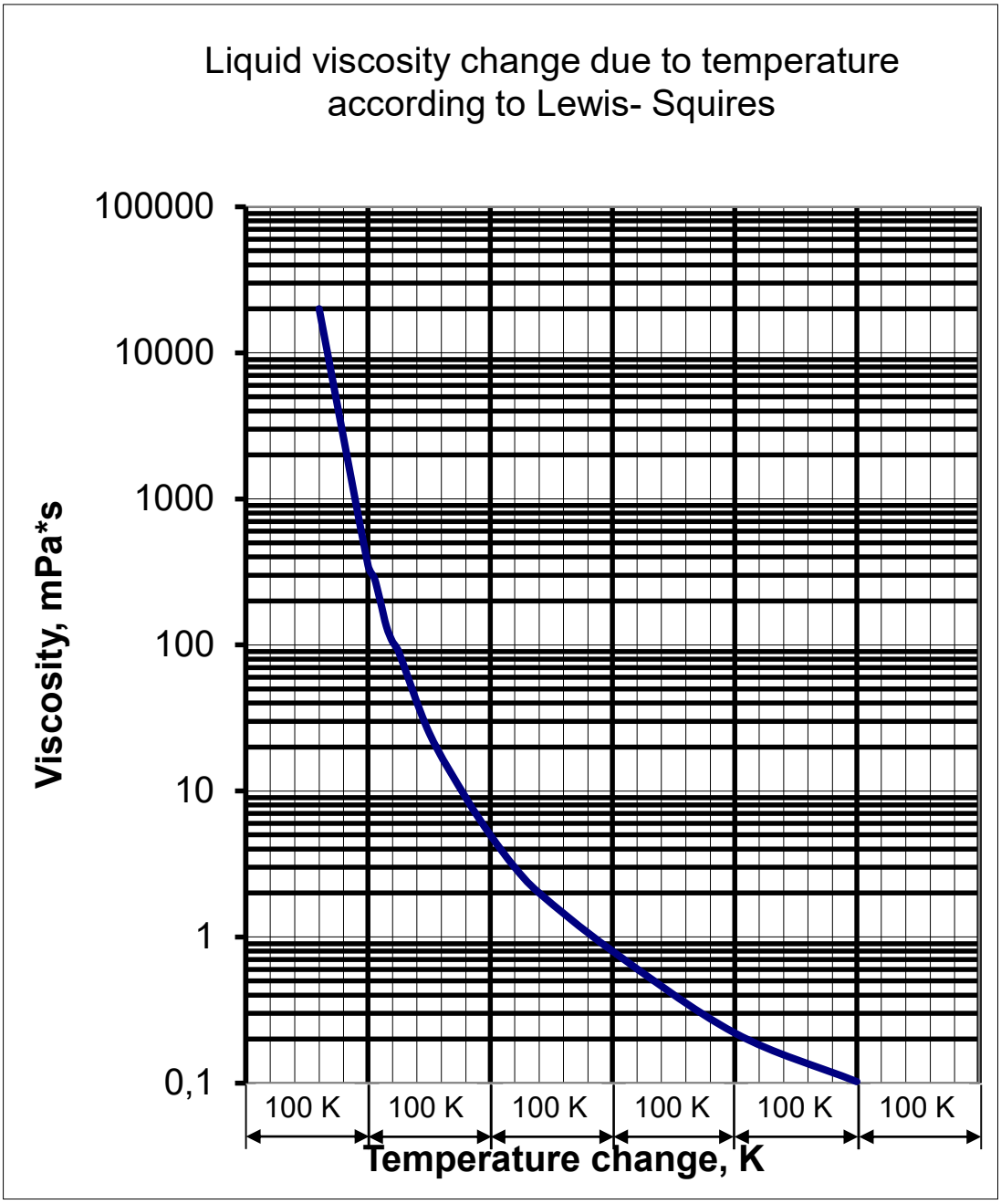

Figure 10- Liquid viscosity change due to temperature according to Lewis- Squires

Example: $\mu_{o1} = 2,4$ MPa*s; $T_1 = 313$ K; $T_2 = 293$ K. Determine μ_{o2}.

Solution : Lay off the point $\mu_{o1} = 2,4$ MPa*s on the ordinate. From this point we go right up to the curve; shift along the curve by $\Delta T = T_1 - T_2 = 313 - 293 = 20$ K. We see what new value of the viscosity corresponds to this shift. $\mu_{o2} = 6,3$ MPa*s.

Thus, when calculating the viscosity of oil as opposed to gas content, density and volume faction calculations, temperature changes have to be taken into account.

Table 9- Output data

Parameter	Symbol	Unit
Oil viscosity	μ_o	MPa*s

3.4.1.5 Calculation of coefficients for oil average density, viscosity, volume factor and gas saturation calculations

If coefficients for calculations of oil density, oil viscosity, GOR and volume factor are unknown, then corresponding coefficients are determined by solution of the following se of equations:

$$\left.\begin{aligned} lg\left(y_{line}\right) &= lg\left(m_y\right) + n_y lg\left(P_{line}\right) \\ lg\left(y_{sat}\right) &= lg\left(m_y\right) + n_y lg\left(P_{sat}\right) \end{aligned}\right\} \quad (3.8)$$

Where y_{line} and y_{sat} -values of a considered function (ρ_o , μ_o , b_o , GOR), taken from the corresponding curve at line pressure P_{line} and saturation pressure P_{sat}.

As the result, output data is $m_\rho, n_\rho, m_\mu, n_\mu, m_b, n_b, m_{GOR}, n_{GOR}$ coefficients.

3.4.1.6 Compressibility factor calculation

Function- compressibility_factor

Table 10- Input data

Parameter	Symbol	Unit
Pressure	P	MPa
Temperature	T	K
Saturation pressure	P_{sat}	MPa
Assosiated gas density	ρ_{gSC}	kg/m3
Nitrogen volume fraction in the associated gas at SC	y_{N_2}	m3/m3

We calculate gas compressibility factor having previously calculated:

Relative gas density:

$$\rho_{g.rel} = \frac{\rho_{gSC}}{1,205} \tag{3.9}$$

Relative density of all HC and non-HC components except nitrogen:

$$\rho_{HC.rel} = \frac{(\rho_{g.rel} - 0,97 y_{N_2})}{1 - y_{N_2}} \tag{3.10}$$

Pseudoreduced pressure and temperature:

$$P_{pr} = \frac{10P}{46,9 - 2,06\rho^2_{HC.rel}} \tag{3.11}$$

$$T_{pr} = \frac{T}{97 + 172\rho_{HC.rel}} \tag{3.12}$$

If the value of T_{pr} is less than 1,05, assume T_{pr} =1,05

Compressibility factor excluding nitrogen is obtained from the following formula:

$$\left.\begin{aligned} z_{HC} &= 1 - 0,23P_{pr} - (1,88 - 1,67T_{pr})P_{pr}^2, 0 \le P_{pr} \le 1,45 \,\&\, 1,05 \le T_{pr} \le 1,17 \\ z_{HC} &= 0,13P_{pr} + (6,05T_{pr} - 6,25)\frac{T_{pr}}{P_{pr}^2}, 1,45 \le P_{pr} \le 4 \,\&\, 1,05 \le T_{pr} \le 1,17 \\ z_{HC} &= 1 - P_{pr}\left(\frac{0,18}{T_{pr} - 0,73} - 0,135\right) + 0,0161\frac{P_{pr}^{3,45}}{T_{pr}^{6,1}}, 0 \le P_{pr} \le 4 \,\&\, 1,17 \le T_{pr} \le 2 \end{aligned}\right\} \tag{3.13}$$

z value is obtained from:

$$z = z_{HC}(1 - y_{N_2}) + z_{HC}y_{N_2} \tag{3.14}$$

Table 11- Output data

Parameter	Symbol	Unit
Compressibility factor	z	-

3.4.1.7 Calculation of gas density

Function– gas_density

Table 12- Input data

Parameter	Symbol	Unit
Pressure	P	MPa
Temperature	T	K
Assosiated gas density	ρ_{gSC}	kg/m3
Compressibility factor	z	-

Table 13- Called functions

Name of the function	Denotation
Compressibility factor calculation	compressibility_factor

Gas density at a certain cross-section area we may get from:

$$\rho_g = \rho_{g.rel} \frac{PT_{SC}}{zP_{SC}T} \tag{3.15}$$

where P_{SC} - Pressure of air at SC, 101,3 kPa

T_{sc} - Temperature of air at SC, 293,2 K

Table 14- Output data

Parameter	Symbol	Unit
Gas density	ρ_g	kg/m3

3.4.1.8 Calculation of fluid's volumetric water fraction

Function– volume_share

Table 15- Input data

Parameter	Symbol	Unit
Pressure	P	MPa
Water volume fraction in produced fluid at SC	$\beta_{w.sc}$	m3/m3
Oil volume factor	b_o	m3/m3

Table 16- Called functions

Name of the function	Denotation
Calculation of oil volume factor	volume_factor

Volumetric water content in liquid is calculated from:

$$\beta_{wl} = \frac{1}{1 + b_o\left(1 - \beta_{w.sc}\right)} \tag{3.16}$$

Volumetric oil content in liquid is calculated from:

$$\beta_o = 1 - \beta_{wl} \tag{3.17}$$

Table 17- Output data

Parameter	Symbol	Unit
Volumetric water content in produced fluid at given temperature and pressure conditions	β_{wl}	m3/m3

3.4.1.9 Calculation of the surface tension between the liquid phase that is the outer phase of the stream and gas

σ_{lg}

Function– surface_tension

Table 18- Input data

Parameter	Symbol	Unit
Zone (annular space or tubing)	-	-
Pressure	P	MPa
Temperature	T	K
Volumetric water content in produced fluid at given temperature and pressure conditions	β_{wl}	m3/m3
Superficial velocity of the mixture at given temperature and pressure conditions	ω_{mix}	m/s
First critical velocity of the mixture at given temperature and pressure conditions	ω_{cr1}	m/s

Table 19- Called functions

Name of the function	Denotation
Calculation of fluid's volumetric water fraction	volume_share
Calculation of oil, water and gas flow rates and first and second critical rates	flow_rate

Zone (annular space or tubing) parameter is introduced. It can have 2 values: "Casing"- when calculating mixture parameters in the annular space and "Tubing"- when calculating in tubing area. We calculate the surface tension value at water-gas contact:

$$\sigma_{wg} = 10^{-1,19+0,01P} \tag{3.18}$$

Then we calculate the surface tension value at oil-gas contact:

$$\sigma_{og} = 10^{-1,58+0,05P} - 72 \cdot 10^{-6} \left(T - 305\right) \tag{3.19}$$

If the value σ_{og} turned out to be below zero, then:

$$\sigma_{og} = 0 \tag{3.20}$$

We calculate the surface tension value at oil-water contact:

$$\sigma_{ow} = \sigma_{wg} - \sigma_{og} \tag{3.21}$$

Eventually, the value of the surface tension at liquid-gas contact σ_{lg} we obtain from the following scheme:

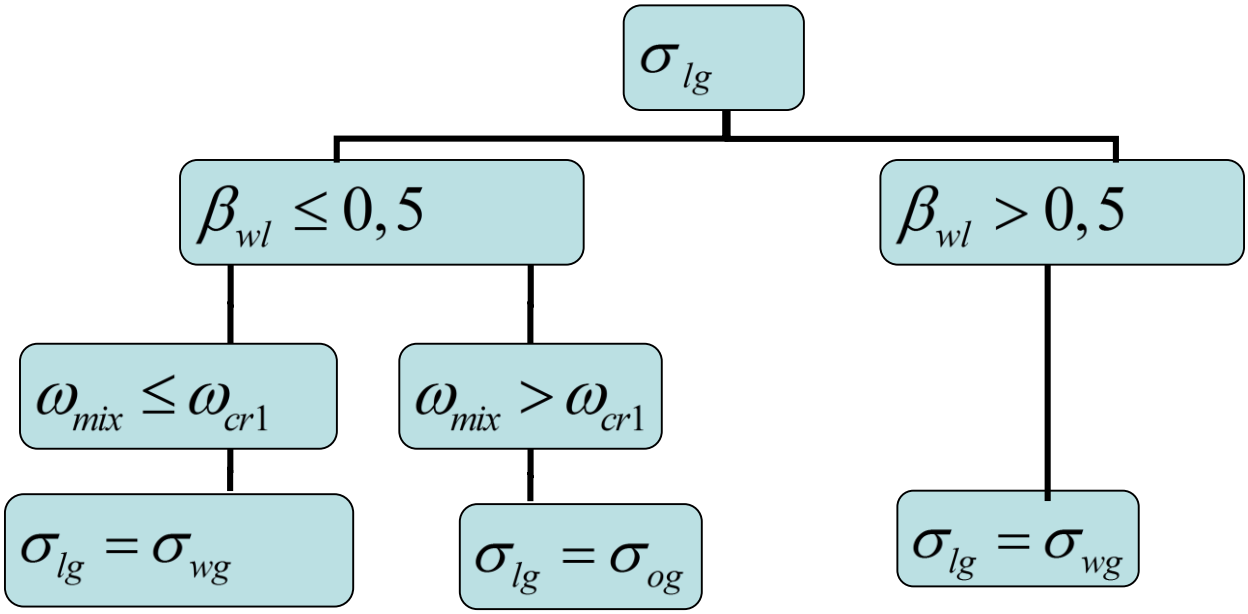

Figure 11– Choice of the surface tension between the liquid phase as the outer phase of the stream and the gas

Table 20- Output data

Parameter	Symbol	Unit
Surface tension at oil-water contact	σ_{ow}	N/m
Surface tension at liquid-gas contact	σ_{lg}	N/m

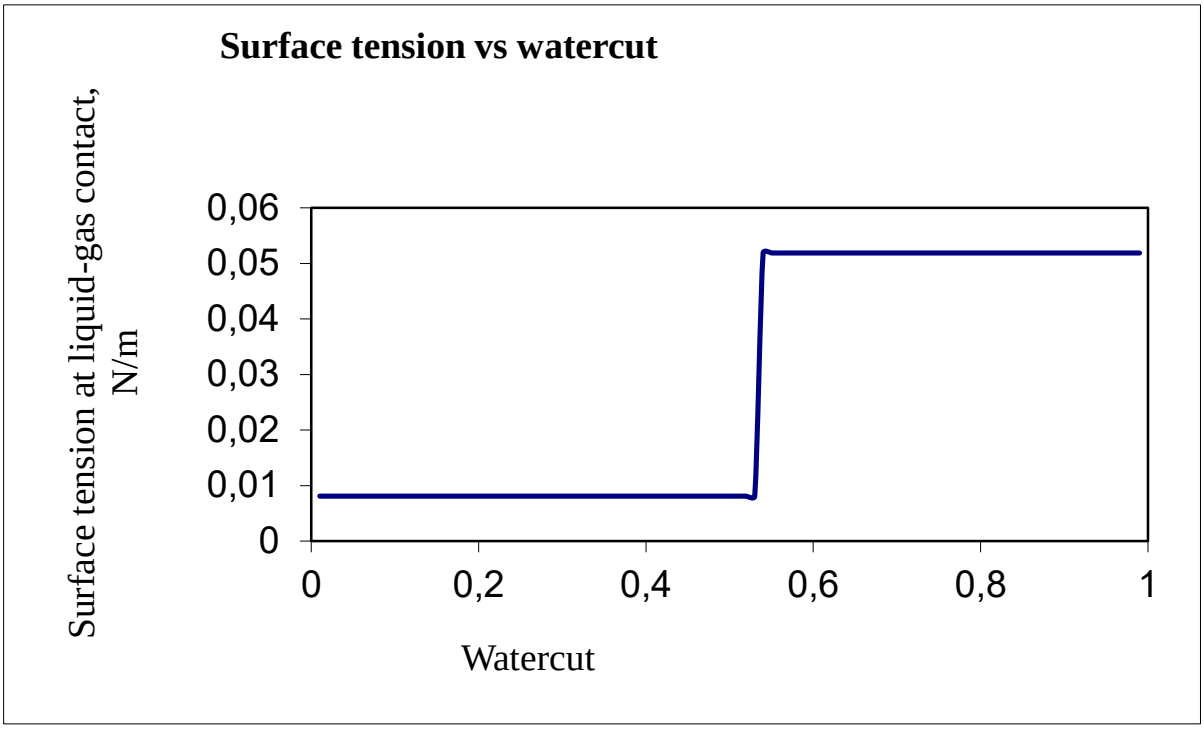

Figure 12– Surface tension vs watercut for Karakuduk oilfield (reservoir J-1/2)

3.4.1.10 Calculation of fluid viscosity

Function–fluid_viscosity

Table 21- Input data

Parameter	Symbol	Unit
Zone (annular space or tubing)	-	-
Pressure	P	MPa
Temperature	T	K
Water density at SC	$\rho_{w.sc}$	kg/m3
Annulus (tubing) diameter	D	m
Water volume fraction in liquid	β_{wl}	m3/m3
Superficial velocity of the mixture at given temperature and pressure conditions	ω_{mix}	m/s

Table 22- Continuation

First critical velocity of the mixture at given temperature and pressure conditions	ω_{cr1}	m/s
Second critical velocity of the mixture at given temperature and pressure conditions	ω_{cr2}	m/s
Oil viscosity at given temperature and pressure conditions	μ_0	MPa*s

Table 23- Called functions

Name of the function	Denotation
Calculation of fluid's volumetric water fraction	volume_share
Calculation of oil, water and gas flow rates and first and second critical rates	flow_rate
Calculation of oil density	oil_density

We calculate water viscosity:

$$\mu_w = \frac{0,0014 + 38 \cdot 10^{-7} (\rho_{w.sc} - 1000)}{10^{0,0065(T-273)}} \tag{3.22}$$

We calculate the value of A parameter:

$$A = \frac{(1 + 20\beta_{wl}^2)}{\left(\frac{8\omega_{mix}}{D}\right)^{0,48\beta_{wl}}} \tag{3.23}$$

Eventually, the value of liquid viscosity μ_l we get from the scheme:

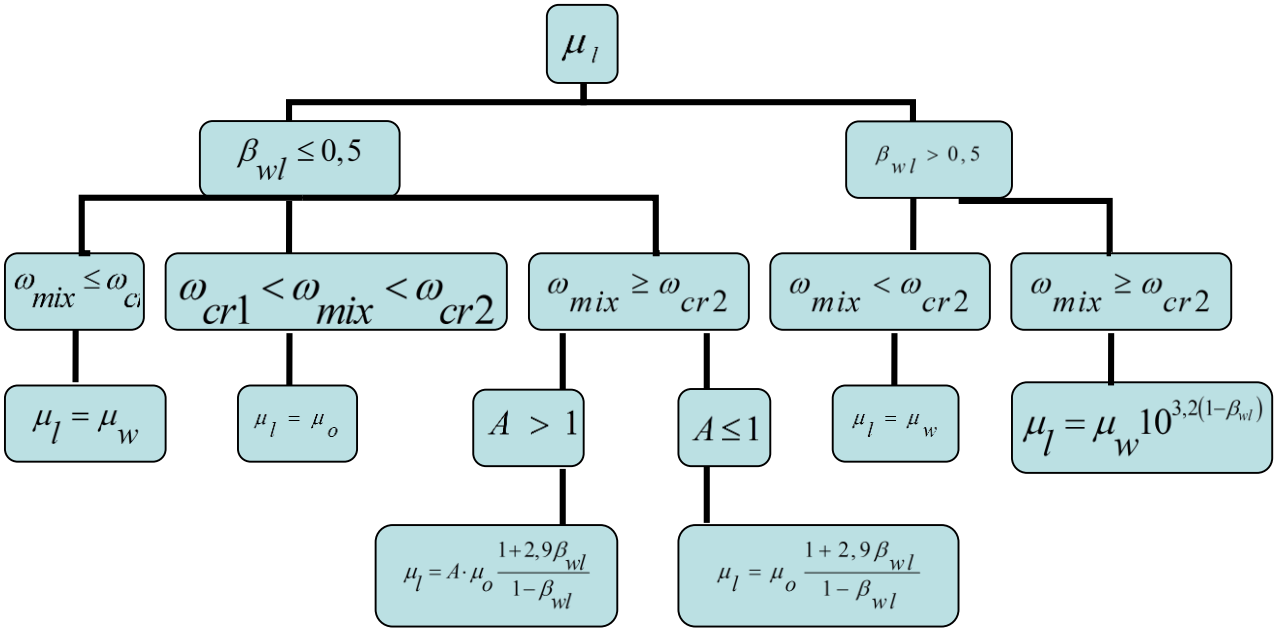

Figure 13- Choice of liquid viscosity

Table 24- Output data

Parameter	Symbol	Unit
Water viscosity	μ_w	MPa*s
Liquid viscosity	μ_l	MPa*s

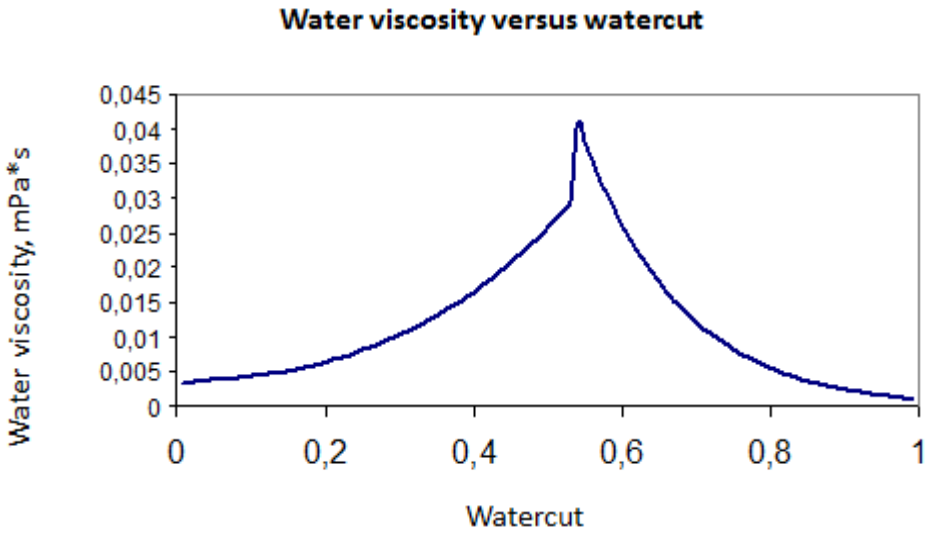

Figure 14- Water viscosity versus watercut for Karakuduk oilfield (reservoir J-1/2) (Gazizullin, 2014)

3.4.2 Calculation of pressure gradient

3.4.2.1 Calculation of oil, water and gas volumetric flowrates

Function– production_in_situ_condition

Table 25- Input data

Parameter	Symbol	Unit
Zone (annular space or tubing)	-	-
Pressure	P	MPa
Temperature	T	K
Well inflow at SC	$Q_{l.sc}$	m3/s
Water volume fraction in produced fluid at SC	$\beta_{w.sc}$	m3/m3
Saturation pressure	P_{sat}	MPa
Gas to oil ratio at saturation pressure	GOR_{sat}	m3/m3
Associated gas solubility coefficient in water	α_g	m3/(m3*MPa)
Oil volume factor at given temperature and pressure conditions	b_o	m3/m3
Water volume fraction in liquid	β_{wl}	m3/m3
Compressibility factor	Z	-
Gas to oil ratio	GOR	m3/m3
Separation factor	K_{sep}	-
Gas to oil ratio at pump intake	GOR_{inl}	MPa
Gas injection rate (for gas lift well)	$Q_{g.inj}$	m3/s
Pressure at pump intake	P_{inl}	m3/m3

Table 26- Called functions

Name of the function	Denotation
Calculation of oil volume factor	volume_factor
Calculation of fluid's volumetric water fraction	volume_share
Calculation of oil density	oil_density
Calculation of gas saturation	gas_saturation
Compressibility factor calculation	compressibility_factor

We calculate oil, water and gas volumetric flowrates:

$$Q_o = Q_{l.sc} \cdot (1-\beta_{w.sc}) \cdot b_o \tag{3.24}$$

$$Q_w = Q_{l.sc} \cdot \beta_{w.sc} \tag{3.25}$$

For annulus:

$$\left.\begin{aligned} Q_g &= Q_{l.sc} \frac{zP_{sc}T}{PT_{sc}}(1-\beta_{w.sc})(GOR_{sat}-GOR), P < P_{sat} \\ Q_g &= 0, P \geq P_{sat} \end{aligned}\right\} \tag{3.26}$$

For tubing:

$$Q_g = Q_{l.sc} \frac{zP_{sc}T}{PT_{sc}} \left\{ \begin{aligned} &(1-\beta_{w.sc})\left[\left(1-K_{sep}\right)(GOR_{sat}-GOR_{inl})-(GOR-GOR_{inl})\right]- \\ &-\alpha_g \beta_{w.sc}\left[\left(1-K_{sep}\right)(P_{sat}-P_{inl})-(P-P_{inl})\right] \end{aligned} \right\} + Q_{g.inj}$$

(3.27)

Table 27- Output data

Parameter	Symbol	Unit
Oil volumetric flowrate at given temperature and pressure conditions	$Q_н$	m3/s
Water volumetric flowrate at given temperature and pressure conditions	$Q_в$	m3/s
Gas volumetric flowrate at given temperature and pressure conditions	$Q_г$	m3/s

3.4.2.2 Calculation of oil, water and gas flow rates and first and second critical rates

Function– flow_rate

Table 28- Input data

Parameter	Symbol	Unit
Zone (annular space or tubing)	-	-
Annulus (tubing) diameter	D	m
Oil volumetric flowrate at given temperature and pressure conditions	Q_o	m3/s
Water volumetric flowrate at given temperature and pressure conditions	Q_w	m3/s
Gas volumetric flowrate at given temperature and pressure conditions	Q_g	m3/s
Volumetric water content in produced fluid at given temperature and pressure conditions	β_{wl}	m3/m3

Table 29- Called functions

Name of the function	Denotation
Calculation of fluid's volumetric water fraction	volume_share
Calculation of oil, water and gas volumetric flowrates	production_in_situ_condition

We calculate superficial velocities for oil, water and gas, previously having calculated the cross-sectional area:

$$S = \frac{\pi D}{4} \tag{3.28}$$

$$\omega_o = \frac{Q_o}{S} \tag{3.29}$$

$$\omega_w = \frac{Q_w}{S} \tag{3.30}$$

$$\omega_g = \frac{Q_g}{S} \tag{3.31}$$

Then we obtain the mixture velocity:

$$\omega_{mix} = \omega_o + \omega_w + \omega_g \tag{3.32}$$

Also first and second critical velocities are calculated:

$$\omega_{cr1} = 0,064 \cdot 56^{\beta_{wl}} (gD_c)^{0,5} \tag{3.33}$$

$$\omega_{cr2} = 0,487(gD_c)^{0,5} \tag{3.34}$$

Table 30- Output data

Parameter	Symbol	Unit
Oil superficial velocity at given temperature and pressure conditions	ω_o	m/s
Water superficial velocity at given temperature and pressure conditions	ω_w	m/s
Gas superficial velocity at given temperature and pressure conditions	ω_g	m/s
Superficial velocity of the mixture at given temperature and pressure conditions	ω_{mix}	m/s
First critical velocity of the mixture at given temperature and pressure conditions	ω_{cr1}	m/s
Second critical velocity of the mixture at given temperature and pressure conditions	ω_{cr2}	m/s

3.4.2.3 Calculation of a mixture type and a flow regime

Function– type_and_structure

Table 31- Input data

Parameter	Symbol	Unit
Zone (annular space or tubing)	-	-
Pressure	P	MPa

Table 32- Continuation

Volumetric water content in produced fluid at given temperature and pressure conditions	β_{wl}	m3/m3
Gas superficial velocity at given temperature and pressure conditions	ω_g	m/s
Superficial velocity of the mixture at given temperature and pressure conditions	ω_{mix}	m/s
First critical velocity of the mixture at given temperature and pressure conditions	ω_{cr1}	m/s
Second critical velocity of the mixture at given temperature and pressure conditions	ω_{cr2}	m/s
Surface tension at liquid-gas contact	σ_{lg}	N/m
Liquid viscosity	μ_l	MPa*s

Table 33- Called functions

Name of the function	Denotation
Calculation of fluid's volumetric water fraction	volume_share
Calculation of oil, water and gas flow rates and first and second critical rates	flow_rate
Calculation of oil, water and gas volumetric flowrates	production_in_situ_condition
Calculation of the surface tension between the liquid phase that is the outer phase of the stream and gas	surface_tension
Calculation of fluid viscosity	fluid_viscosity

As a condition of existence for a flow type and a flow regime, true gas fraction is used. It is calculated further as it depends on the flow regime. However, we can estimate the true gas fraction by the equation:

$$\varphi_g = \frac{\dfrac{\omega_{gs}}{\omega_{mix} + 0,23\left(\dfrac{\sigma_{lg}}{\sigma^*_{wg}}\right)^{0,83}\left(\dfrac{\mu_l}{\mu^*_w}\right)^{0,44}\cdot e^{-0,01\frac{\mu_l}{\mu^*_w}}} + \dfrac{\omega_{gs}}{\omega_{mix} + 0,41\left(\dfrac{\mu_l}{\mu^*_w}\right)^{0,1}\left(\dfrac{\sigma_{lg}}{\sigma^*_{wg}}\cdot\omega^2_{gs}\right)^{\frac{1}{3}}}}{2} \qquad (3.35)$$

Where $\sigma^*_{wg} = 0,067$ N/m,

$\mu^*_w = 0,0011$ Pa*s

We determine the mixture type and the flow regime from the table:

Table 34- Choice of mixture type and flow regime

Phase composition of the stream	Proportion of water in liquid	Mixture type	Flow regime	Existence boundaries of mixture type and structure
o+g	$\beta_{wl} = 0$	g/o	P	$\varphi_g \le 0,65$ or $P > 0,7$
		g/o	S	$\varphi_g > 0,65$ or $P \le 0,7$
o+w	$0 < \beta_{wl} \le 0,5$	o/w	D	$\omega_{mix} \le \omega_{cr1}$
		w/o	D	$\omega_{cr1} < \omega_{mix} < \omega_{cr2}$
		w/o	E	$\omega_{mix} \ge \omega_{cr2}$
	$\beta_{wl} > 0,5$	o/w	D	$\omega_{mix} < \omega_{cr2}$
		o/w	E	$\omega_{mix} \ge \omega_{cr2}$
o+w+g	$0 < \beta_{wl} \le 0,5$	(o+g)/w	D-P	$\omega_{mix} \le \omega_{cr1}$ and ($\varphi_g \le 0,65$ or $P > 0,7$)
		(w+g)/o	D-P	$\omega_{cr1} < \omega_{mix} < \omega_{cr2}$ and ($\varphi_g \le 0,65$ or $P > 0,7$)
		(w+g)/o	D-P	$\omega_{mix} \ge \omega_{cr2}$ and ($\varphi_g \le 0,65$ or $P > 0,7$)
		(w+g)/o	E-S	$\omega_{mix} \ge \omega_{cr2}$ and ($\varphi_g > 0,65$ or $P \le 0,7$)
	$0,5 < \beta_{wl} < 1$	(o+g)/w	D-P	$\omega_{mix} < \omega_{cr2}$ and ($\varphi_g \le 0,65$ or $P > 0,7$)
		(o+g)/w	E-P	$\omega_{mix} \ge \omega_{cr2}$ and ($\varphi_g \le 0,65$ or $P > 0,7$)
		(o+g)/w	E-S	$\omega_{mix} \ge \omega_{cr2}$ and ($\varphi_g > 0,65$ or $P \le 0,7$)

Where for flow regime:

B- Bubble,

S- Slug,

D- Droplet,

E- Emulsion.

Table 35- Output data

Parameter	Symbol	Unit
Mixture type	type	-
Flow regime	regime	-

3.4.2.4 Calculation of oil, water and gas fractions

Function- fraction_share

Table 36- Input data

Parameter	Symbol	Unit
Zone (annular space or tubing)	-	-
Oil superficial velocity at given temperature and pressure conditions	ω_o	m/s
Water superficial velocity at given temperature and pressure conditions	ω_w	m/s
Gas superficial velocity at given temperature and pressure conditions	ω_g	m/s
Superficial velocity of the mixture at given temperature and pressure conditions	ω_{mix}	m/s
Volumetric water content in produced fluid at given temperature and pressure conditions	β_{wl}	m3/m3
Water density at SC	$\rho_{w.sc}$	kg/m3
Oil density at given temperature and pressure conditions	ρ_o	kg/m3
Mixture type	type	-
Flow regime	regime	-
Liquid viscosity	μ_l	MPa*s

Table 37- Continuation

Annulus (tubing) diameter	D	m
Surface tension at oil-water contact	σ_{ow}	N/m
Surface tension at liquid-gas contact	σ_{lg}	N/m

Table 38- Called functions

Name of the function	Denotation
Calculation of the surface tension between the liquid phase that is the outer phase of the stream and gas	surface_tension
Calculation of fluid's volumetric water fraction	volume_share
Calculation of oil, water and gas flow rates and first and second critical rates	flow_rate
Calculation of oil density	oil_density
Calculation of a mixture type and a flow regime	type_and_structure
Calculation of fluid viscosity	fluid_viscosity

True gas fraction s determined from :

Table 39- Choice of true gas fraction

Flow regime	True gas fraction
B, D-B, E-B	$\varphi_g = \dfrac{\omega_{gs}}{\omega_{mix} + 0,23\left(\dfrac{\sigma_{lg}}{\sigma^*_{wg}}\right)^{0,83}\left(\dfrac{\mu_l}{\mu^*_w}\right)^{0,44} \cdot e^{-0,01\frac{\mu_l}{\mu^*_w}}}$
S, E-S	$\varphi_g = \dfrac{\omega_{gs}}{\omega_{mix} + 0,41\left(\dfrac{\mu_l}{\mu^*_w}\right)^{0,1}\left(\dfrac{\sigma_{lg}}{\sigma^*_{wg}} \cdot \omega^2_{gs}\right)^{\frac{1}{3}}}$
D	$\varphi_g = 0$

Where one may assume $\sigma^*_{wg} = 0,067$ N/m,

$\mu^*_w = 0,0011$ Pa*s

Then we calculate the true fraction share of water and oil in the liquid

Table 40- Choice of true fraction share of water and oil in the liquid

Flow type	Flow regime	True fraction share of water and oil in the liquid
o/w, (o+g)/w	D, D-B	$\varphi_{ol} = \dfrac{\omega_o}{\omega_{mix} + \left[0,54\left(0,01+\beta_{wl}^{0,152}\right) - \dfrac{\omega_{mix}}{\sqrt{gD}}\right]\left(4g\sigma_{ow}\dfrac{\lvert\rho_{w.sc}-\rho_o\rvert}{\rho_{w.sc}^2}\right)^{0,25}}$ $\varphi_{wl} = 1-\varphi_{ol}$
	E, E-B, E-S	$\varphi_{ol} = \dfrac{\omega_o}{\omega_{mix}}$ $\varphi_{wl} = 1-\varphi_{ol}$
w/o, (w+g)/o	D, D-B	$\varphi_{wl} = \dfrac{\omega_w}{\omega_{mix} - \left(0,425-0,827\dfrac{\omega_{mix}}{\sqrt{gD}}\right)\left(4g\sigma_{ow}\dfrac{\lvert\rho_{w.sc}-\rho_o\rvert}{\rho_o^2}\right)^{0,25}}$ $\varphi_{ol} = 1-\varphi_{wl}$
	E, E-B, E-S	$\varphi_{wl} = \dfrac{\omega_w}{\omega_{mix}}$ $\varphi_{ol} = 1-\varphi_{wl}$

True water and oil fractions are obtained from:

$$\varphi_o = \varphi_{ol}\left(1-\varphi_g\right) \tag{3.36}$$

$$\varphi_w = \varphi_{wl}\left(1-\varphi_g\right) \tag{3.37}$$

Table 41- Output data

Parameter	Symbol	Unit
Oil fraction	φ_o	-
Water fraction	φ_w	-
Gas fraction	φ_g	-

3.4.2.5 Calculation of pressure gradient

$\frac{\partial P}{\partial L}$

Function– pressure_gradient

Table 42- Input data

Parameter	Symbol	Unit
Zone (annular space or tubing)	-	-
Oil fraction	φ_o	-
Water fraction	φ_w	-
Gas fraction	φ_g	-
Oil superficial velocity at given temperature and pressure conditions	ω_o	m/s
Water superficial velocity at given temperature and pressure conditions	ω_w	m/s
Gas superficial velocity at given temperature and pressure conditions	ω_g	m/s
Oil density at given temperature and pressure conditions	ρ_o	kg/m3
Water density at SC	$\rho_{w.sc}$	kg/m3
Gas density at given temperature and pressure conditions	ρ_g	kg/m3
Mixture viscosity	μ_{mix}	MPa*s
Average inclination	θ	deg.
Annulus (tubing) diameter	D	m

Table 43- Called functions

Name of the function	Denotation
Calculation of oil, water and gas flow rates and first and second critical rates	flow_rate
Calculation of oil density	oil_density
Calculation of gas density	gas_density
Calculation of fluid viscosity	fluid_viscosity
Calculation of oil, water and gas fractions	fraction_share

The calculation is done by the formula:

$$\frac{\partial P}{\partial L} = g \cdot (\varphi_o \cdot \rho_o + \varphi_w \cdot \rho_{w.sc} + \varphi_g \cdot \rho_g) \cos\theta + \frac{\lambda}{2D_c}\left(\frac{\rho_o \omega_o^2}{\varphi_o} + \frac{\rho_w \omega_w^2}{\varphi_w} + \frac{\rho_g \omega_g^2}{\varphi_g}\right) \tag{3.38}$$

In order to determine hydraulic friction coefficient we calculate the value of Re number:

$$\mathrm{Re} = \frac{D}{\mu_{mix}}\left(\rho_o \omega_o + \rho_w \omega_w + \rho_g \omega_g\right) \tag{3.39}$$

Hydraulic friction coefficient is calculated from:

$$\left.\begin{aligned} \lambda &= \frac{64}{\mathrm{Re}}, \mathrm{Re} \le 2000 \\ \lambda &= 0{,}11\left(\frac{68}{\mathrm{Re}} + \frac{k_e}{D}\right), \mathrm{Re} > 2000 \end{aligned}\right\} \tag{3.40}$$

One may assume that for an oil producing well $k_e = 15 \cdot 10^{-6}$ m.

Table 44- Output data

Parameter	Symbol	Unit
Pressure gradient	$\frac{\partial P}{\partial L}$	MPa/m

3.4.2.6 Calculation of temperature gradient

$\frac{\partial T}{\partial L}$

Function– temperature_gradient

Table 45- Input data

Parameter	Symbol	Unit
Zone (annular space or tubing)	-	-
Geothermal gradient	G	K/m
Well inflow at SC	$Q_{l.sc}$	m3/d
Annulus (tubing) diameter	D	m

We calculate temperature gradient:

$$\frac{\partial T}{\partial L} = \frac{(0,0034 + 0,79G)}{10^{\frac{Q_{l.sc}}{20D^{2,67}}}} \tag{3.41}$$

Table 46- Output data

Parameter	Symbol	Unit
Temperature gradient	$\frac{\partial T}{\partial L}$	K/m

3.4.2.7 Calculation of pressure and temperature on the next stage

Function– P_and_T

Table 47- Input data

Parameter	Symbol	Unit
Zone (annular space or tubing)	-	-
Pressure	P	MPa
Temperature	T	K

Table 48- Continuation

Pressure gradient	$\frac{\partial P}{\partial L}$	MPa/m
Temperature gradient	$\frac{\partial T}{\partial L}$	K/m
Distance from the wellhead to the upper holes of the filter of the casing	H_f	m

Table 49- Called functions

Name of the function	Denotation
Calculation of pressure gradient	pressure_gradient
Calculation of temperature gradient	temperature_gradient

The interval L - O is divided into 100 equal steps $\Delta L_1 \ldots \Delta L_{100}$:

$$\Delta L = \frac{H_f}{100} \tag{3.42}$$

Gradient by definition is:

$$\frac{\partial A}{\partial L} = \frac{A_1 - A_2}{L_1 - L_2} \tag{3.43}$$

where A -Pressure and Temperature P, T respectively.

Let the pressure in a cross-sectional area be $P = P_{in}$ -pressure at the inlet of i stage, and the temperature in a cross-sectional area be $T = T_{in}$ - temperature at the inlet of i stage. Then pressure and temperature at the outlet of i stage are:

Table 50- Pressure and temperature at the outlet of i stage

Zone (annular space or tubing) / Parameters	Casing	Tubing
Calculation method	Upwards (from the bottom to the mouth)	Upwards (from the bottom to the mouth)
Pressure on the next stage	$P_{out} = P_{in} - \frac{\partial P}{\partial L}\Delta L$	$P_{out} = P_{in} - \frac{\partial P}{\partial L}\Delta L$
Temperature on the next stage	$T_{out} = T_{in} - \frac{\partial T}{\partial L}\Delta L$	$T_{out} = T_{in} - \frac{\partial T}{\partial L}\Delta L$

Thus, output data:

Table 51- Output data

Parameter	Symbol	Unit
Pressure on the next stage	P_{out}	MPa
Temperature on the next stage	T_{out}	K

3.4.2.8 Calculation of bottowhole pressure

Function– bottomhole_pressure

Table 52- Input data

Parameter	Symbol	Unit
Reservoir pressure	P_{res}	MPa
Productivity coefficient	K	m3/(d*MPa)
Well inflow at SC	$Q_{l.sc}$	m3/d

We calculate the value of the bottomhole pressure from the equation:

$$P_{bh} = P_{res} - 86400\frac{Q_{l.sc}}{K} \tag{3.44}$$

Table 53- Output data

Parameter	Symbol	Unit
Bottomhole pressure (BHP)	P_{bh}	MPa

3.4.2.9 Calculation of pressure and temperature distribution curves along casing

$P(L)_c$, $T(L)_c$

Function– PDC_casing

Table 54- Input data

Parameter	Symbol	Unit
BHP	P_{bh}	MPa
Distance from the wellhead to the upper holes of the filter of the casing	H_f	m
Reservoir temperature	T_{res}	K
Average inclination	θ	deg.
Pressure in well flow line	P_l	MPa
Pressure on the next stage	P_{out}	MPa
Temperature on the next stage	T_{out}	K
Water volume fraction in produced fluid at SC	$\beta_{w.sc}$	m3/m3
Gas superficial velocity at given temperature and pressure conditions	ω_g	m/s
Superficial velocity of the mixture at given temperature and pressure conditions	ω_{mix}	m/s

Table 55- Called functions

Name of the function	Denotation
Calculation of bottowhole pressure	bottomhole_pressure
Calculation of pressure and temperature on the next stage	P_and_T
Calculation of oil, water and gas flow rates and first and second critical rates	flow_rate

Pressure distribution curve (PDC) and temperature distribution curve along the annulus is built from the bottom towards the surface of the well. That means that for the starting point bottomhole parameters are taken:

$$P_1 = P_{bh} \tag{3.45}$$

$$T_1 = T_{res} \tag{3.46}$$

$$L_1 = H_f \tag{3.47}$$

Then the calculation of i value of depth, pressure and temperature is performed according to the following flowchart:

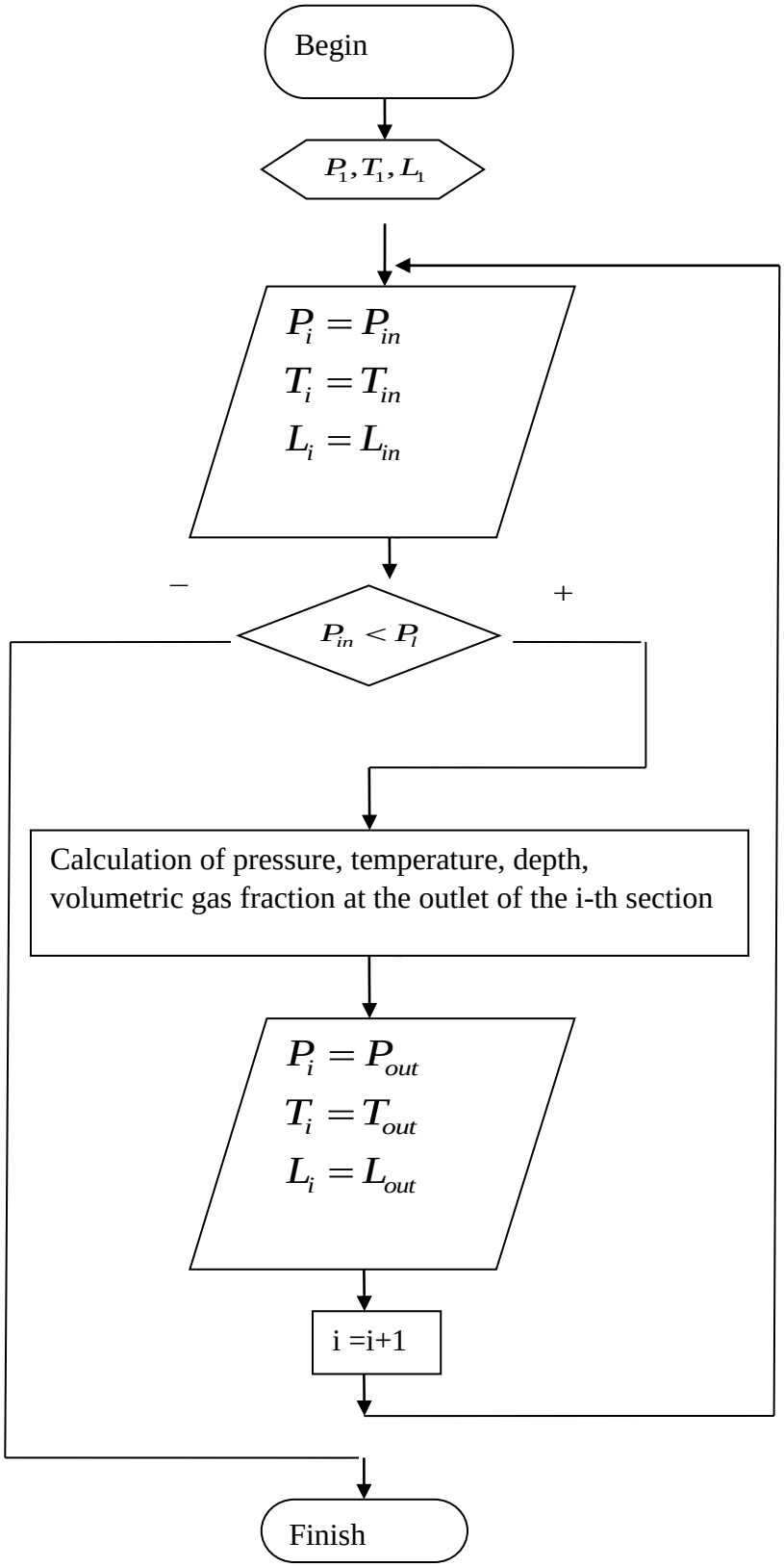

Figure 15- Flowchart for PDC along annulus calculation

Pressure and temperature calculation is performed in the respective chapters.

We calculate the depth value as shown below:

$$L_{out} = L_{in} - \Delta L \tag{3.48}$$

Thus, not only pressure and temperature, but also any other characteristic of the flow may be determined for any annulus section.

3.4.3 Calculation of pressure and temperature distribution curves along tubing

$P(L)_{tub}$, $T(L)_{tub}$

Function- PDC_tubing

Table 56- Input data

Parameter	Symbol	Unit
Pressure in well flow line	P_l	MPa
Reservoir temperature	T_{res}	m3/(d*MPa)
Distance from the wellhead to the upper holes of the filter of the casing	H_f	m
Average inclination	θ	deg.
Geothermal gradient	G	K/m
Well inflow at SC	$Q_{l.sc}$	m3/s
Casing diameter	D_c	m
Flow temperature increment caused by heating it with pump heat and engine	ΔT_p	deg.
Pump setting depth	L_{inl}	m
Pressure on the next stage	P_{out}	MPa
Temperature on the next stage	T_{out}	K

Table 57- Called functions

Name of the function	Denotation
Calculation of flow temperature increment caused by heating it with pump heat and engine	temperature_increment
Calculation of pressure and temperature on the next stage	P_and_T

Pressure distribution curve (PDC) and temperature distribution curve along the tubing is built from the surface towards the pump setting depth. That means that for the starting point mouth parameters are taken:

$$P_1 = P_l \tag{3.49}$$

$$T_1 = T_l = T_{res} - (H_f - L_{inl}\cos\theta)\cdot\left(\frac{\partial T}{\partial L}\right)_c + \Delta T_p - L_{inl}\cdot\cos\theta\cdot\left(\frac{\partial T}{\partial L}\right)_{tub} \tag{3.50}$$

$$L_1 = 0 \tag{3.51}$$

Then the calculation of i value of depth, pressure and temperature is performed according to the following flowchart:

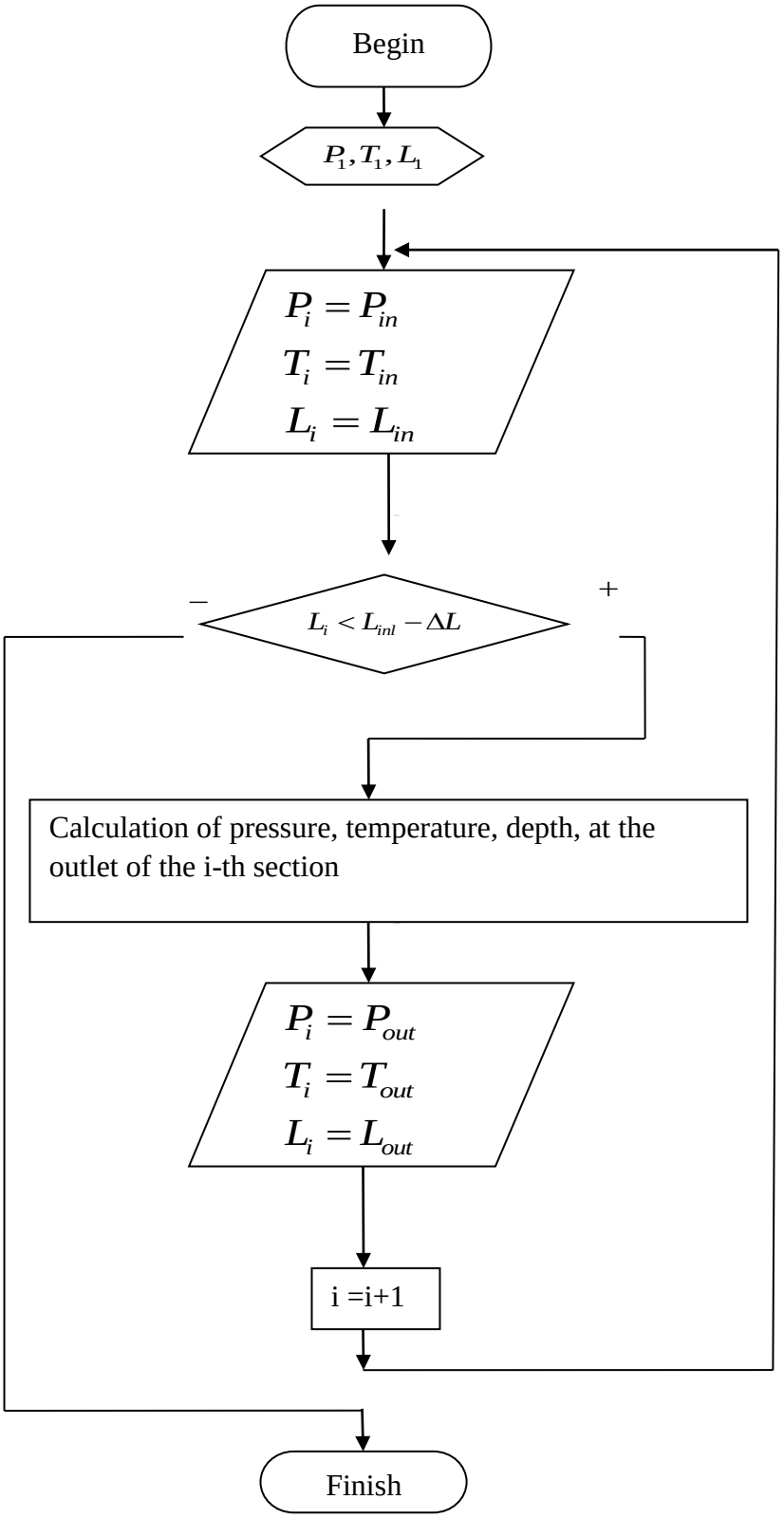

Figure 16- Flowchart for PDC along tubing calculation

Pressure and temperature calculation is performed in the respective charpters.

We calculate the depth value as shown below:

$$L_{out} = L_{in} - \Delta L \tag{3.52}$$

Temperature can be calculated from:

$$T_{in} = T_{res} - (H_f - L_{inl}\cos\theta)\cdot\left(\frac{\partial T}{\partial L}\right)_c - \left(L_{inl} - L_{out}\right)\cdot\cos\theta\cdot\left(\frac{\partial T}{\partial L}\right)_{tub}$$

(3.53)

Thus, not only pressure and temperature, but also any other characteristic of the flow may be determined for any tubing section.

These functions united into one loop allow to build the pressure distribution curve (PDC). As a result, true liquid flowrate is obtained. Later a set of gas injection rates is tested out to see, how the liquid flowrate is changed. The obtained array of gas injection rates and liquid production rates is used to produce a production curve for a well, that can be analyzed for the optimization.

3.5. Optimization of calculation process

As it has been noted in paragraph "3.3 Calculation steps", the whole calculation process consists of several loops, folded into each other (from PDC calculation, which is level 1 loop to the loop, testing out different gas injection rates, which is level 3-see Figure 5). Thus, number of calculation times inside the loops may reach high values if no optimization is done. By optimization it is considered certain values, changing which allows the user to minimize the calculation time. Another question is precision of calculation, which can be affected if wrong optimization is done. Here the balance must be kept between the optimization and precision, however the second one is of higher importance.

A part of the program code is shown below in order to explain the optimization parameter, that have been used (from "maim_program" matlab file- more fully shown in Appendix A):

```
%definition of resolution-strongly affects the speed of calculation process
%(recommended n_q=30 P_tol=0.025 for good results)
n_q=10; %number of steps- define precision
P_tol=0.025;
K_tol=1.1; % tolerance coefficient- increases calculation speed
 %-------------------------------------------------------------

counter1=0;
for i_q=1:n_q
x0(101)=0;
P_bh(i_q)=8;
y17=P_bh(i_q);
Ql_SC(i_q)=  K*(P_res - P_bh(i_q)) / 86400;
    counter1=counter1+1;
    counter=0;
    while abs(x0(101)-P_l)>P_tol
        counter=counter+1;
        counter1=counter1+1;
P_bh(i_q)=P_bh(i_q)- K_tol*P_tol;

     …

     end

…

end
```

The following values have been ranged in order to obtain better timing results:

n_q=10- number of time the level 3 loop is done. It defines the resolution of "liquid production" curve and "gas lift operating pressure vs. gas injection" curve, the eventual result, which is presented in a plot further in "Results and Discussion" section.

P_bh(i_q)=8- Initial “guessed bottomhole pressure”. It should not be much far away from the true bottomhole pressure value.

P_tol=0.025- tolerance of calculated wellhead pressure in relation to the factual wellhead pressure. It affects the number of times level 2 loop is done.

K_tol=1.1; - another tolerance coefficient in the level 2 loop. After several attempts of testing out the program it have turned out, that the factual calculation time, when the program code is run is around 5 minutes. After introducing this coefficient the timing have been reduced to 2 minutes, as this value increases the value of pressure that must be distracted from the “P_bh” value. Several attempts have been made to make the tolerance coefficient be proportional to the absolute difference between factual and true wellhead pressures. It resulted in false results along with increased calculation time. So, the last method have been rejected.

Two counters have been added to visualize number of step done in the loops. “counter” is a counter for the level 2 loop and counter “counter1” is for level 3 loop. It turned out, that “counter” equals to 7 and “counter1” equals to 73, which is pretty good results.

4 Discussion of simulation results

4.1 Simulation part

In the following section the results produced by the Matlab program are discussed. The results are mostly represented in plots, built in the Matlab workspace for the given well with input parameters shown earlier in the Chapter 3. To begin with, pressure distribution curve for the oil producing well with gaslift installed (with gas injection rate 0,5 Sm3/s) is shown below:

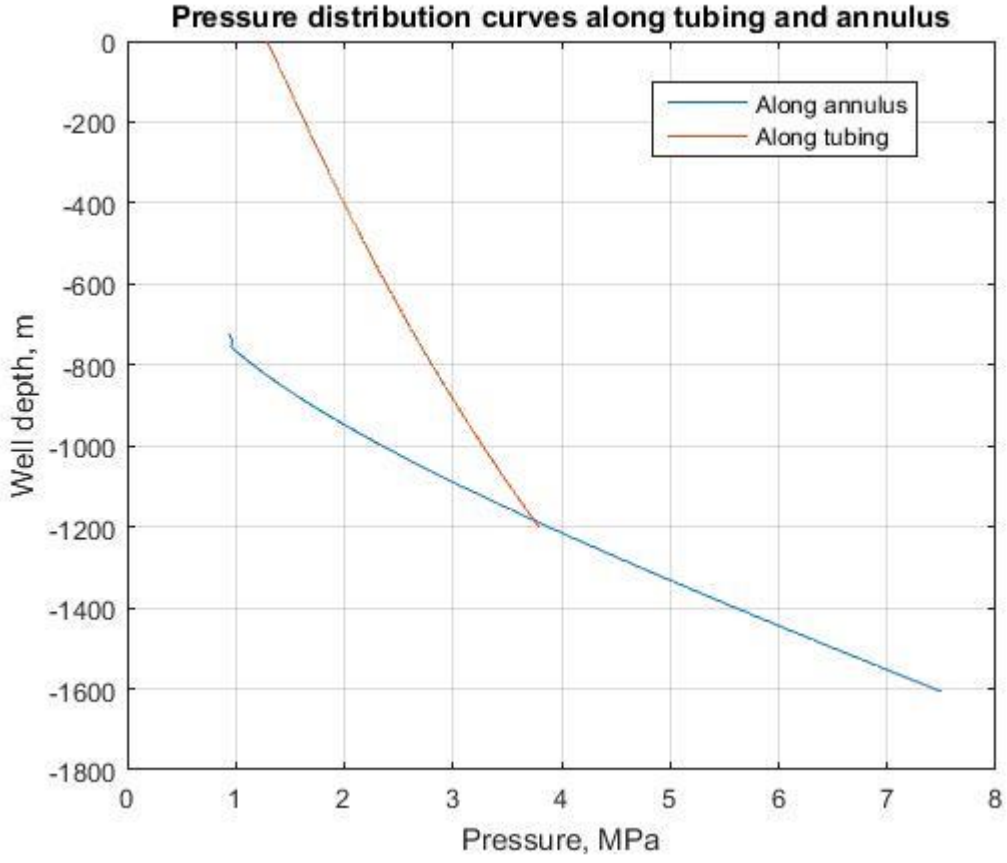

Figure 17- Pressure distribution curves along tubing and annulus

From this figure it can be seen that the well is producing the reservoir fluid at the bottomhole pressure of around 7,5 MPa. The tubing is installed until the depth of 1200 m, from where gas-oil-water mixture is being delivered to the surface at 1,3 MPa wellhead pressure. The two curves are

bended out due to degassing process, since the gas saturation pressure is given to be 8,5 MPa, which is higher than the bottomhole pressure.

As it has been shown before in Chapter 2 and Chapter 3, local pressures are comprised of local pressure gradients multiplied by the length interval. Pressure and temperature gradients for the given well are shown below:

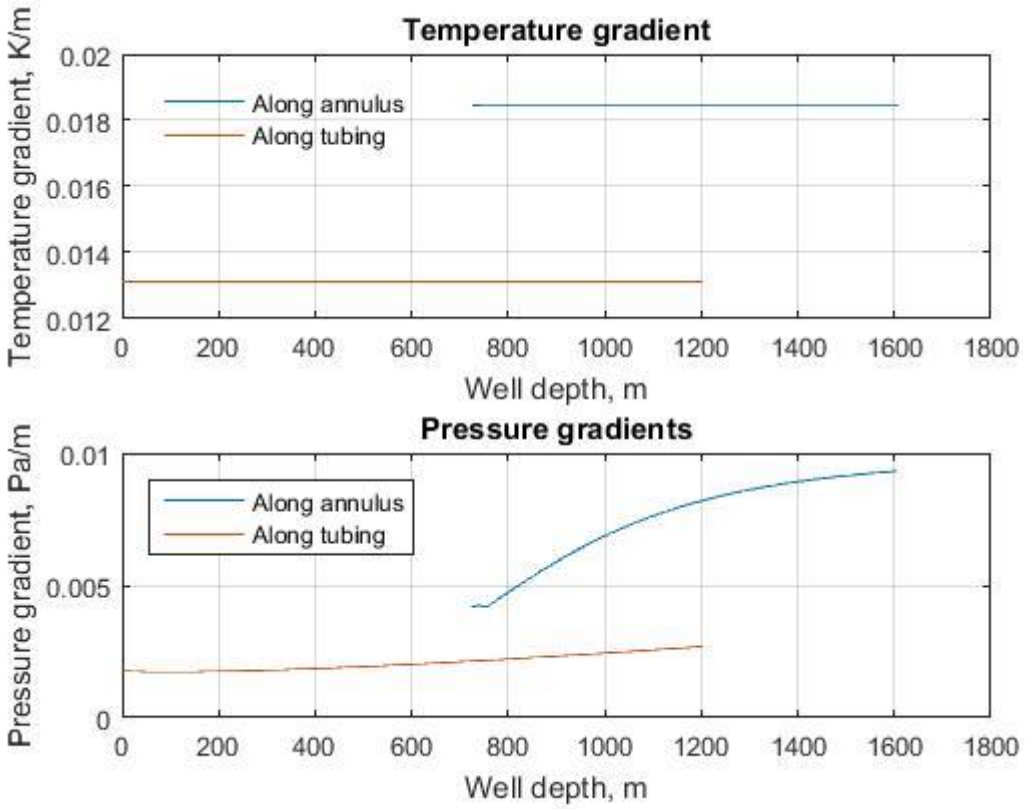

Figure 18- Pressure and temperature gradients along the well

By looking at the first subplot, one may conclude that temperature gradients are constant and that the gradient is higher in annulus rather than in tubing. That means that temperature in tubing does not change much due to its lower cross-section area and, as a sequence, due to higher flow velocities. In other words, the well fluid does not have “enough time” to cool down.

The second flowchart describes pressure gradients. Here it is important to emphasize, that given results are obtained for a gas lift well with injected gas at 0,5 m3/s. Pressure gradients for annulus and tubing show different behavior. The first one decreases gradually as the well position goes up. The second pressure gradient has a minimum at a certain point, and due to the gas lift effect slightly increases near the wellhead area, where pressure is minimum and gas bubbles have maximum diameter and, consequently, the highest efficiency. The efficiency of gas lift, how the injected gas affects the pressure gradient and liquid production in particular, will be considered further.

It is also interesting to look at the intermediate results obtain during PDC calculation, namely, PVT properties of the well mixture as well as dynamic properties of the fluid.

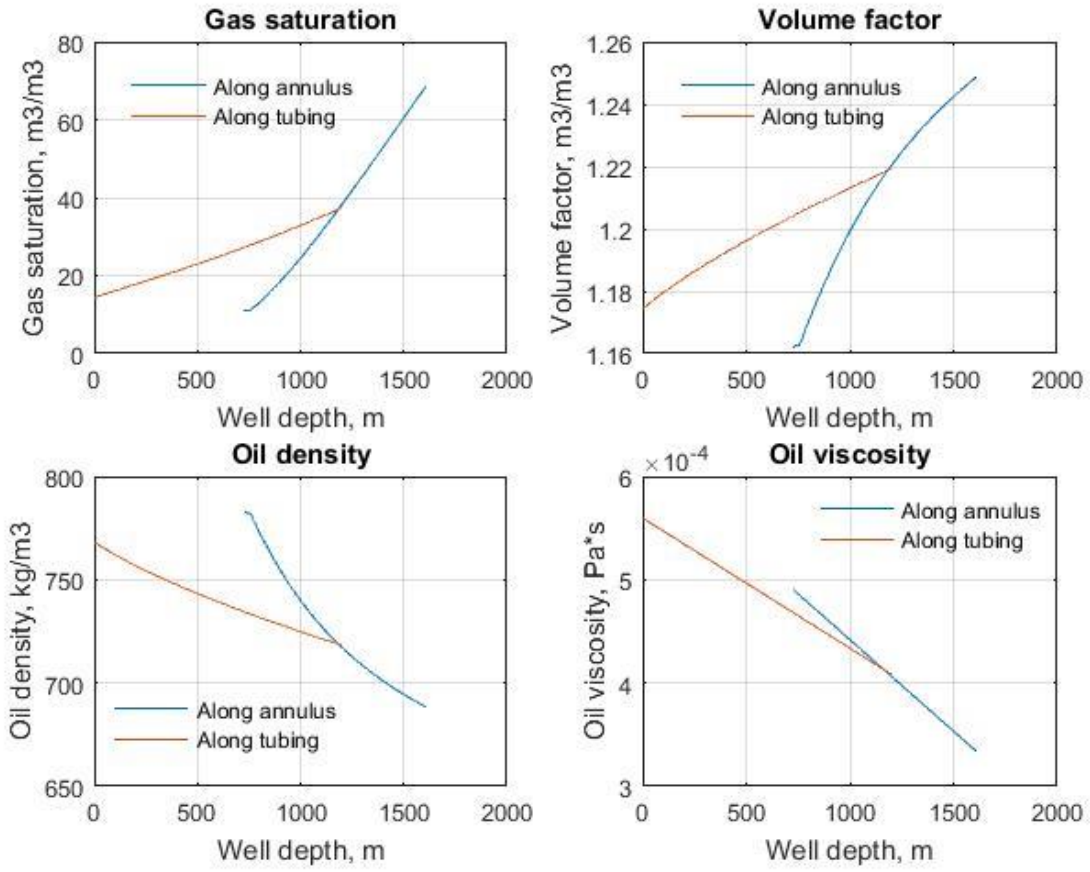

Figure 19- PVT properties of oil in the well along tubing and annulus

The first subplot represents gas saturation in oil (natural gas that is dissolved in oil). It is constant up to a certain pressure- gas saturation pressure, below which gradually decreases as more and more gas is extracted from oil.

The second plot represents formation volume factor. It has similar behavior to gas saturation function. It is constant up to a certain pressure- gas saturation pressure, below which it gradually decreases as oil loses mass due to gas extraction; temperature change and oil expansion- pressure decreases from the bottomhole pressure to the wellhead pressure.

The third plot represents oil density function. Oil density has a local maximum at the lower part of the well, where the pressure is maximum (in case all gas is dissolved in oil), then linearly goes down due to pressure-temperature effects until the gas saturation point (not visible here), from where logarithmically goes up again as the well position is closer to the surface.

Finally, the forth subplot represents oil viscosity function which has the similar behavior to the well density factor due to the same effects.

Other important gas and mixture PVT properties are depicted below:

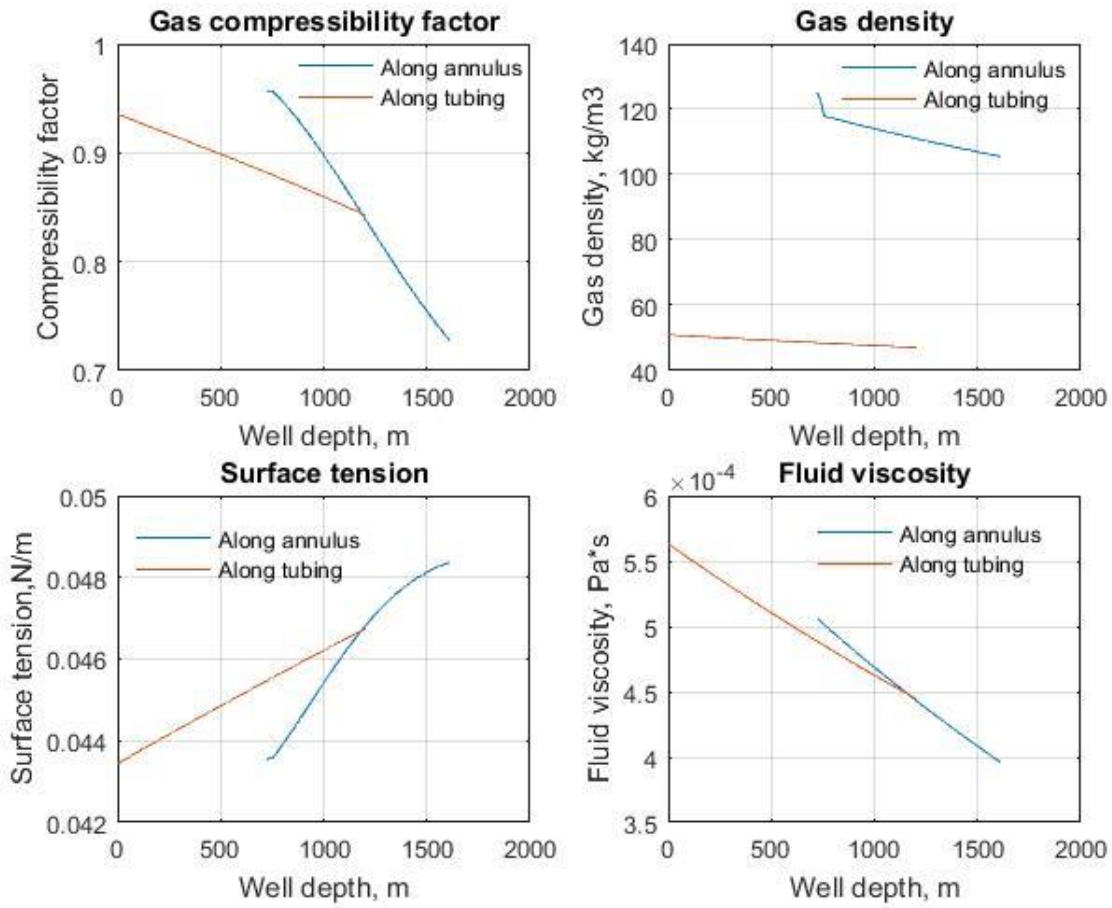

Figure 20- PVT properties of gas and gas-oil-water mixture in the well along tubing and annulus

The first subplot represents gas compressibility factor. It depends on gas composition, pseudoreduced pressure and temperature and local pressures and temperature. Eventually, the behavior of this function is complicated, but the main trend is that it increases upwards from the well bottom to the wellhead.

The second subplot represents gas density. It linearly increases upwards according to the barometric formula for gases.

The third subplot represents surface tension function at oil-water contact. Surface tension depends on pressure and temperature and has its maximum and minimum at the wells' bottom and head respectively.

The last subplot fluid viscosity as a function of well depth. Fluid viscosity has a difficult behavior depending on many factors. The most significant factor is watercut, that affects the mixture viscosity as follows:

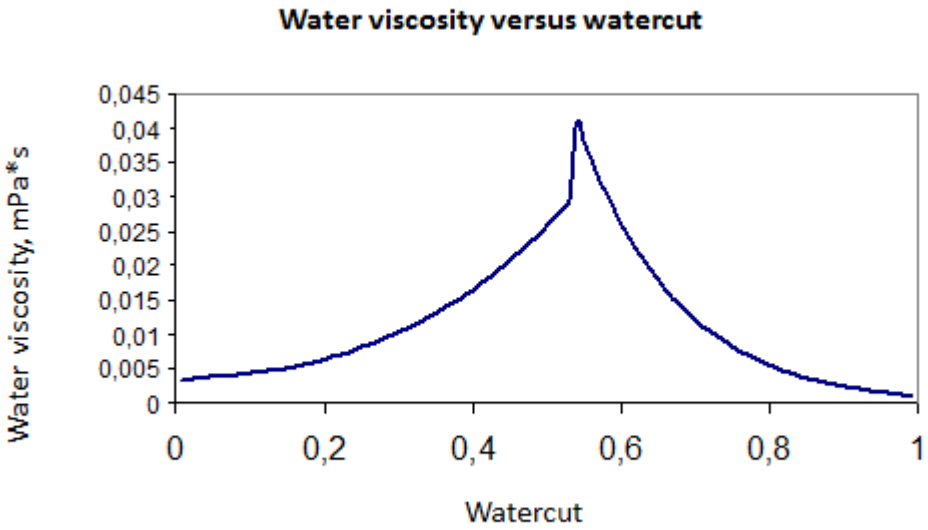

Figure 21- Fluid viscosity versus watercut

As can be seen from the plot, mixture viscosity is significantly higher that water and oil viscosities separately. The maximum is observes at water concentration of around 50%, where a strong emulsion is created.

The next figure represents different parameters of the flow for tubing and annulus space along the well.

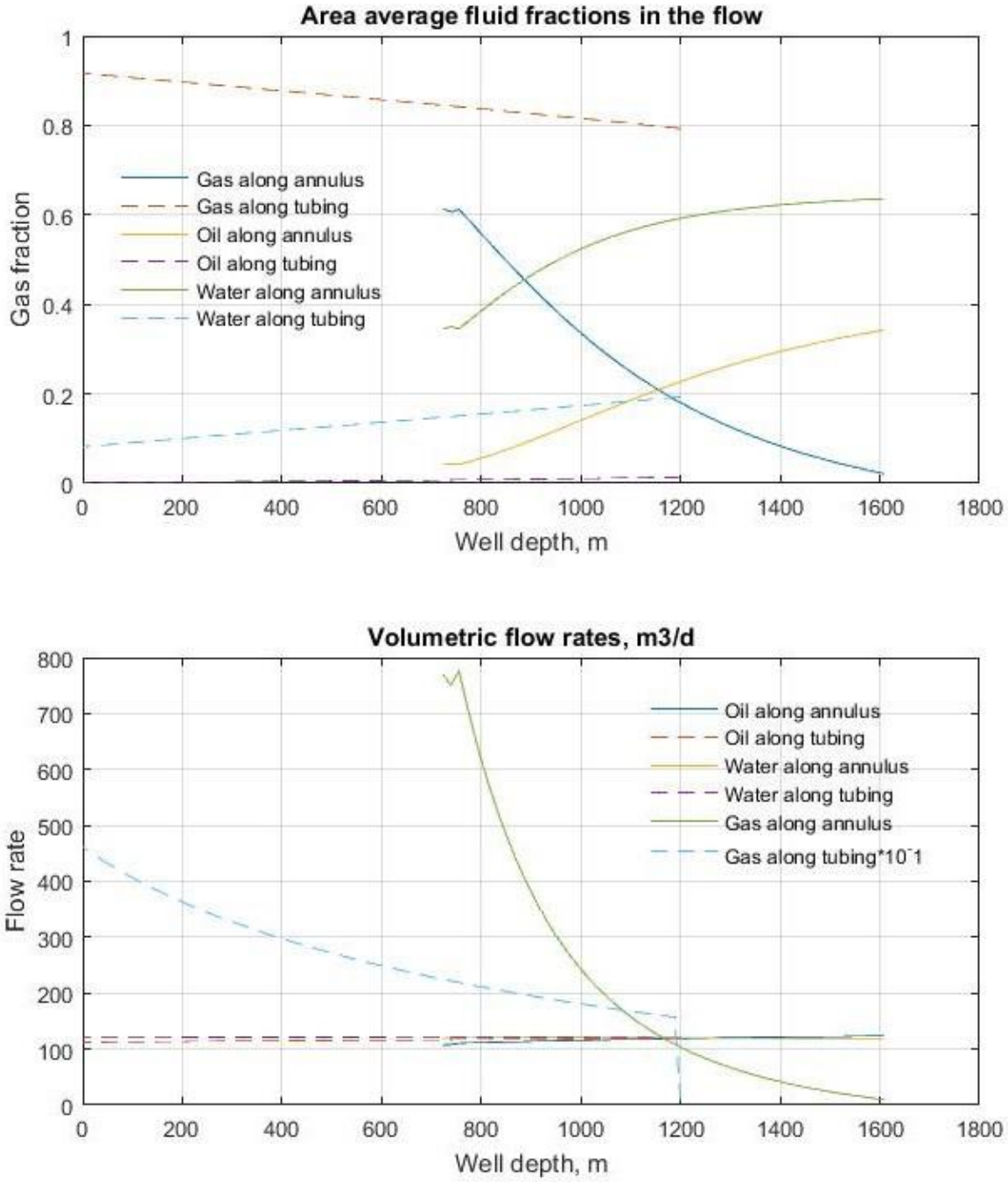

Figure 22- Different fluid properties in the well along tubing and annulus

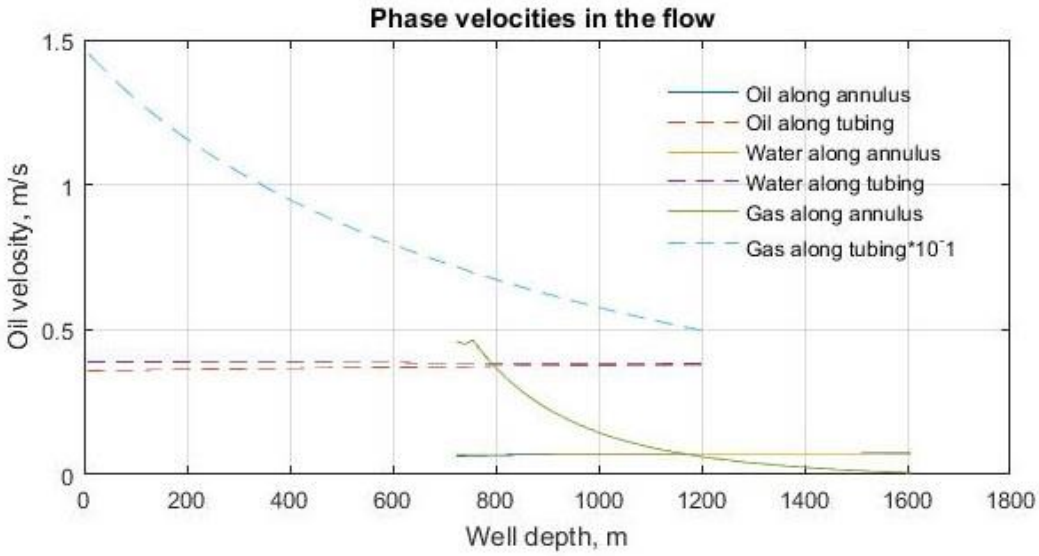

Figure 23- Different fluid properties in the well along tubing and annulus (continuation)

The first subplot represents area average fluid fractions in the flow for oil, water and gas. Since the following case is considered for a gaslift injection case, gas parameters are expected to be higher than the ones for liquids. For example, here gas volume takes almost all space in tubing. Also, the more gas is expected from oil, the more fraction it takes in the cross-sectional area (relevant for both tubing and annulus), and oil and water fraction are being reduced respectively.

The second plot and the third plot represent phase velocities of the flow and volumetric low rates respectively. Notice, that gas velocity is ten times reduced in order to show compatible figures. As expected, the general behavior is similar to the previous plot.

4.2 Gas lift optimization

Let us consider a case when the given well is producing the reservoir fluid on a natural production (no gas injection system is implemented). Considering given initial well, reservoir and reservoir fluid data, pressure distribution curves have been built, using the Matlab program:

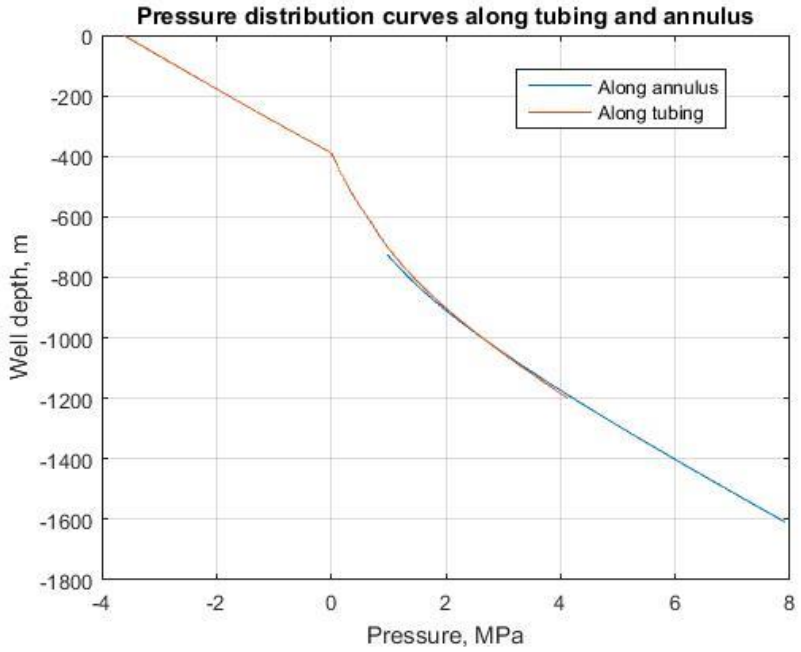

Figure 24 – PDC along tubing and annulus when no gas lift in the well is installed

The program gives a “mistake”, as the pressure values go below the atmospheric pressure level. From here, it can be concluded that reservoir energy is not enough to lift the fluid to the surface. The gas-oil-water mixture is lifted along the tubing to the depth of around 400 meter, where the local pressure is equal to the atmospheric pressure. It is necessary to use additional methods, gas lift is a good solution. After gas lift has been set, pressure distribution curves will look as in Figure 17, meaning that oil reservoir production reaches the surface and gaslift is an efficient tool. Here it is important to note few assumptions, used when designing gaslift:

1-gas is injected to the lower part of the tubing, meaning absence of gaslift valves or orifices along tubing;

2- gaslift is injected from an imaginary tube, meaning that friction losses due to the additional equipment are not considered;

3- gas injected into the well has the same composition as natural gas;

4- amount of gas available for injection is not limited.

Once the efficiency of gaslift has been proved, optimization of gaslift must be considered.

Different gas injection rates have been tested out to see, how liquid production will be changed due to it. Gas injection rate range was selected to be 0-2,1 m3/s (0-181440 m3/d). Based on that range, liquid flow rate was calculated, as well as gaslift operating pressure at the gas injection valve. The results can be observed below:

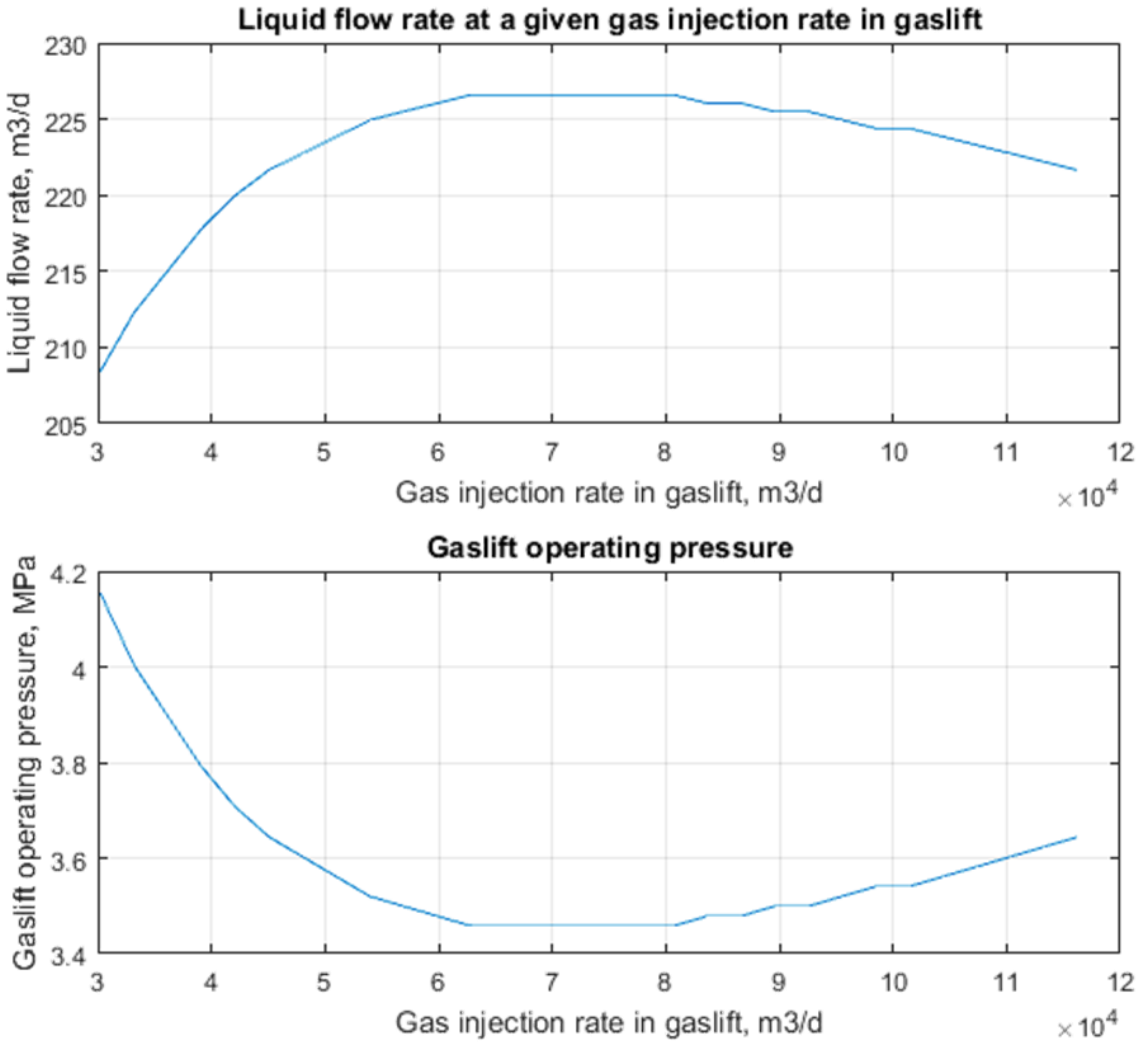

Figure 25 - Liquid production and gas lift operating pressure vs. gas injection rate

Figure 10 represents liquid production and gas lift operating pressure vs. gas injection rate. Analyzing the plot it can be concluded, that for given conditions the minimum amount of injected gas when the well can produce reservoir liquid is equal to approximately 35000 m3/d that gives 208 m3/d of liquid. Gaslift operating pressure is maximum and equals to 4,15 MPa. Further, as amount of injected gas increases, amount of produced liquid increases as well, as mixture density becomes lower. The maximum liquid production can be reached in the range of 65000-85000 m3/d of gas injection rate and equals to 226,6 m3/d at operating pressure 3,46 MPa. *That is the optimal regime of gaslift at which maximum amount of liquid can be produced.*

As the amount of gas increases even more, efficiency of gaslift falls down due to higher gas-oil slip ratio and higher friction losses. Eventually, at a certain rate (2,1 m3/s or 181440 m3/d) friction losses are so high that the well stops producing.

5 Experimental part

5.1 Experimental setup and method

The goal of the planned experimental work is to simulate continuous gas lift by means of injection gas in a vertical pipe at the laboratory at the University of Stavanger. The first step is to mount all necessary equipment and to make preparation works in the laboratory loop for the experiments.

The prime part of the experiment is installation of a new flowmeter from Alicat Company, which allows to measure a high range of gas rates- from 0 to 50 standard liters per minute (SLPM) with high precision at very small gas rates, which is a zone of the highest interest for the experiments; installation of a new Sensirion SQT-QL500 liquid flowmeter with measuring limits up to 120 milliliters per minute for water with extremely high precision. Then it is planned to measure gas injection rates and liquid rates. As a result, a production curve along with other parameters is to be obtained.

After the research has been taken on previous experience, full understanding of numerical simulation and experiments was obtained.

This chapter presents the experimental setup, improvements and measuring procedures executed on the gas-lift model.

Gas-lift model

Gas lift model is illustrated in Figure 26:

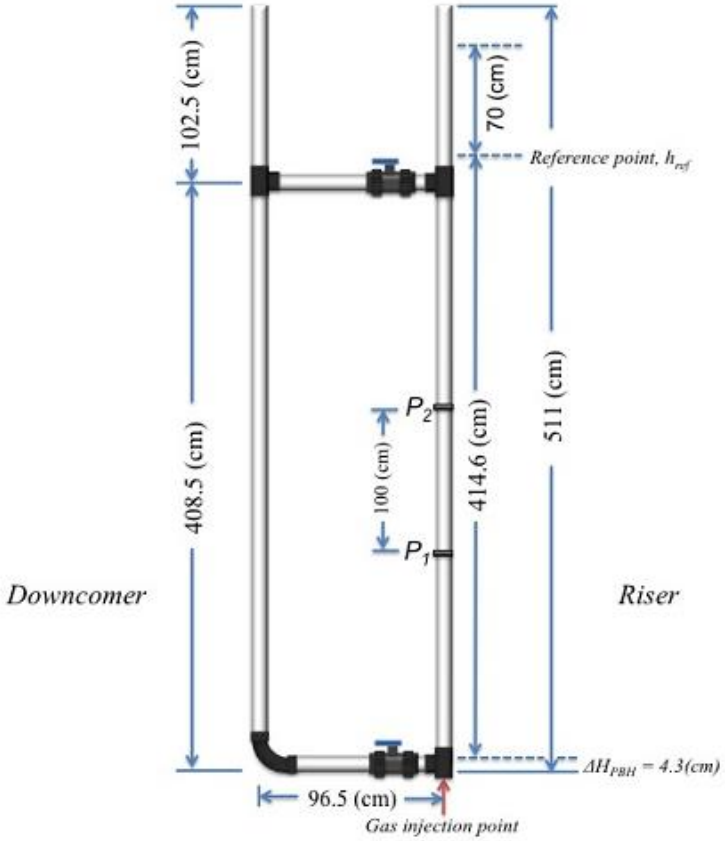

Figure 26- Illustration of the gas-lift model (Ostvold & Marvik, 2014)

It is comprised of two vertical pipes. The vertical pipe on the left hand side is called the downcomer, the one on the right hand side is called the riser. The horizontal pipes are distinguished by their vertical placement (upper and lower). The two pressure taps measure differential pressure, they are placed in the riser on the distance of 1 meter from each other.

The acrylic pipes have an inner diameter of 4.0 cm and outer diameter, 5.0 cm. The two vertical pipes are arched with two parallel horizontal pipes of a smaller size. There is a gas injection point in the lower horizontal section of the loop where gas can be injected at different rated by changing them by a gas flowmeter (Ostvold & Marvik, 2014).

Measuring procedure

Data logging method

Data logging system is shown on Figure 27:

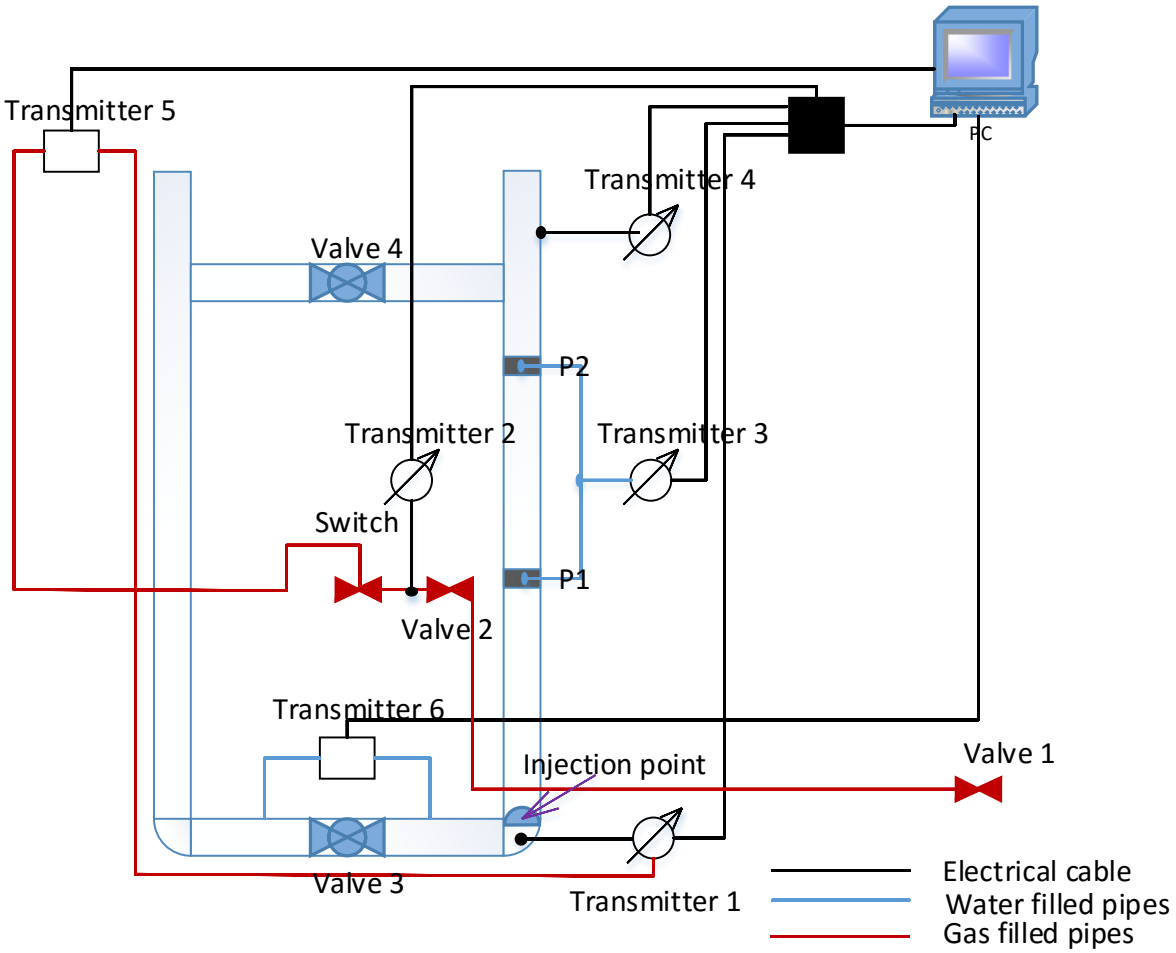

Figure 27- Flowchart of the data logging setup

Data logging components are shown in Appendix B. Figure 27 represents a flow chart of the data logging setup. The black lines, connecting various transmitters to the computer, show electrical cables here. Gas pipes are shown by the red lines, which supply the injector with gas flow from the compressor and pipes, leading to the Alicat gas flowmeter. Water filled pipes are represented by the blue lines, that are connected to the Sensirion liquid flowmeter and differential pressure manometers.

Transmitter 1 and 2 are Crystal Digital test Gauge XP manometers that measure the bottomhole pressure and the inlet gas pressure respectively. Transmitter 3 is a Rosemount transmitter 3051C, which measures the differential pressure between P_1 and P_2. The pressure taps are positioned 1 meter apart. Transmitter 4 is Rosemount transmitter, which measures the atmospheric pressure. Transmitter 5 is Alicat gas flowmeter, the inlet of which is connected to the switch after the valve 2 and the outlet in connected to the Transmitter 1. Transmitter 6 is Sensirion SQL-QT500 liquid flowmeter that measures the liquid flow from the downcomer to the riser, when there is injection of gas through the injection point.

Compressed air is delivered through the valve 1. Valve 2 is the inlet gas regulator. It was fully open during the experiments. Then the gas is directed into the switch. Switch is a three-way valve. If the switch is positioned in direction 1, the gas line is closed; in direction 2 gas is bled into the atmosphere; in direction 3 gas enters further to the transmitter 5.

The gas comes dried before it reaches the transmitter 5 (flow meter), the gas injection rate is measured and logged. The switch is positioned towards “gaslift”. Gas quantity is regulated by the Alicat flowmeter and transmitter 2 logs the inlet gas pressure. Bottomhole pressure is continuously logged by transmitter 1. The injected air creates bubbles in the lower part of the riser. Differential pressure is measured between P_1 and P_2. The air injected into the pipe reduces the density of the flow forcing the mixture to flow along the loop. Valve 3 is closed, allowing liquid to flow through the transmitter 6 liquid flowmeter. It sends the measured signal to the computer.

5.2 Preparation for experiments

As stated in the previous work, Bronkhorst gas pressure measurer was inadequate for the project (Ostvold & Marvik, 2014). There was a need for a new gas flowmeter. So, a flowmeter from Alicat Company had been chosen. The advantage of this flowmeter was measuring fluid flow at very low rates up to 50 SLPM (standard liters per minute) and high precision. For this purpose the decision had been made to mount the flowmeter.

The flowmeter installation procedure consisted of several steps. First, appropriate mounting materials had to be chosen. The flowmeter mounted on an aluminum rectangle plate by four screws. The plate by itself was mounted on an aluminum beam by two screws. Appropriate holes were drilled. Finally, the installation was mounted to the laboratory loop at the level higher the liquid level in order to avoid possible water penetration into the flowmeter.

The experimental loop was filled up with water solution. It has been drained and filled up again for several reasons:

- The loop has not been used for long time, liquid condition was moderate;
- It turned out, that water was diluted with another substance. In the current experiment water properties were required from the liquid;
- In previous experiments air was injected from a needle, which limited the required range for the following experiment. In order to detach the needle, water had to be drained.

After the experimental setup was dewatered, the Alicat gas flowmeter was connected to the setup by thin acrylic pipes. The inlet of the flowmeter was connected by a 9 meters long pipe to the “P-inn” (Inlet pressure) gauge node, the outlet was connected by a 7 meters long pipe to the “P-bunn” (bottomhole pressure node). Necessary screw connections were sealed with Teflon tape.

Liquid flow is measured by a Sensirion SLQ-QT500 model flowmeter (see Appendix B, Figure 43), it features a flow range up to 120 ml/min for water-based liquids. The whole fluidic path is straight and there are no obstacles or moving parts in the sensor. The flowmeter is based on a thermal micro sensor technology; it possesses the short response time and high precision.

It was decided to install the liquid flowmeter in the lower horizontal section of the loop at two points on the outer sides of the valve. In order to perform measurements, the valve must be closed, so that water will run through the flowmeter, serving as a bypass.

In order to mount the liquid flowmeter, two orifices in the lower horizontal pipe were to be drilled. The pipe is made of 0,5 mm thick acrylic material, which is difficult to work with due to its fragility. So, first, a peace of soft-plastic around 0,5 mm thick material was glued with silicon to the pipe at the desired place to drill, so that the thickness (now 1 cm) could be sufficient for the drilling operation and further adapter screwing . After the lapse of approximately 24 (needed for the silicon to harden) the pipe was drilled with a 3,5 mm thick drill throughout its the whole thickness and then with a 8,5 mm thick drill to the depth of 0,5 mm. Later a thread maker was used inside the two orifices. Finally, two adapters were sealed with a Teflon tape and screwed in the holes by 4 turns (this value must not be exceeded due to the depth of the tread). The flowmeter was connected to the loop by these adaptors.

After all measuring tools and equipment were installed, a proper logging system must be used. For these purposes there was a need in a computer with logging software. First, a horizontal platform, serving as a desk had to be made. It was made out of a wooden plate and a metal beam, bounded with nuts by the author. The deck was mounted by two metal plated to vertical railings on the wall behind the setup. The PC, the keyboard and the mouse then stood on that desk. The monitor was screwed into the wall by two screws.

Much time have been spent on launching the PC due to some unknown failure. Eventually, the computer had been launched and the engineer Svein Myhren helped the author to install LabVIEW software, connect all logging systems into the PC (namely, Alicat flowmeter, Sensirion flowmeter). All pressure gauges were connected to a wire box with a USB outlet, also connected to the computer. The detailed scheme of the LabVIEW logging system can be found in Appendix B, Figure 49.

By that time the experimental loop was ready to use. It was again filled with water. Few leakages were discovered and fixed with silicon.

5.3 Experiments

The experiment consists of measuring gas and liquid flowrates along with the other gauges readings for series of steady-state flow. Each series represents a constant gas injection rate within the interval 0,05-5 SLPM (standard liters per minute). The gas injection rate is controlled from the LabVIEW.

The goal of the experiment is to obtain plots of liquid production and other parameters vs. gas injection rate. In order to understand how the experimental data is obtained, let us have a closer look at the LabVIEW interface:

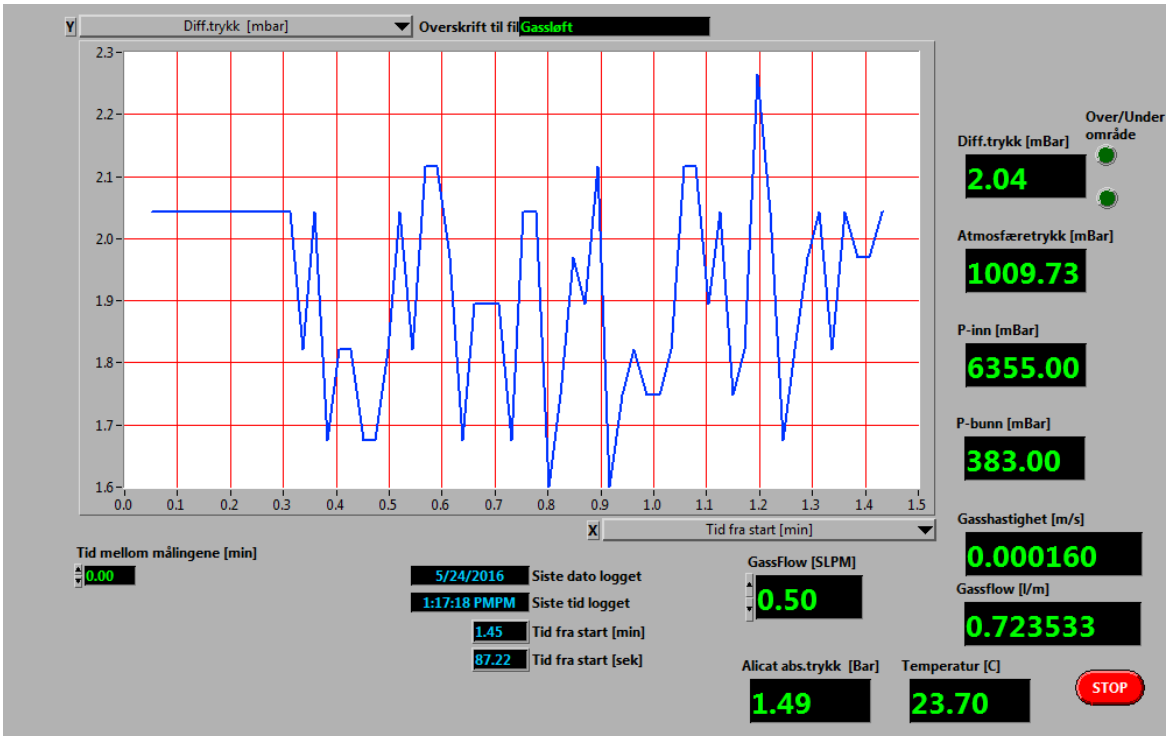

Figure 28- LabVIEW interface

The series of parameters is being logged into the program in real time:

- "Diff. trykk"- Differential pressure in mBar;
- "Atmosfæretrykk"- Atmospheric pressure, mBar;
- "P-inn"- Gas injection pressure in mBar;
- "P-bunn"- Bottomhole pressure in mBar;
- "Gashastighet" and "Gassflow" are not valid;
- ""Gassflow [SLPM]"- Gas flow in SLPM;

- "Alicat abs.trykk"- Alicat outlet pressure in Bar;
- "Temperatur"- Ambient temperature in C measured by the Alicat flowmeter;
- "Tid mellom målingene"- Time interval between the measurements.

Each parameter can be shown in the real-time diagram in the program.

The measured values are saved into a file (that can later be opened with Notepad or MS Excel).

Liquid flowmeter is being logged into another program, provided by the developer. The interface is shown below:

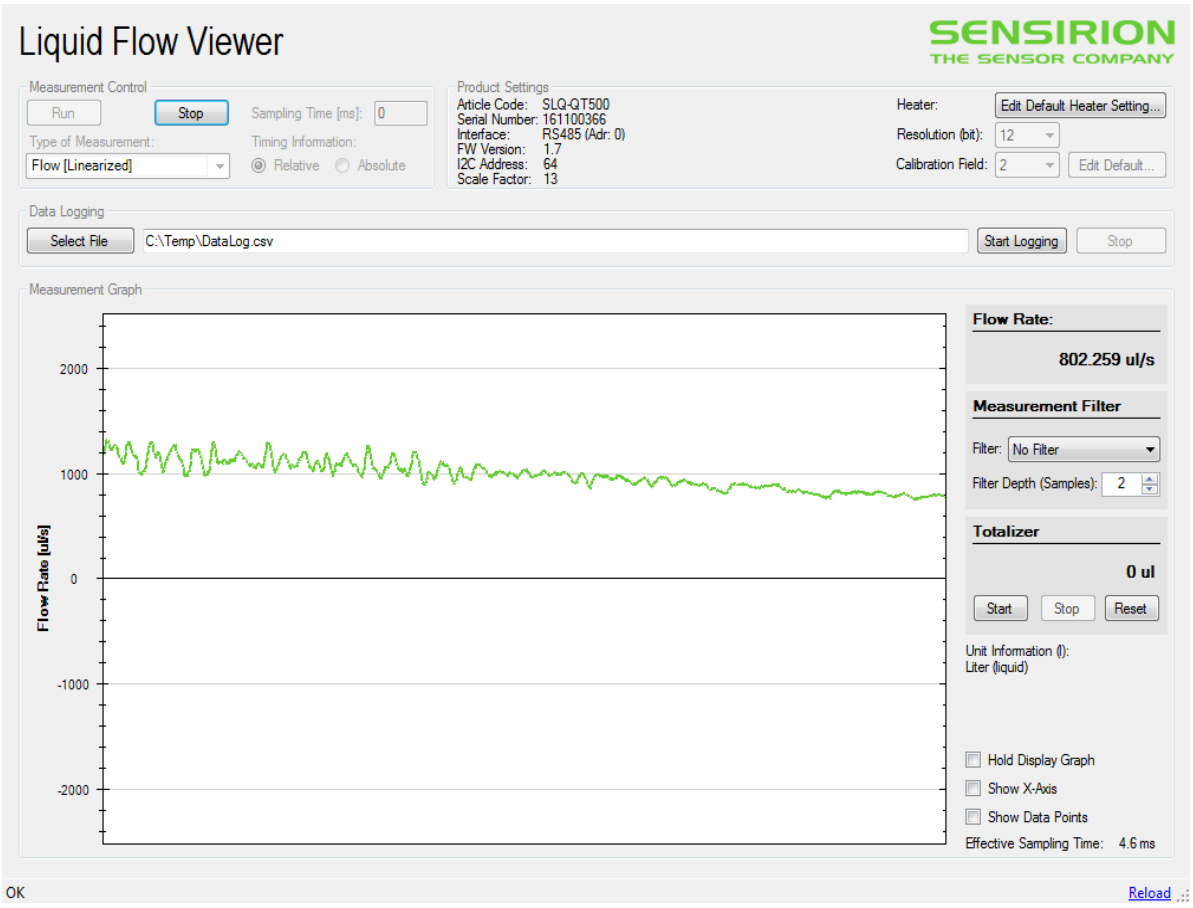

Figure 29- Sensirion program interface

Before running the program, the parameter "Calibration Field" was set to 2, which means the measurements have been calibrated for water (it could also be changed to "0" meaning alcohol as the liquid)

The logging data- the flowrate in microliters per second is displayed in the diagram in real-time. Sampling time can be controlled manually. It has been chosen to be 200 ms (0,2 sec) during the experiments.

The measured values are saved into an Excel file.

Three sets of experiments were carried out. The first set of experiments was rejected due to incorrect results of liquid flow values (the reason is explained in the Chapter 6). In the second experiment gas rate was increased from the lowest value to the highest value and in the third experiment it was decreasing respectively to observe possible hysteresis. There were 40 series of measurements during the experiments for the gas injection rates in the range of 0,01-5 SLPM. Each series was from 1 to 2 minutes long. This time is sufficient to establish steady state flow and to obtain representative samplings.

The considered range is covers the desired range and is limited by the maximum capacity of the liquid flowmeter and by the gas pipes small diameter and long total lengths, which leads to high friction losses at high gas rates.

A series of pictures have been taken for different gas injection rates. They represent flow patterns inside the vertical pipe:

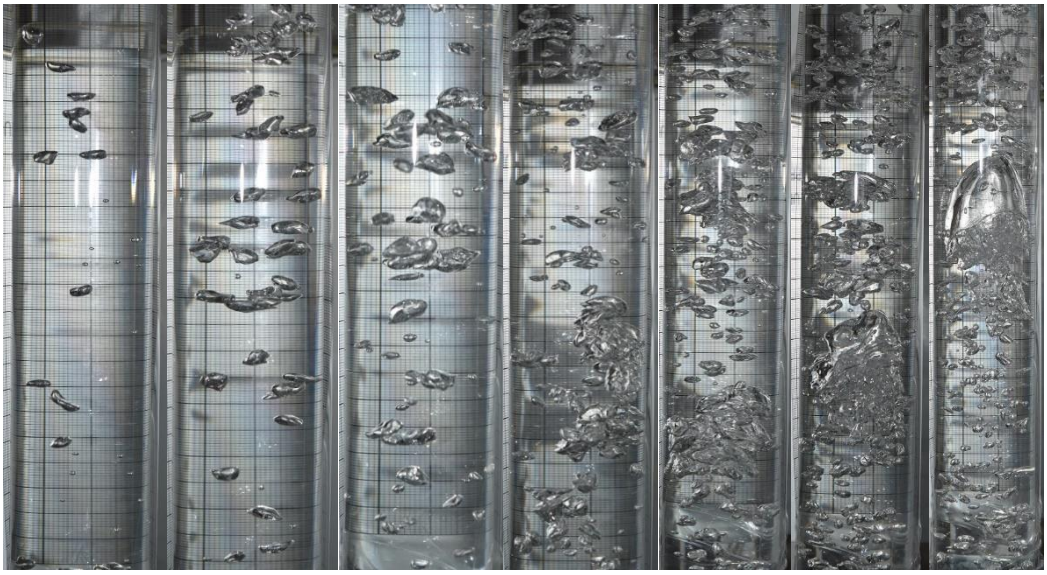

Figure 30- Flow pattern at 0,2; 0,5; 1,0; 1,5; 2,0; 2,5; 3,0 SPLM of gas (air) respectively

It can be seen that at low gas velocities gas bubbles are evenly distributed along the flow. Then while the gas injection rate increases, bubbles start to coalesce and eventually form a Taylor bubble, that can be observed at the 3,0 SLPM gas rate.

After the experimental data was obtained, it then needed to be processed in MS Excel. The main difficulty in data processing was the fact that it was logged into two different files. These files were united into one Excel file, based on the same time intervals for different time series.

5.4 Experimental data processing

The experimental data has to be processed in order to obtain representative information shown in a table or in a plot. A standard procedure of processing of multiple direct measurements has been performed in order to calculate a confidence interval and a relative error for series of measurements of liquid flow rate and other parameters.

Average value of the measurement (for example, liquid flow rate) is calculated by:

$$\overline{Q_{liq}} = \frac{1}{n}\sum_{i=1}^{n} Q_{liq.i} \tag{5.1}$$

Where

$Q_{liq.i}$ is an i-th measurement of a series;

n is number of readings within one series.

Standard deviation is calculated by:

$$S_{\overline{Q_{liq}}} = \sqrt{\frac{\sum_{i=1}^{n}(Q_{liq.i} - \overline{Q_{liq}})^2}{n(n-1)}} \tag{5.2}$$

Average deviation from the mean is calculated by:

$$\overline{S_{\overline{Q_{liq}}}} = \frac{S_{\overline{Q_{liq}}}}{\sqrt{N}} \tag{5.3}$$

Where “N” is number of degrees of freedom, taken as 10;

With the help of Excel’s standard functions, *Student’s distribution* is calculated:

$t_{\alpha,\mathrm{x}}$ =T.DIST(x, degrees_freedom-1),

Where “x” is probability:

$$x = 1 - 0,95 = 0,05; \tag{5.4}$$

“degrees_freedom” is number of degrees of freedom;

Confidence interval is calculated by:

$$\Delta_{\overline{Q_{liq}}} = t_{\alpha,\mathrm{x}}\,\overline{S_{\overline{Q_{liq}}}} \tag{5.5}$$

Finally, *relative error* is given as:

$$\varepsilon_{Q_{liq}} = \frac{\Delta_{\overline{Q_{liq}}}}{\overline{Q_{liq}}} \tag{5.6}$$

A series of tables were obtained based on the previous calculation. As a result, they were depicted in several plots, discussion of which is given below in the “Result and Discussion” Chapter.

6 Experiments' results and discussion

6.1 Discussions of experiment's results

The experimental data was processed in the forms of tables. As an example, tables for liquid flow vs. injected gas rate for two experiments are given in the Appendix C. However, it may be more clearly presented by diagrams.

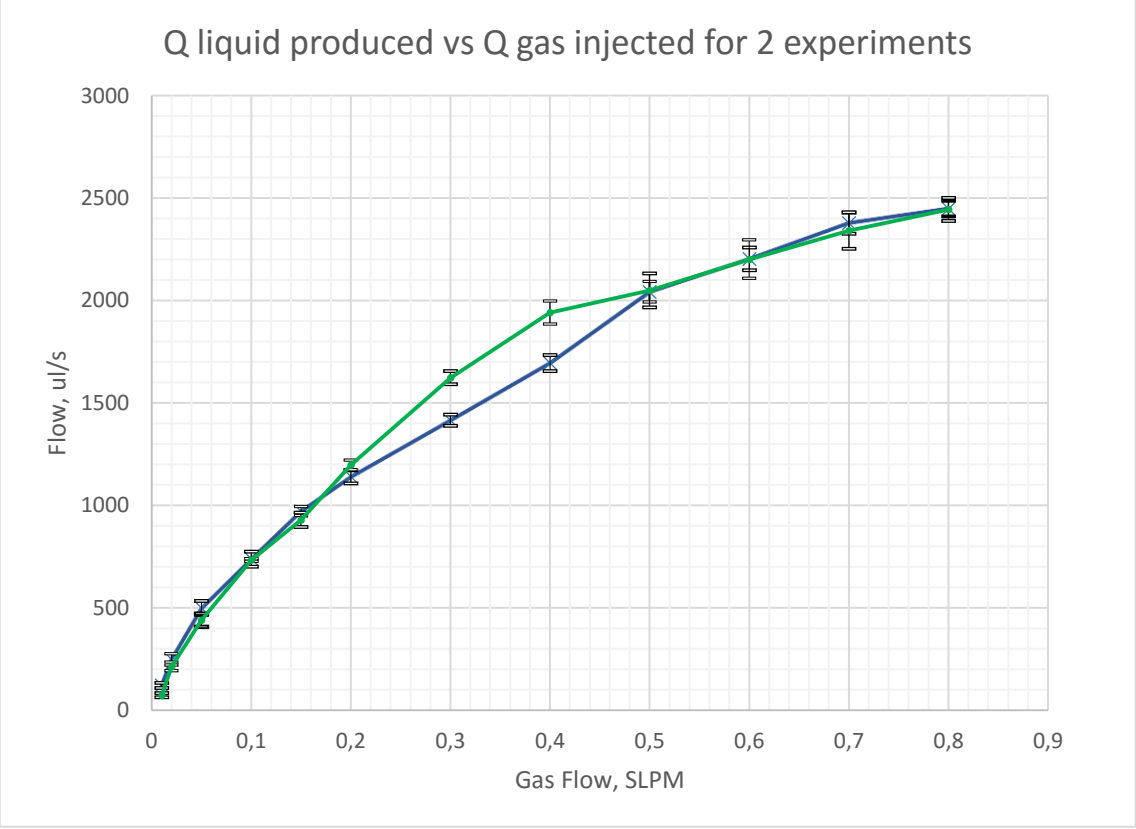

Figure 31- liquid rate as a function of gas injected into the system

The given plot describes the mean value of liquid rate as a function of gas injected into the system for two experiments (experiment 1 in blue and experiment 2 in green respectively). The confidence intervals are given by black vertical lines.

It can be clearly seen that the liquid flow has a strong growing trend. The minimum liquid flow is around 120 microliters per second (mcLPS) at 0,01 SLPM gas injection rate. It rapidly increases with the increase of gas rate up to 1 SLPM reaching the 2440 mcLPS value.

It is interesting to notice, that the relative error range is linearly decreasing with the growth of gas rate. For instance, the value of the relative error at 0,01 SLPM is equal to 10 % and 2 % at 1 SLPM of gas respectively.

The experiment has not covered the full expected gas range, when the curve would bend and go down due to gas slip and frictional losses in the production pipe due to insufficient gas injection pressure and/or high frictional losses in the gas pipes. Liquid flowrate values were limited by the liquid flowmeter capacity, which is 2500 microliters/s (120 ml/min); this value were reached at gas injection rate 0,9 SLPM. However, for other measurements from pressure gauges the gas injection rate range was increased to 5 SLPM.

Let us take a closer look at other equally important graphs:

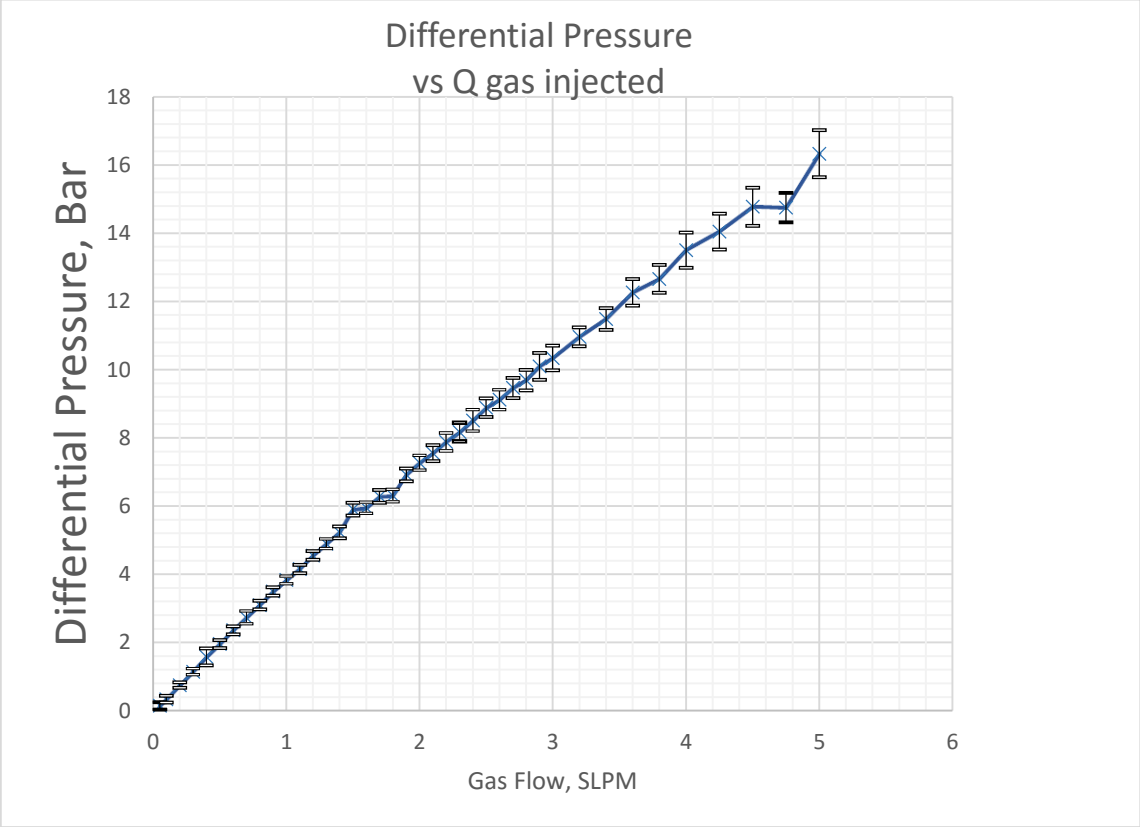

Figure 32- differential pressure as a function of gas injected into the system

The given plot describes differential pressure as a function of gas injected into the system. Similarly to the previous plot, the mean value for each measurement is given by crosses, the confidence intervals are given by black vertical lines.

As can be seen, the differential pressure is linearly dependent on gas flowrate and reaches 18 Bar at 5 SLPM of gas. The uncertainty also grows with the increase of gas flow and reaches 0,7 bar at 5 SLPM.

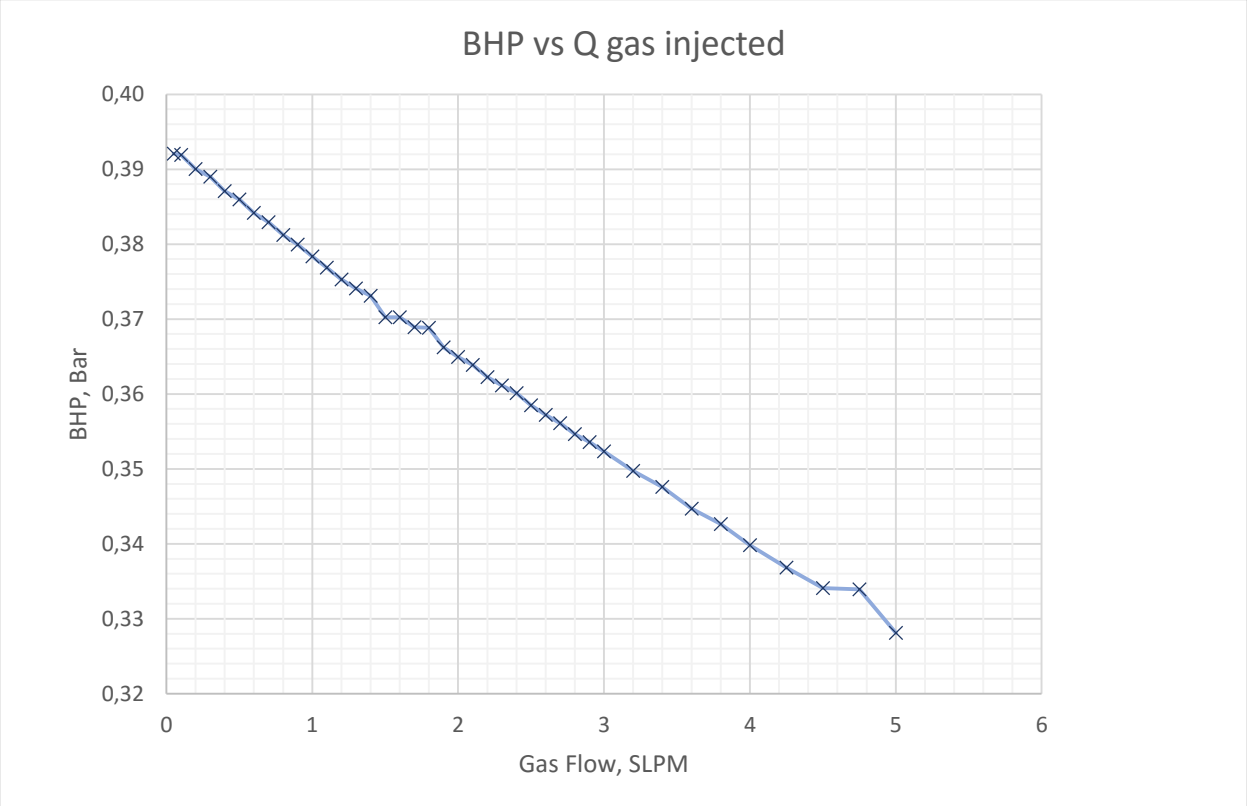

Figure 33- Bottomhole pressure as a function of gas injected into the system

Figure 33 depicts the bottomhole pressure as a function of gas injection rate. A clear trend can be seen here. Bottomhole pressure linearly decreases while more gas is being injected into the system. The maximum value is 393 mBar, which is the weight of the liquid column without gas; the minimum value of 328 mBar is at the highest gas rate respectively.

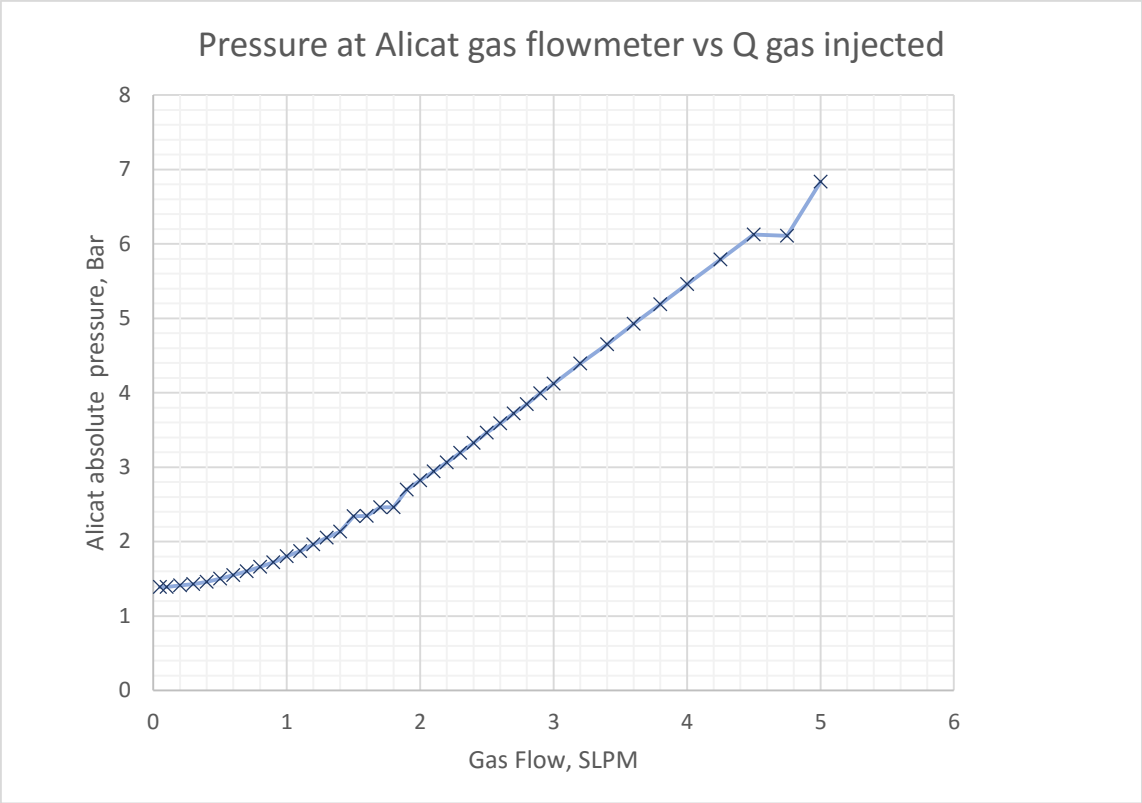

Figure 34- Alicat absolute gas pressure as a function of gas injected into the system

Finally, the given plot represents Alicat absolute gas pressure as a function of gas injected into the system. According to the documentation, it should not exceed 10 Bar. In the following case at the lowest rates the pressure was a little higher than the atmospheric (1,39 Bar) and steadily grew with the increase of gas injection rates, reaching the maximum value of 6,84 Bar at 5 SLPM. The experimental systematic error was minimum for these measurements.

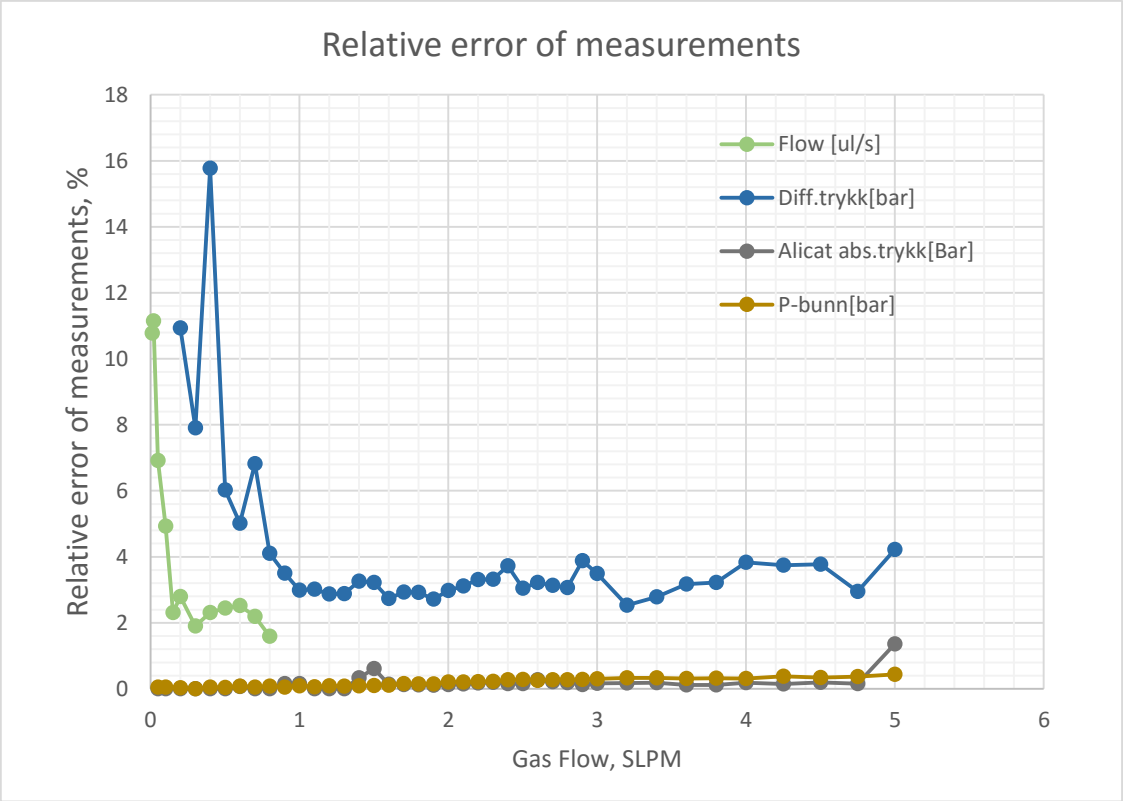

Figure 35- Relative errors for different measurements

It is worth considering the relative errors for the 4 cases. The least presice measuring imstruments were differential pressure gauge and the flowmeter readings. Their behaviour is similar in principle. Differential pressure gauge gives uncertain results at low gas flowrates, having an initial instrumental error (which is around 0,09 Bar). Thus, when the gauge reading reach higher values (16 Bar at the end), the relative error stabilizes at the level of 3-4 per cent. Sensirion liquid flow meter's relative error is also inverely proportional to the gas flow rate, from around 10% for low gas rates to satisfactory 2 %. The other flow parameters have very low measurment relative error of less than 1 percent.

6.2 Results comparison

Now, when the experimental part have been analyzed, a comparison must be done between the experimental values of the liquid flow flowrate and the calculated ones.

The idea of the following section is calculation of liquid flow and further comparison with the factual liquid flow, obtained from the Sensirion flowmeter readings. The calculation process is based on the Bernoulli's equation for a simple section of pipe, one phase non-compressible liquid. It is reduced to the following form:

$$H + \frac{P_1 - P_2}{\rho g} = \frac{v^2}{2g}(\lambda \frac{L}{D} + \sum \xi) \quad (6.1)$$

Where:

H is height difference;

$\varphi_o, \varphi_w, \varphi_g$ is oil, water and gas fractions respectively;

P_1, P_2 is pressures at the pipe's ends;

ρ - is fluid density;

v is fluid flowrate;

L - is pipe length;

D is pipe diameter;

λ - hydraulic friction coefficient;

$\sum \xi$ - local friction loses.

Experiments were carried out for low liquid rates, the Reynolds numbers do not exceed 600 value, the flow is laminar. Using the formula:

$$\lambda = \frac{64}{\mathrm{Re}} \quad (6.2)$$

And neglecting local friction loses, the Bernoulli's equation is converted to (in terms of liquid flow):

$$Q = \frac{\pi D^4 \Delta P}{128 \mu L} \quad (6.3)$$

Where:

ΔP - is pressure drop $P_1 - P_2$;

μ - liquid viscosity.

Hereafter it is considered, that liquid flow is measured in the lower horizontal pipe of the loop from left to right. Boundary pressures are measured by a pressure gauge "P_bunn" (bottomhole pressure) at the lower section of the right vertical pipe. P1 is hydrostatic water column pressure when no flow is observed. Since the two vertical pipes are communicating vessels, the pressure at the lower left corner of the loop is also equal to P1. P2 is pressure measured by the pressure gauge when injecting gas and it is the pressure on the right boundary. Bernoulli's equation

is then applied for a section of the pipe where the flowmeter is installed with the pressures at the end P1 and P2 respectively:

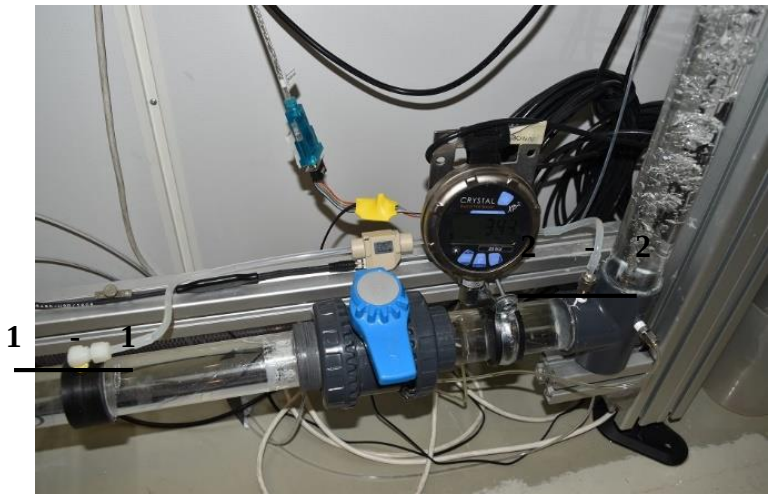

Figure 36-Section of the pipe, to which Bernoulli's equation is applied

Hydrostatic drop is taken as zero due to the horizontal flow. Pipe inner diameter is 3 mm and length is 70 cm (36 cm of the flowmeter length and 17 cm of flexible pipes with adapter on two sides). During the experiments, pure water was used, hence viscosity is 1 mPa*s.

A series of liquid flow rates for the given section of the pipe for different pressure drops was calculated. Since the dependency between the bottomhole pressure and the gas injection rates is known from the previous section, a plot "Liquid production versus gas injection rates" can be built for experimental and calculated values of liquid flow:

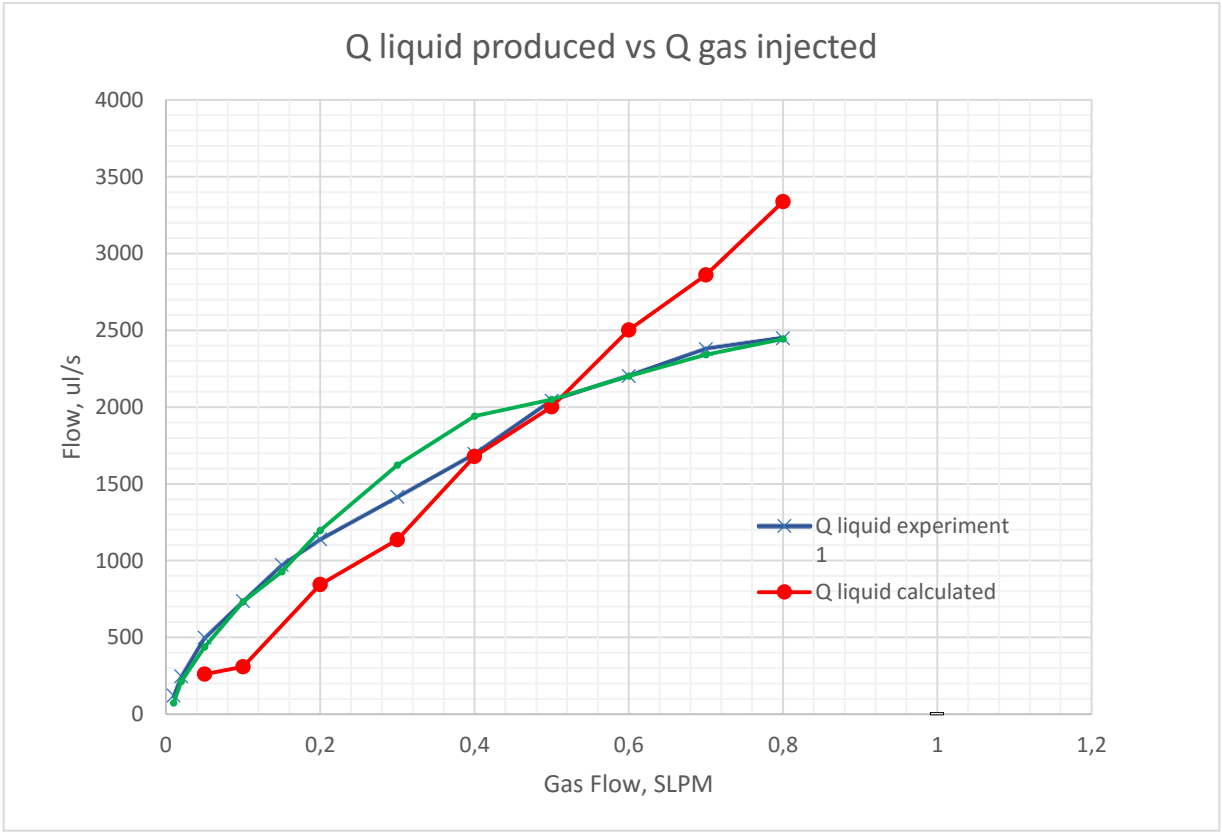

Figure 37-Comparison of calculated values of liquid flowrate and the factual value, obtained during the experiments

In Figure 37 the comparison of theoretical values of liquid flowrate and the factual value, obtained during the experiments is shown. The theoretical liquid flow is in red color and is based on the theory, given above. The experimental values are shown in blue and green color for experiment 1 and 2 respectively.

The theoretical line of flowrates is linearly dependent on the pressure drop due to laminar flow. The pressure drops linearly depend on the bottomhole pressure, which, in its tern, linearly depends on the gas injection rate as can be seen from the previous section. Thus, the line is close to a straight line.

The two experimental curves nearly coincide with each other, meaning good repeatable results. By looking at the plot it can be seen, that the experimental values and the theoretical values have some divergence. The author made an assumption, that there are local friction losses in pipe connectors due to sudden diameter change and bending of pipes. Since the linearity of the velocity profile in a cross-sectional area in laminar flow is based on the assumption, that the pipe has a constant diameter without sudden constriction and expansion, the flow during the experiments does not fully obey the laminar flow rules.

Distortion of measurements has been noticed, in case the presence of tiny gas bubbles, accumulation in the liquid flowmeter. Moreover, the very first experiments showed wrong results

(for example, the liquid rate at 5SLPM of gas rate was around 1400 microliters per minute; later the same value was reached at 0,25-0,35 SLPM), however the pattern of the curve strongly resembled the blue and the green curve on Figure 37. Here it can be concluded, that *the Sensirion liquid flowmeter gives low reliable results in case of presence of any amount of gas.*

The next plot is a reproduction of Figure 37 in terms of differential pressure:

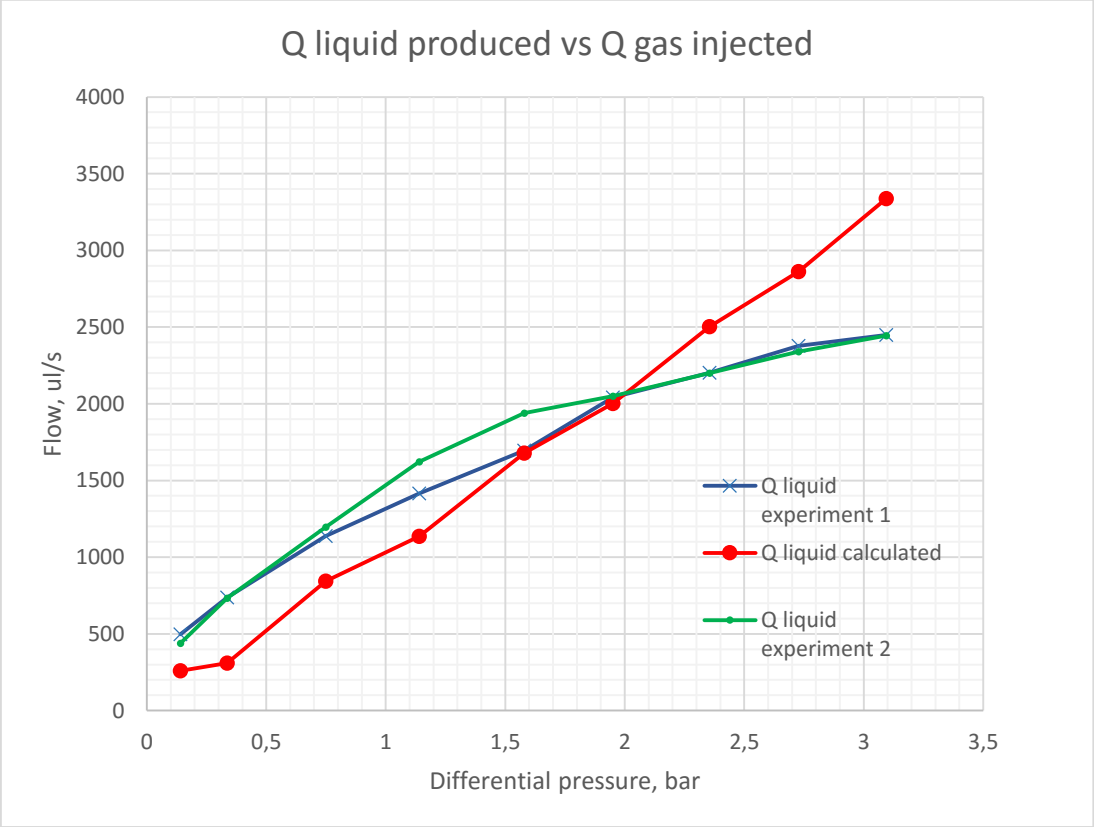

Figure 38- Comparison of calculated values of liquid flowrate and the factual value, obtained during the experiments as a function of differential pressure

In Figure 38 the x-axis is shown in differential pressure units. The differential pressure here is measured by the pressure gauge between two points in the riser and represents pressure difference between riser's and downcomer's column weight, which causes the flow. As in the previous plot, the liquid flow is directly proportional to the pressure drop.

7 Conclusion

In the present master's thesis a gas lift issue for a simple vertically inclined oil producing well has been considered. A program have been successfully developed, which describes multiphase flow behavior in a gas lift well. A step-by-step guide was created by the author. The strong points of this program is displaying all important parameters of the flow, such as PVT properties of reservoir fluid, flow regimes and dynamic parameters for any local point in a well, as well as building pressure curves in tubing string and annulus space for a given gas injection rate. Thus, these options make the program suitable for studying purposes. Numerical implementation makes the calculation process fast and simple for the user. Division the program into several functions makes it easy to add new PVT correlations if necessary.

Simulation in the program proved that liquid production rate changes depending on gas injection rate. It has been show, that at the certain moment (at gas rates higher that 83000 Sm3/day for a given well) the increase of gas rate leads to liquid production decrease due to friction and slip energy loses.

The existing experimental gas lift loop in the UiS laboratory was modified. The new gas flow meter from Alicat company and Sensirion liquid flowmeter were mounted on the loop. The author also install a PC-station for monitoring flow parameters.

Experiments were carried out for a simplified case, where reservoir liquid was replaced with water and natural gas was replaced with air, the well was represented by a vertical pipe. Two sets of experiments covered gas injection rate 0-5 SLMP and liquid rates up to 120 mLPM. The production curve (liquid rate versus gas injection rate) was obtained and compared with theoretical liquid flow values. It was concluded, that the curves have similar behavior; however, there is a small divergence due to local friction losses in flow, resulting in divergence from laminar flow regime and due to inaccuracy of the Sensirion liquid flowmeter related to presence of small amounts of gas in measured liquid flow.

8 Further work

- In this project only one set of correlations was used. It would be interesting to compare other correlation results.
- In simulation part only an open gas lift case was investigated. It is possible to modify the program for gas injection through injection orifices or valves or more complicated gas lift installation types.
- In the program only linearly inclined well was considered. In practice wells have more sophisticated shape. In the future works well inclination might be considered.
- In the experiments only simplified well loop was available, where reservoir liquid was replaced with water and natural gas was replaced with air, the well was represented by a vertical pipe. If possible, it is interesting to simulate more real conditions.
- In future the program might be developed into an independent software package for wide use on oilfields.

References

1. Lyapkov P. D., 1987. “ESP Selection to a Well” (in Russian). Gubkin University, Moscow.
2. Dunushkin I. I., Mishenko I. T., 1982. “Calculation of the Basic Properties of Reservoir Oils When Oil Production and Treatment” (in Russian). Gubkin University, Moscow.
3. Mishenko I. T., 2003. “Oil Production” (in Russian). Gubkin University, Moscow.
4. Takacs, G., 2005”Gas Lift manual”. Tulsa, Oklahoma.
5. Time, R. W., 2009. “Two-Phase Flow in Pipelines”. Course compendium, UiS.
6. Ostvold, T. D., Marvik, E., 2014. “Optimization of the Gas Lift Flow Loop”. Bachelor’s Thesis. UiS.
7. Gazizullin, E. R., 2014. “ESP Selection Program on the Example of Karakuduk Oilfield”. Bachelor’s Thesis. Gubkin University.
8. Szilas, A. P., 1985. “Production and transport of oil and gas”. 2nd Ed. Part A. Elsevier Publishing Co.
9. Barnea, D., 1987. “A Unified Model for Predicting Flow-Pattern Transitions for the Whole Range of Pipe Inclinations.” Int. J. of Multiphase flow. No. 1:1-12.
10. Vazquez- Roman, R., Palafox-Hernandez, P., 2005. “A New Approach for Continuous Gas Lift Simulation and Optimization”. SPE, 95949.
11. Chia, Y. C. and Sies Hussain, 1999. “ Gas Lift Optimization Effort and Challenges”. SPE, 5731.3
12. Wang.. P, and Litvak, 2004. “Gas Lift Optimization for Long-Term Reservoir Simulations”. SPE, 90506.
13. Bahadori, A., Ayatollahi, Ah., and Shirazz, M. , 2001. “Simulation and Optimization of Continuous Gas Litf System in Aghajari Oil Field”. SPE, 72169.
14. Pablano, E., Camacho, R. and Fairuzov Y. V., 2005. “Stability Analysis of Continuous-Flow Gas Lift Wells”. SPE, 77732.

15. Schlumberger Well Completions and Productivity. Chevron, 1999. Optimization Project. Gas Lift Design and Technology
16. James P. Brill, 1987. “Multiphase Flow in Wells”., U. of Tulsa, Journal of Petroleum Technology. SPE.
17. F. Zavareh, A.D., Hill and Podia, A.L., 1988. “Flow Regimes in Vertical and Inclined Oil/Water Flow in Pipes”. U. of Texas. SPE, 18215.
18. Stoisits, R.F. , 1992. “Dynamic Production System Nodal Analysis”, ARC0 Alaska Inc. SPE, 24791.
19. Griffith, P., 1984. “Multiphase Flow in Pipes”. Massachusetts Inst. of Technology.
20. Aliev, F. ; Dzhamalbekov, M. ; Il’yasov, M. 2011. :Mathematical Simulation and Control of Gas Lift”. Journal of Computer and Systems Sciences International, Vol.50(5), pp.805-814
21. Gimatudinov, S. K., 1983. “Manual for Oil Fields Exploitation Design” (in Russian). Gubkin University, Moscow.
22. Gimatudinov, S. K., 1974. “Handbook of Oil Production” ” (in Russian). Gubkin University, Moscow.
23. Buhalenko, E.I, Ibragimov, E. G., Kurbanov, N. G., Rasi-Zade, A. T., Jafarov, S. T., Baikov, N. M., Vershkova, V. V., 1983. “Handbook of Oilfield Equipment” (in Russian). Gubkin University, Moscow.
24. Trebin, G. F., Charigin, N. V., Obuhova, T. M., 1980 “Oils of the Soviet Union” (in Russian). Gubkin University, Moscow.
25. Shtof, M. D., 1974 “Calculation of the Properties of Reservoir Oils” (in Russian). Gubkin University, Moscow.
26. Agapova, E. G., 2012 “Experimental data processing in MS Excel: guidelines to perform laboratory work for full-time students “ (in Russian). Pacific State University, Khabarovsk.
27. Kurepin, V. V., Baranov, I. V. “Processing of the experimental data:Method. instructions to laboratory works for students of 1st, 2nd and 3rd year” (in Russian). Saint Petersburg State University of Refrigeration and Food Technologies, Saint Petersburg.

Appendices

Appendix A

Program code

main_file

```
clear % Start with clear command to delete old stuff
clc
clf

P_mtr = 1;
H_tub=1200;
P_res = 17.4;
Tf = 103 + 273.15;
G = 0.02;
Hf = 1607;

tetta = 0.2;
D_ann =157 / 1000;
K = 22;
kappa = 0.6;
P_l = 1.2;

D_tub = 68 / 1000;
Pnas = 8.5;
go_nas = 76.6;
ro_gSC = 1.333;
y_azot = 0.0339;
ro_oSC = 819.9;

beta_wSC = 60 / 100;
ro_wSC = 1120;
alpha_g = 0.15;
Qg_inj_SC(1)=0.35; %min gas injection rate
Qg_inj_SC0_max=1.38; %max gas injection rate

%-------------------------------------------------------------
% Calculation of coefficients for oil average density, viscosity, volume
factor and gas saturation calculations

[b_n_t_lin, ro_og_lin, g_om_t_lin, b_n_t_nas, ro_og_t_nas, g_om_t_nas]=
reaga(P_res, P_l, Tf, Pnas, go_nas, ro_gSC, ro_oSC, ro_wSC);
[ny,my,ny2,my2]=constPVT(g_om_t_lin, g_om_t_nas, P_l, Pnas) ;
n_g=ny;
m_g=my;

[ny,my,ny2,my2]=constPVT(b_n_t_lin, b_n_t_nas, P_l, Pnas) ;
n_b =ny;
m_b =my;

[ny,my,ny2,my2]=constPVT(ro_og_lin, ro_og_t_nas, P_l, Pnas) ;
```

```
n_ro = ny2;
m_ro = my2;

%Here are the values of the coefficients to have an idea, what they should
%look like (values given for the existing case)
%m_g=8.161;
%n_g=1.046;
%m_b=1.1341;
%n_b=0.0634;
%m_ro=764.627;
%n_ro=0.0328;
%m_mu =0.04;
%n_mu =1; %
m_mu =0.04; % No correlation has been found, assumed
n_mu =1; % No correlation has been found, assumed
%-----------------------------------------------------------------
%Calculation of pressure and temperature distribution curves along casing

x0(101)=0;
P_bh(1)=8;
y17=P_bh(1);
Ql_SC(1)=  K*(P_res - P_bh(1)) / 86400;
 %-----------------------------------------------------------------
%definition of resolution-strongly affects the speed of calculation process
%(recommended n_q=30 P_tol=0.025 for good results)
n_q=10; %number of steps- define precision
P_tol=0.025;
K_tol=1.1; % tolerance coefficient- increases calculation speed
 %-----------------------------------------------------------------

counter1=0;
for i_q=1:n_q
x0(101)=0;
P_bh(i_q)=8;
y17=P_bh(i_q);
Ql_SC(i_q)=  K*(P_res - P_bh(i_q)) / 86400;
    counter1=counter1+1;
    counter=0;
    while abs(x0(101)-P_l)>P_tol
        counter=counter+1;
        counter1=counter1+1;
        if x0(101) <0
            break
        end

    P_bh(i_q)=P_bh(i_q)- K_tol*P_tol;
    Ql_SC(i_q)=  K*(P_res - P_bh(i_q)) / 86400;
    a=P_mtr; % define minimum x value
    b=P_bh(i_q); % define maximum x value
    n=100;
    x(1)=b;
    b1=Tf; % define maximum x value
    x1(1)=b1;
    L_ann(1) = Hf / cos(tetta / 180 * pi);
    deltaL = Hf / 100;
    zone=1;
    gruppa=1;

    y1(1)=gas_saturation(x(1), m_g , n_g , Pnas , go_nas ) ;
    y2(1)=volume_factor(x(1), m_b , n_b , Pnas) ;
```

```
    y3(1)=oil_density(x(1), m_ro , n_ro , Pnas);
    y4(1)=oil_viscosity(x(1)  , x1(1)  , m_mu  , n_mu  , Pnas  , Tf    )  ;
    y5(1)=compressibility_factor(x(1)  , x1(1) , ro_gSC  , y_azot ,Pnas   )
;
    y6(1)=gas_density(x(1)  , x1(1)  , ro_gSC  , y_azot  , Pnas     )  ;
    y7(1)=volume_share(x(1) , beta_wSC , m_b , n_b , Pnas  ) ;
    [y81(1),y82(1),y83(1)]= production_in_situ_condition(1  , x(1)  , x1(1)
, P_res  , Tf  , G  , Hf  , tetta  , D_ann  , K  , kappa  , P_mtr  ,
Ql_SC(i_q)  , D_tub  , Pnas  , go_nas  , ro_gSC  , y_azot  , ro_oSC  ,
beta_wSC  , ro_wSC  , alpha_g  , m_g  , n_g  , m_b  , n_b  , m_ro  , n_ro  ,
m_mu  , n_mu  , gruppa  , P_mtr , Qg_inj_SC(i_q) );
    [y91(1),y92(1),y93(1),y94(1),y95(1)]=flow_rate(zone  , x(1)  , x1(1)  ,
P_res  , Tf  , G  , Hf  , tetta  , D_ann  , K  , kappa  , P_mtr  , Ql_SC(i_q)
, D_tub  , Pnas  , go_nas  , ro_gSC  , y_azot  , ro_oSC  , beta_wSC  , ro_wSC
, alpha_g  , m_g  , n_g  , m_b  , n_b  , m_ro  , n_ro  , m_mu  , n_mu  ,
gruppa  , P_mtr , Qg_inj_SC(i_q));
    y10(1)=surface_tension(zone  , x(1)  , x1(1)  , P_res  , Tf  , G  , Hf  ,
tetta  , D_ann  , K  , kappa  , P_mtr  , Ql_SC(i_q)  , D_tub  , Pnas  ,
go_nas  , ro_gSC  , y_azot  , ro_oSC  , beta_wSC  , ro_wSC  , alpha_g  , m_g
, n_g  , m_b  , n_b  , m_ro  , n_ro  , m_mu  , n_mu  , gruppa  , P_mtr  ,
Qg_inj_SC(i_q)  )  ;
    y11(1)=fluid_viscosity(zone  , x(1)  , x1(1)  , P_res  , Tf  , G  , Hf  ,
tetta  , D_ann  , K  , kappa  , P_mtr  , Ql_SC(i_q)  , D_tub  , Pnas  ,
go_nas  , ro_gSC  , y_azot  , ro_oSC  , beta_wSC  , ro_wSC  , alpha_g  , m_g
, n_g  , m_b  , n_b  , m_ro  , n_ro  , m_mu  , n_mu  , gruppa  , P_mtr ,
Qg_inj_SC(i_q) )  ;
    [y121(1),y122(1)]= type_and_structure(zone  , x(1)  , x1(1)  , P_res  ,
Tf  , G  , Hf  , tetta  , D_ann  , K  , kappa  , P_mtr  , Ql_SC(i_q)  , D_tub
, Pnas  , go_nas  , ro_gSC  , y_azot  , ro_oSC  , beta_wSC  , ro_wSC  ,
alpha_g  , m_g  , n_g  , m_b  , n_b  , m_ro  , n_ro  , m_mu  , n_mu  , gruppa
, P_mtr  , Qg_inj_SC(i_q)  )  ;
    [y131(1),y132(1),y133(1)]=fraction_share(zone  , x(1)  , x1(1)  , P_res
, Tf  , G  , Hf  , tetta  , D_ann  , K  , kappa  , P_mtr  , Ql_SC(i_q)  ,
D_tub  , Pnas  , go_nas  , ro_gSC  , y_azot  , ro_oSC  , beta_wSC  , ro_wSC
, alpha_g  , m_g  , n_g  , m_b  , n_b  , m_ro  , n_ro  , m_mu  , n_mu  ,
gruppa  , P_mtr  , Qg_inj_SC(i_q) ) ;
    y14(1)=pressure_gradient(zone  , x(1)  , x1(1)  , P_res  , Tf  , G  , Hf
, tetta  , D_ann  , K  , kappa  , P_mtr  , Ql_SC(i_q)  , D_tub  , Pnas  ,
go_nas  , ro_gSC  , y_azot  , ro_oSC  , beta_wSC  , ro_wSC  , alpha_g  , m_g
,n_g  , m_b  , n_b  , m_ro  , n_ro  , m_mu  , n_mu  , gruppa  , P_mtr ,
Qg_inj_SC(i_q)  );
    y15(1)=temperature_gradient(zone , G , Ql_SC(i_q) , D_ann , D_tub );
    [y161(1),y162(1)]= P_and_T(zone  , x(1)  , x1(1)  , P_res  , Tf  , G  ,
Hf  , tetta  , D_ann  , K  , kappa  , P_mtr  , Ql_SC(i_q)  , D_tub  , Pnas  ,
go_nas  , ro_gSC  , y_azot  , ro_oSC  , beta_wSC  , ro_wSC  , alpha_g  , m_g
,n_g  , m_b  , n_b  , m_ro  , n_ro  , m_mu  , n_mu  , gruppa  , P_mtr  ,
Qg_inj_SC(i_q),H_tub  )  ;
    y17=bottomhole_pressure(P_res  , Ql_SC(i_q)  , K    );

    for i=1:n
    L_ann(i+1) = L_ann(i) - deltaL;
        if  abs(L_ann(i)- H_tub)<=deltaL
        x0(1)=x(i);
        x01(1)=x1(i);
        end
    x(i+1)=y161(i);
    x1(i+1)=y162(i);
    y1(i+1)=gas_saturation(x(i+1), m_g , n_g , Pnas , go_nas ) ;
    y2(i+1)=volume_factor(x(i+1), m_b , n_b , Pnas) ;
    y3(i+1)=oil_density(x(i+1), m_ro , n_ro , Pnas);
```

```
    y4(i+1)=oil_viscosity(x(i+1)  , x1(i+1)  , m_mu  , n_mu  , Pnas  , Tf
)  ;
    y5(i+1)=compressibility_factor(x(i+1)  , x1(i+1) , ro_gSC  , y_azot ,Pnas
)  ;
    y6(i+1)=gas_density(x(1)  , x1(i+1)  , ro_gSC  , y_azot  , Pnas     )  ;
    y7(i+1)=volume_share(x(i+1) , beta_wSC , m_b , n_b , Pnas  ) ;
    [y81(i+1),y82(i+1),y83(i+1)]= production_in_situ_condition(zone  , x(i+1)
, x1(i+1)  , P_res  , Tf  , G  , Hf  , tetta  , D_ann  , K  , kappa  , P_mtr
, Ql_SC(i_q)  , D_tub  , Pnas  , go_nas  , ro_gSC  , y_azot  , ro_oSC  ,
beta_wSC  , ro_wSC  , alpha_g  , m_g  , n_g  , m_b  , n_b  , m_ro  , n_ro  ,
m_mu  , n_mu  , gruppa  , P_mtr , Qg_inj_SC(i_q) );
    [y91(i+1),y92(i+1),y93(i+1),y94(i+1),y95(i+1)]=flow_rate(zone  , x(i+1)
, x1(i+1)  , P_res  , Tf  , G  , Hf  , tetta  , D_ann  , K  , kappa  , P_mtr
, Ql_SC(i_q)  , D_tub  , Pnas  , go_nas  , ro_gSC  , y_azot  , ro_oSC  ,
beta_wSC  , ro_wSC  , alpha_g  , m_g  , n_g  , m_b  , n_b  , m_ro  , n_ro  ,
m_mu  , n_mu  , gruppa  , P_mtr, Qg_inj_SC(i_q) );
    y10(i+1)=surface_tension(zone  , x(i+1)  , x1(i+1)  , P_res  , Tf  , G  ,
Hf  , tetta  , D_ann  , K  , kappa  , P_mtr  , Ql_SC(i_q)  , D_tub  , Pnas  ,
go_nas  , ro_gSC  , y_azot  , ro_oSC  , beta_wSC  , ro_wSC  , alpha_g  , m_g
, n_g  , m_b  , n_b  , m_ro  , n_ro  , m_mu  , n_mu  , gruppa  , P_mtr  ,
Qg_inj_SC(i_q)  )  ;
    y11(i+1)=fluid_viscosity(zone  , x(i+1)  , x1(i+1)  , P_res  , Tf  , G  ,
Hf  , tetta  , D_ann  , K  , kappa  , P_mtr  , Ql_SC(i_q)  , D_tub  , Pnas  ,
go_nas  , ro_gSC  , y_azot  , ro_oSC  , beta_wSC  , ro_wSC  , alpha_g  , m_g
, n_g  , m_b  , n_b  , m_ro  , n_ro  , m_mu  , n_mu  , gruppa  , P_mtr ,
Qg_inj_SC(i_q) )  ;
    [y121(i+1),y122(i+1)]= type_and_structure(zone  , x(i+1)  , x1(i+1)  ,
P_res  , Tf  , G  , Hf  , tetta  , D_ann  , K  , kappa  , P_mtr  , Ql_SC(i_q)
, D_tub  , Pnas  , go_nas  , ro_gSC  , y_azot  , ro_oSC  , beta_wSC  , ro_wSC
, alpha_g  , m_g  , n_g  , m_b  , n_b  , m_ro  , n_ro  , m_mu  , n_mu  ,
gruppa  , P_mtr  , Qg_inj_SC(i_q)  )  ;
    [y131(i+1),y132(i+1),y133(i+1)]=fraction_share(zone  , x(i+1)  , x1(i+1)
, P_res  , Tf  , G  , Hf  , tetta  , D_ann  , K  , kappa  , P_mtr  ,
Ql_SC(i_q)  , D_tub  , Pnas  , go_nas  , ro_gSC  , y_azot  , ro_oSC  ,
beta_wSC  , ro_wSC  , alpha_g  , m_g  , n_g  , m_b  , n_b  , m_ro  , n_ro  ,
m_mu  , n_mu  , gruppa  , P_mtr , Qg_inj_SC(i_q)  ) ;
    y14(i+1)=pressure_gradient(zone  , x(i+1)  , x1(i+1)  , P_res  , Tf  , G
, Hf  , tetta  , D_ann  , K  , kappa  , P_mtr  , Ql_SC(i_q)  , D_tub  , Pnas
, go_nas  , ro_gSC  , y_azot  , ro_oSC  , beta_wSC  , ro_wSC  , alpha_g  ,
m_g  ,n_g  , m_b  , n_b  , m_ro  , n_ro  , m_mu  , n_mu  , gruppa  , P_mtr ,
Qg_inj_SC(i_q)  );
    y15(i+1)=temperature_gradient(zone , G , Ql_SC(i_q) , D_ann , D_tub );
    [y161(i+1),y162(i+1)]= P_and_T(zone  , x(i+1)  , x1(i+1)  , P_res  , Tf
, G  , Hf  , tetta  , D_ann  , K  , kappa  , P_mtr  , Ql_SC(i_q)  , D_tub  ,
Pnas  , go_nas  , ro_gSC  , y_azot  , ro_oSC  , beta_wSC  , ro_wSC  , alpha_g
, m_g  ,n_g  , m_b  , n_b  , m_ro  , n_ro  , m_mu  , n_mu  , gruppa  , P_mtr
, Qg_inj_SC(i_q), H_tub )  ;
    y17(i+1)=bottomhole_pressure(P_res  , Ql_SC(i_q)  , K    );
        if x(i+1) <= P_mtr %!!!!!!!!!!!!!!!!!!!!!!!!!!!!!!!!!! x(i+1) <=
1.28*P_l
            break
        end
    end


    %-------------------------------------------------------------
    %Calculation of pressure and temperature distribution curves along tubing
    n=100;
    L_tub(1) =H_tub/ cos(tetta / 180 * pi);
    deltaL = H_tub / 100;
    zone=0;
```

```
        y01(1)=gas_saturation(x0(1), m_g , n_g , Pnas , go_nas ) ;
        y02(1)=volume_factor(x0(1), m_b , n_b , Pnas) ;
        y03(1)=oil_density(x0(1), m_ro , n_ro , Pnas);
        y04(1)=oil_viscosity(x0(1)  , x01(1)  , m_mu  , n_mu  , Pnas  , Tf
)  ;
        y05(1)=compressibility_factor(x0(1)  , x01(1) , ro_gSC  , y_azot
,Pnas   )  ;
        y06(1)=gas_density(x0(1)  , x01(1)  , ro_gSC  , y_azot  , Pnas     )
;
        y07(1)=volume_share(x0(1) , beta_wSC , m_b , n_b , Pnas  ) ;
        [y081(1),y082(1),y083(1)]= production_in_situ_condition(1  , x0(1)  ,
x01(1)  , P_res  , Tf  , G  , Hf  , tetta  , D_ann  , K  , kappa  , P_l  ,
Ql_SC(i_q)  , D_tub  , Pnas  , go_nas  , ro_gSC  , y_azot  , ro_oSC  ,
beta_wSC  , ro_wSC  , alpha_g  , m_g  , n_g  , m_b  , n_b  , m_ro  , n_ro  ,
m_mu  , n_mu  , gruppa  , P_mtr , Qg_inj_SC(i_q) );
        [y091(1),y092(1),y093(1),y094(1),y095(1)]=flow_rate(zone  , x0(1)  ,
x01(1)  , P_res  , Tf  , G  , Hf  , tetta  , D_ann  , K  , kappa  , P_l  ,
Ql_SC(i_q)  , D_tub  , Pnas  , go_nas  , ro_gSC  , y_azot  , ro_oSC  ,
beta_wSC  , ro_wSC  , alpha_g  , m_g  , n_g  , m_b  , n_b  , m_ro  , n_ro  ,
m_mu  , n_mu  , gruppa  , P_mtr, Qg_inj_SC(i_q) );
        y010(1)=surface_tension(zone  , x0(1)  , x01(1)  , P_res  , Tf  , G
, Hf  , tetta  , D_ann  , K  , kappa  , P_l  , Ql_SC(i_q)  , D_tub  , Pnas  ,
go_nas  , ro_gSC  , y_azot  , ro_oSC  , beta_wSC  , ro_wSC  , alpha_g  , m_g
, n_g  , m_b  , n_b  , m_ro  , n_ro  , m_mu  , n_mu  , gruppa  , P_mtr  ,
Qg_inj_SC(i_q)  )  ;
        y011(1)=fluid_viscosity(zone  , x0(1)  , x01(1)  , P_res  , Tf  , G
, Hf  , tetta  , D_ann  , K  , kappa  , P_l  , Ql_SC(i_q)  , D_tub  , Pnas  ,
go_nas  , ro_gSC  , y_azot  , ro_oSC  , beta_wSC  , ro_wSC  , alpha_g  , m_g
, n_g  , m_b  , n_b  , m_ro  , n_ro  , m_mu  , n_mu  , gruppa  , P_mtr ,
Qg_inj_SC(i_q) )  ;
        [y0121(1),y0122(1)]= type_and_structure(zone  , x0(1)  , x01(1)  ,
P_res  , Tf  , G  , Hf  , tetta  , D_ann  , K  , kappa  , P_l  , Ql_SC(i_q)
, D_tub  , Pnas  , go_nas  , ro_gSC  , y_azot  , ro_oSC  , beta_wSC  , ro_wSC
, alpha_g  , m_g  , n_g  , m_b  , n_b  , m_ro  , n_ro  , m_mu  , n_mu  ,
gruppa  , P_mtr  , Qg_inj_SC(i_q)  )  ;
        [y0131(1),y0132(1),y0133(1)]=fraction_share(zone  , x0(1)  , x01(1)
, P_res  , Tf  , G  , Hf  , tetta  , D_ann  , K  , kappa  , P_l  , Ql_SC(i_q)
, D_tub  , Pnas  , go_nas  , ro_gSC  , y_azot  , ro_oSC  , beta_wSC  , ro_wSC
, alpha_g  , m_g  , n_g  , m_b  , n_b  , m_ro  , n_ro  , m_mu  , n_mu  ,
gruppa  , P_mtr , Qg_inj_SC(i_q)  ) ;
        y014(1)=pressure_gradient(zone  , x0(1)  , x01(1)  , P_res  , Tf  , G
, Hf  , tetta  , D_ann  , K  , kappa  , P_l  , Ql_SC(i_q)  , D_tub  , Pnas  ,
go_nas  , ro_gSC  , y_azot  , ro_oSC  , beta_wSC  , ro_wSC  , alpha_g  , m_g
,n_g  , m_b  , n_b  , m_ro  , n_ro  , m_mu  , n_mu  , gruppa  , P_mtr ,
Qg_inj_SC(i_q)  );
        y015(1)=temperature_gradient(zone , G , Ql_SC(i_q) , D_ann , D_tub );
        [y0161(1),y0162(1)]= P_and_T(zone  , x0(1)  , x01(1)  , P_res  , Tf
, G  , Hf  , tetta  , D_ann  , K  , kappa  , P_l  , Ql_SC(i_q)  , D_tub  ,
Pnas  , go_nas  , ro_gSC  , y_azot  , ro_oSC  , beta_wSC  , ro_wSC  , alpha_g
, m_g  ,n_g  , m_b  , n_b  , m_ro  , n_ro  , m_mu  , n_mu  , gruppa  , P_mtr
, Qg_inj_SC(i_q) ,H_tub)  ;
        y017=bottomhole_pressure(P_res  , Ql_SC(i_q)  , K    );
            for i=1:n
            L_tub(i+1) = L_tub(i) - deltaL;
            x0(i+1)=y0161(i);
            x01(i+1)=y0162(i);
            y01(i+1)=gas_saturation(x0(i+1), m_g , n_g , Pnas , go_nas ) ;
            y02(i+1)=volume_factor(x0(i+1), m_b , n_b , Pnas) ;
            y03(i+1)=oil_density(x0(i+1), m_ro , n_ro , Pnas);
            y04(i+1)=oil_viscosity(x0(i+1)  , x01(i+1)  , m_mu  , n_mu  ,
Pnas  , Tf    )  ;
```

```
            y05(i+1)=compressibility_factor(x0(i+1)  , x01(i+1) , ro_gSC  ,
y_azot ,Pnas   )  ;
            y06(i+1)=gas_density(x0(1)  , x01(i+1)  , ro_gSC  , y_azot  ,
Pnas    )  ;
            y07(i+1)=volume_share(x0(i+1) , beta_wSC , m_b , n_b , Pnas  ) ;
            [y081(i+1),y082(i+1),y083(i+1)]=
production_in_situ_condition(zone  , x0(i+1)  , x01(i+1)  , P_res  , Tf  , G
, Hf  , tetta  , D_ann  , K  , kappa  , P_l  , Ql_SC(i_q)  , D_tub  , Pnas  ,
go_nas  , ro_gSC  , y_azot  , ro_oSC  , beta_wSC  , ro_wSC  , alpha_g  , m_g
, n_g  , m_b  , n_b  , m_ro  , n_ro  , m_mu  , n_mu  , gruppa  , P_mtr ,
Qg_inj_SC(i_q) );

[y091(i+1),y092(i+1),y093(i+1),y094(i+1),y095(i+1)]=flow_rate(zone  , x0(i+1)
, x01(i+1)  , P_res  , Tf  , G  , Hf  , tetta  , D_ann  , K  , kappa  , P_l
, Ql_SC(i_q)  , D_tub  , Pnas  , go_nas  , ro_gSC  , y_azot  , ro_oSC  ,
beta_wSC  , ro_wSC  , alpha_g  , m_g  , n_g  , m_b  , n_b  , m_ro  , n_ro  ,
m_mu  , n_mu  , gruppa  , P_mtr, Qg_inj_SC(i_q) );
            y010(i+1)=surface_tension(zone  , x0(i+1)  , x01(i+1)  , P_res  ,
Tf  , G  , Hf  , tetta  , D_ann  , K  , kappa  , P_l  , Ql_SC(i_q)  , D_tub
, Pnas  , go_nas  , ro_gSC  , y_azot  , ro_oSC  , beta_wSC  , ro_wSC  ,
alpha_g  , m_g  , n_g  , m_b  , n_b  , m_ro  , n_ro  , m_mu  , n_mu  , gruppa
, P_mtr   , Qg_inj_SC(i_q))  ;
            y011(i+1)=fluid_viscosity(zone  , x0(i+1)  , x01(i+1)  , P_res  ,
Tf  , G  , Hf  , tetta  , D_ann  , K  , kappa  , P_l  , Ql_SC(i_q)  , D_tub
, Pnas  , go_nas  , ro_gSC  , y_azot  , ro_oSC  , beta_wSC  , ro_wSC  ,
alpha_g  , m_g  , n_g  , m_b  , n_b  , m_ro  , n_ro  , m_mu  , n_mu  , gruppa
, P_mtr , Qg_inj_SC(i_q) )  ;
            [y0121(i+1),y0122(i+1)]= type_and_structure(zone  , x0(i+1)  ,
x01(i+1)  , P_res  , Tf  , G  , Hf  , tetta  , D_ann  , K  , kappa  , P_l  ,
Ql_SC(i_q)  , D_tub  , Pnas  , go_nas  , ro_gSC  , y_azot  , ro_oSC  ,
beta_wSC  , ro_wSC  , alpha_g  , m_g  , n_g  , m_b  , n_b  , m_ro  , n_ro  ,
m_mu  , n_mu  , gruppa  , P_mtr   , Qg_inj_SC(i_q) )  ;
            [y0131(i+1),y0132(i+1),y0133(i+1)]=fraction_share(zone  , x0(i+1)
, x01(i+1)  , P_res  , Tf  , G  , Hf  , tetta  , D_ann  , K  , kappa  , P_l
, Ql_SC(i_q)  , D_tub  , Pnas  , go_nas  , ro_gSC  , y_azot  , ro_oSC  ,
beta_wSC  , ro_wSC  , alpha_g  , m_g  , n_g  , m_b  , n_b  , m_ro  , n_ro  ,
m_mu  , n_mu  , gruppa  , P_mtr , Qg_inj_SC(i_q)  ) ;
            y014(i+1)=pressure_gradient(zone  , x0(i+1)  , x01(i+1)  , P_res
, Tf  , G  , Hf  , tetta  , D_ann  , K  , kappa  , P_l  , Ql_SC(i_q)  , D_tub
, Pnas  , go_nas  , ro_gSC  , y_azot  , ro_oSC  , beta_wSC  , ro_wSC  ,
alpha_g  , m_g  ,n_g  , m_b  , n_b  , m_ro  , n_ro  , m_mu  , n_mu  , gruppa
, P_mtr , Qg_inj_SC(i_q)  );
            y015(i+1)=temperature_gradient(zone , G , Ql_SC(i_q) , D_ann ,
D_tub );
            [y0161(i+1),y0162(i+1)]= P_and_T(zone  , x0(i+1)  , x01(i+1)  ,
P_res  , Tf  , G  , Hf  , tetta  , D_ann  , K  , kappa  , P_l  , Ql_SC(i_q)
, D_tub  , Pnas  , go_nas  , ro_gSC  , y_azot  , ro_oSC  , beta_wSC  , ro_wSC
, alpha_g  , m_g  ,n_g  , m_b  , n_b  , m_ro  , n_ro  , m_mu  , n_mu  ,
gruppa  , P_mtr  , Qg_inj_SC(i_q) ,H_tub )  ;
            y017(i+1)=bottomhole_pressure(P_res  , Ql_SC(i_q)  , K    );
            P_oper(i_q)=x0(1);
            end
    end
        if i_q == n_q
            break
        end
Qg_inj_SC(i_q+1)=Qg_inj_SC(i_q)+(Qg_inj_SC0_max-Qg_inj_SC(1))/n_q;
end


%-------------------------------------------------------------
```

```
%Plotting graphs

%------------------
%PVT properties p.1
%------------------
figure(1)
subplot(2,2,1);
plot(L_ann,y1,L_tub,y01);
legend('Along annulus','Along tubing','Location','northwest');
legend('boxoff')
title('Gas saturation');
xlabel('Well depth, m');
ylabel('Gas saturation, m3/m3');
grid on;
axis auto

subplot(2,2,2);
plot(L_ann,y2,L_tub,y02);
legend('Along annulus','Along tubing','Location','northwest');
legend('boxoff')
title('Volume factor');
xlabel('Well depth, m');
ylabel('Volume factor, m3/m3');
grid on;
axis auto

subplot(2,2,3);
plot(L_ann,y3,L_tub,y03 );
legend('Along annulus','Along tubing','Location','northwest');
legend('boxoff')
title('Oil density');
xlabel('Well depth, m');
ylabel('Oil density, kg/m3');
grid on;
axis auto

subplot(2,2,4);
plot(L_ann,y4,L_tub,y04 );
legend('Along annulus','Along tubing','Location','northwest');
legend('boxoff')
title('Oil viscosity');
xlabel('Well depth, m');
ylabel('Oil viscosity, Pa*s');
grid on;
axis auto

%------------------
%PVT properties p.2
%------------------
figure(2)
subplot(2,2,1);
plot(L_ann,y5,L_tub,y05);
legend('Along annulus','Along tubing','Location','northwest');
legend('boxoff')
title('Gas compressibility factor');
xlabel('Well depth, m');
ylabel('Compressibility factor');
grid on;
axis auto
```

```
subplot(2,2,2);
plot(L_ann,y6',L_tub,y06);
legend('Along annulus','Along tubing','Location','northwest');
legend('boxoff')
title('Gas density');
xlabel('Well depth, m');
ylabel('Gas density, kg/m3');
grid on;
axis auto

subplot(2,2,3);
plot(L_ann,y10,L_tub,y010);
legend('Along annulus','Along tubing','Location','northwest');
legend('boxoff')
title('Surface tension');
xlabel('Well depth, m');
ylabel('Surface tension,N/m');
grid on;
axis auto

subplot(2,2,4);
plot(L_ann,y11,L_tub,y011);
legend('Along annulus','Along tubing','Location','northwest');
legend('boxoff')
title('Fluid viscosity');
xlabel('Well depth, m');
ylabel('Fluid viscosity, Pa*s');
grid on;
axis auto

%------------------
%Other flow parameters
%------------------
figure(3)
subplot(2,2,1);
plot(L_ann,y131,L_tub,y0131,'--',L_ann,y132,L_tub,y0132,'--
',L_ann,y133,L_tub,y0133,'--');
legend('Gas along annulus','Gas along tubing','Oil along annulus','Oil along
tubing','Water along annulus','Water along tubing','Location','northwest');
legend('boxoff')
title('Area average fluid fractions in the flow');
xlabel('Well depth, m');
ylabel('Gas fraction');
grid on;
axis auto

subplot(2,2,2);
plot(L_ann,y91,L_tub,y091,'--',L_ann,y92,L_tub,y092,'--
',L_ann,y93,L_tub,y093*10^-1,'--');
legend('Oil along annulus','Oil along tubing','Water along annulus','Water
along tubing','Gas along annulus','Gas along tubing*10^-
1','Location','northwest');
legend('boxoff')
title('Phase velocities in the flow ');
xlabel('Well depth, m');
ylabel('Oil velosity, m/s');
grid on;
axis auto

subplot(2,2,3);
```

```
plot(L_ann,y81*86400,L_tub,y081*86400,'--
',L_ann,y82*86400,L_tub,y082*86400,'--',L_ann,y83*86400,L_tub,y083*86400*10^-
1,'--');
legend('Oil along annulus','Oil along tubing','Water along annulus','Water
along tubing','Gas along annulus','Gas along tubing*10^-
1','Location','northwest');
legend('boxoff')
title('Volumetric flow rates, m3/d');
xlabel('Well depth, m');
ylabel('Flow rate');
grid on;
axis auto

subplot(2,2,4);
plot(L_ann,y121,...
    L_tub,y0121,...
    L_ann,y122,...
    L_tub,y0122);

legend('Flow regime along annulus','Flow regime along tubing','Type of
emulsion along annulus','Type of emulsion along
tubing','Location','northwest');
legend('boxoff')
title('Flow regimes (1-12)');
xlabel('Well depth, m');
ylabel('Flow regimes');
grid on;
axis auto

%flow regimes: (in russian- varies from 1 -bubble flow to 12 - annular
%wavy)
%'capelnaya'=1;
%'emulsionnaya'=2;
%'capelno - puzirkovaya'=3;
%'emulsionno - puzirkovaya'=4;
%'emulsionno - snoryadnaya'=5;
%'error1'=6;
%'error2'=7;
%'error3'=8;
%'error4'=9;
%'puzirkovo-snoryadnaya'=10;
%'puzirkovaya'=11;
%'snoryadnaya'=12;

%type:
%'n / w'=1;
%'(n + g) / w'=2;
%'w / n'=3;
%'(w + g) / n'=4;
%'g / n'=5;

%zone:
%'_ann'=1;
%'_tub'=0;

%------------------
%Pressure and temperature gradients
%------------------
figure(4)
subplot(2,1,1);
```

```
plot(L_ann,y15,L_tub,y015);
legend('Along annulus','Along tubing','Location','northwest');
legend('boxoff')
title('Temperature gradient');
xlabel('Well depth, m');
ylabel('Temperature gradient, K/m');
grid on;
axis auto

subplot(2,1,2);
plot(L_ann,y14,L_tub,y014);
legend('Along annulus','Along tubing','Location','northwest')
title('Pressure gradients');
xlabel('Well depth, m');
ylabel('Pressure gradient, Pa/m');
grid on;
axis auto

%------------------
%Other plots
%------------------

figure(5)
plot(x,(-1)*L_ann,x0,(-1)*L_tub);
title('Pressure distribution curves along tubing and annulus');
legend('Along annulus','Along tubing','Location','northwest');
xlabel('Pressure, MPa');
ylabel('Well depth, m');
grid on;
axis auto

P_bash(1)=14;
increment=(P_bash(1)-0)/100;
n1=100;
for i=1:100
    if  i>1
    P_bash(i)=P_bash(i-1)-increment;
    end
Q(i)= K*(P_res-P_bash(i)-((Hf-H_tub)*9.81*oil_density((1.1*P_bash(i)), m_ro ,
n_ro , Pnas))/10^6);
Q_max(i)=86400*1.8*D_tub^3*((P_bash(i)-P_l)/(10^(-
6)*oil_density((1.1*P_bash(i)), m_ro , n_ro , Pnas)*H_tub))^1.5;
Q_opt(i)=Q_max(i)*(oil_density((1.1*P_bash(i)), m_ro , n_ro ,
Pnas)*9.81*H_tub/10^6-P_bash(i)-P_l)/(oil_density((1.1*P_bash(i)), m_ro ,
n_ro , Pnas)*9.81*H_tub*10^(-6));
min1(i)=abs(Q(i)-Q_max(i));
min2(i)=abs(Q(i)-Q_opt(i));
M1 = min(min1);
M2 = min(min2);
end

for i=1:n1
    if min1(i)==M1
    ind1= i ;
    end
    if min2(i)==M2
    ind2= i ;
    end
end
```

```
P_bash_isk=6.2;
Bhp=P_bash_isk+10^(-6)*(Hf-H_tub)*9.81*oil_density(P_bash_isk, m_ro , n_ro ,
Pnas);
display(Q(ind1), 'Maximum liquid flow rate')      %Maximum liquid flow rate
display(Q(ind2), 'Optimal liquid flow rate')      %Optimal liquid flow rate
display(x0(1), 'Operating gaslift pressure')      %Operating gaslift pressure

figure(6)
plot(P_bash,Q,P_bash,Q_max,P_bash,Q_opt);
legend('IPR curve','Maximum flow','Optimal flow','Location','northwest')
title('Q-P');
xlabel('Pressure, MPa');
ylabel('Q');
grid on;
axis auto

figure(7)
subplot(2,1,1);
plot(Qg_inj_SC*86400,Ql_SC*86400);
title('Liquid flow rate at a given gas injection rate in gaslift');
xlabel('Gas injection rate in gaslift, m3/d');
ylabel('Liquid flow rate, m3/d');
grid on;
axis auto

subplot(2,1,2);
plot(Qg_inj_SC*86400,P_oper);
title('Gaslift operating pressure');
xlabel('Gas injection rate in gaslift, m3/d');
ylabel('Gaslift operating pressure, MPa');
grid on;
axis auto
display(counter, 'counter')% equials to 7
display(counter1, 'counter1')% equials to 73
```

gas_saturation_function

```
function [go]=gas_saturation(P_vh, m_g , n_g , Pnas , go_nas )
    if P_vh < Pnas
    go = (m_g * P_vh ^ n_g);
    else go = go_nas;
    end
end
```

volume_factor

```
function [bo] =volume_factor(P_vh, m_b , n_b , Pnas)
    if P_vh < Pnas
    bo = (m_b * P_vh ^ n_b);
    else bo = (m_b * Pnas ^ n_b);
    end
end
```

oil_density

```
function [ro_n]=oil_density(P_vh, m_ro , n_ro , Pnas)
    if P_vh < Pnas
    ro_n = (m_ro / P_vh ^ n_ro);
    else ro_n = (m_ro / Pnas ^ n_ro);
```

```
    end
end
```

oil_viscosity

```
function [mu_n]=oil_viscosity(P_vh  , T_vh  , m_mu  , n_mu  , Pnas  , Tf    )
    if P_vh < Pnas
    mu_n = (m_mu / P_vh ^ n_mu);
    else mu_n = (m_mu / Pnas ^ n_mu);
    end

 parx(1) = 60;
 parx(2) = 100;
 parx(3) = 105;
 parx(4) = 110;
 parx(5) = 115;
 parx(6) = 120;
 parx(7) = 125;
 parx(8) = 150;
 parx(9) = 180;
 parx(10) = 190;
 parx(11) = 200;
 parx(12) = 210;
 parx(13) = 220;
 parx(14) = 230;
 parx(15) = 240;
 parx(16) = 250;
 parx(17) = 260;
 parx(18) = 270;
 parx(19) = 280;
 parx(20) = 290;
 parx(21) = 300;
 parx(22) = 400;
 parx(23) = 500;
 pary(1) = 20;
 pary(2) = 0.35;
 pary(3) = 290 * 10 ^ -3;
 pary(4) = 200 * 10 ^ -3;
 pary(5) = 134 * 10 ^ -3;
 pary(6) = 105 * 10 ^ -3;
 pary(7) = 90 * 10 ^ -3;
 pary(8) = 25 * 10 ^ -3;
 pary(9) = 9 * 10 ^ -3;
 pary(10) = 7 * 10 ^ -3;
 pary(11) = 5 * 10 ^ -3;
 pary(12) = 4 * 10 ^ -3;
 pary(13) = 3 * 10 ^ -3;
 pary(14) = 2.4 * 10 ^ -3;
 pary(15) = 2 * 10 ^ -3;
 pary(16) = 1.8 * 10 ^ -3;
 pary(17) = 1.4 * 10 ^ -3;
 pary(18) = 1.23 * 10 ^ -3;
 pary(19) = 0.99 * 10 ^ -3;
 pary(20) = 0.8 * 10 ^ -3;
 pary(21) = 0.7 * 10 ^ -3;
 pary(22) = 0.22 * 10 ^ -3;
 pary(23) = 0.102 * 10 ^ -3;

deltaT = Tf - T_vh;
```

```
    for i = 2: 23

        if and((mu_n < pary(i - 1)), (mu_n > pary(i)) )
        Tfictivn1 = (mu_n - pary(i - 1)) * (parx(i) - parx(i - 1)) / (pary(i)
- pary(i - 1)) + parx(i - 1);
        else Tfictivn1 =T_vh;
        end
    end

Tfictivn2 = Tfictivn1 - deltaT;
    for i = 2 : 23
        if and ((Tfictivn2 > parx(i - 1)) , (Tfictivn2 < parx(i)) )
        mu_n = (Tfictivn2 - parx(i - 1)) / (parx(i) - parx(i - 1)) * (pary(i)
- pary(i - 1)) + pary(i - 1) ;
        end
    end
end
```

compressibility_factor

```
function [z]=compressibility_factor(P_vh  , T_vh  , ro_gSC  , y_azot ,Pnas
)

ro_g_otn = ro_gSC / 1.205;
ro_HC_otn = (ro_g_otn - 0.97 * y_azot) / (1 - y_azot);
Prc = 10 * P_vh / (46.9 - 2.06 * ro_HC_otn ^ 2);
Trc = T_vh / (97 + 172 * ro_HC_otn);

    if Trc < 1.05
    Trc = 1.05;
    end

    if and(and((0 <= Prc) , (Prc < 4)), and( (1.17 <= Trc) , (Trc < 2) ))
    zHC = 1 - Prc * (0.18 / (Trc - 0.73) - 0.135) + 0.0161 * Prc ^ 3.45 / Trc
^ 6.1;
    elseif and(and((0 <= Prc) , (Prc < 1.45)) , and((1.05 <= Trc) , (Trc <
1.17) ))
    zHC = 1 - 0.23 * Prc - (1.88 - 1.67 * Trc) * Prc ^ 2;
    elseif and(and((1.45 <= Prc) , (Prc < 4)), and( (1.05 <= Trc) , (Trc <
1.17) ))
    zHC = 0.13 * Prc + (6.05 * Trc - 6.25) * Trc / Prc ^ 2;
    else
    zHC = 0.771;
    end

z_azot = 1 + 564 * 10 ^ -13 * (T_vh - 273) ^ 3.71 * P_vh ^ (14.7 / (T_vh -
273)^2);
z = zHC * (1 - y_azot) + z_azot * y_azot;
end
```

gas_density

```
function [ro_g]=gas_density(P_vh  , T_vh  , ro_gSC  , y_azot  , Pnas     )
[z]=compressibility_factor(P_vh, T_vh, ro_gSC, y_azot, Pnas );
ro_g = ro_gSC * P_vh * 293.2 / (z * 0.1013 * T_vh);
end
```

volume_share

```
function [beta_w_l]=volume_share(P_vh , beta_wSC , m_b , n_b , Pnas  )
[bo]= volume_factor(P_vh, m_b, n_b, Pnas );
beta_w_l = 1 / (1 + bo * (1 / beta_wSC - 1));
beta_n = 1 - beta_w_l;
end
```

production_in_situ_conditions

```
function [Qo  , Qw  , Qg ]= production_in_situ_condition(zone  , P_vh  , T_vh
, P_res  , Tf  , G  , Hf  , tetta  , D_ann  , K  , kappa  , P_l  , Ql_SC  ,
D_tub  , Pnas  , go_nas  , ro_gSC  , y_azot  , ro_oSC  , beta_wSC  , ro_wSC
, alpha_g  , m_g  , n_g  , m_b  , n_b  , m_ro  , n_ro  , m_mu  , n_mu  ,
gruppa  , P_mtr ,Qg_inj_SC )

[bo]= volume_factor(P_vh, m_b, n_b, Pnas );
[beta_w_l]= volume_share(P_vh, beta_wSC, m_b, n_b, Pnas );

Qo = Ql_SC * (1 - beta_w_l) * bo;
Qw = Ql_SC * beta_w_l;
    if P_vh >= Pnas
    Qg = 0;
    else
    [ go]= gas_saturation(P_vh, m_g, n_g, Pnas, go_nas);
    [z]= compressibility_factor(P_vh, T_vh, ro_gSC, y_azot, Pnas );
    [z_SC]= compressibility_factor(P_vh, T_vh, ro_gSC, y_azot, Pnas );
        if zone >= 1
        Qg_nat = Ql_SC * z * 0.1013 * T_vh / (P_vh * 293) * (1 - beta_w_l) *
(go_nas - go);
        Qg_inj=0;
        Qg=Qg_nat+Qg_inj;
        elseif zone <=0
        Qg_nat = Ql_SC * z * 0.1013 * T_vh / (P_vh * 293) * (1 - beta_w_l) *
(go_nas - go);
        Qg_inj=Qg_inj_SC*z * 0.1013 * T_vh / (P_vh * 293*z_SC);
        Qg=Qg_nat+Qg_inj;
            if Qg < 0.0001
            Qg = 12345;
            end
        else
        Qg = 0;
        end
    end

end
```

flow_rate

```
function [omega_n  , omega_w  , omega_priv_g  , omega_mix  , omega_cr1  ,
omega_cr2]=flow_rate(zone  , P_vh  , T_vh  , P_res  , Tf  , G  , Hf  , tetta
, D_ann  , K  , kappa  , P_l  , Ql_SC  , D_tub  , Pnas  , go_nas  , ro_gSC  ,
y_azot  , ro_oSC  , beta_wSC  , ro_wSC  , alpha_g  , m_g  , n_g  , m_b  , n_b
, m_ro  , n_ro  , m_mu  , n_mu  , gruppa  , P_mtr , Qg_inj_SC)
```

```
[beta_w_l]= volume_share(P_vh, beta_wSC, m_b, n_b, Pnas );
[Qo, Qw, Qg]= production_in_situ_condition(zone, P_vh, T_vh, P_res, Tf, G,
Hf, tetta, D_ann, K, kappa, P_l, Ql_SC, D_tub, Pnas, go_nas, ro_gSC, y_azot,
ro_oSC, beta_wSC, ro_wSC, alpha_g, m_g, n_g, m_b, n_b, m_ro, n_ro, m_mu,
n_mu, gruppa, P_mtr, Qg_inj_SC);

    if zone >=1
    D = D_ann;
    elseif zone <=0
    D = D_tub;
    else
    D = 12345;
    end

S = pi * D ^ 2 / 4;
omega_cr1 = 0.064 * 56 ^ beta_w_l * (9.81 * D) ^ 0.5;
omega_cr2 = 0.487 * (9.81 * D) ^ 0.5;
omega_n = Qo / S;
omega_w = Qw / S;
omega_priv_g = Qg / S;
omega_mix = omega_priv_g + omega_n + omega_w;
end
```

surface_tension

```
function [sigma_ow  , sigma_l]=surface_tension(zone  , P_vh  , T_vh  , P_res
, Tf  , G  , Hf  , tetta  , D_ann  , K  , kappa  , P_l  , Ql_SC  , D_tub  ,
Pnas  , go_nas  , ro_gSC  , y_azot  , ro_oSC  , beta_wSC  , ro_wSC  , alpha_g
, m_g  , n_g  , m_b  , n_b  , m_ro  , n_ro  , m_mu  , n_mu  , gruppa  , P_mtr
, Qg_inj_SC  )
[beta_w_l]= volume_share(P_vh, beta_wSC, m_b, n_b, Pnas);
[omega_n, omega_w, omega_priv_g, omega_mix, omega_cr1, omega_cr2]=
flow_rate(zone, P_vh, T_vh, P_res, Tf, G, Hf, tetta, D_ann, K, kappa, P_l,
Ql_SC, D_tub, Pnas, go_nas, ro_gSC, y_azot, ro_oSC, beta_wSC, ro_wSC,
alpha_g, m_g, n_g, m_b, n_b, m_ro, n_ro, m_mu, n_mu, gruppa, P_mtr,
Qg_inj_SC);
sigma_wg = 10 ^ -(1.19 + 0.01 * P_vh);
sigma_og = 10 ^ -(1.58 + 0.05 * P_vh) - 72 * 10 ^ -6 * (T_vh - 305);
    if sigma_og < 0
    sigma_og = 0;
    end
sigma_ow = sigma_wg - sigma_og;
    if beta_w_l > 0.5
    sigma_l = sigma_wg;
    else
        if omega_mix < omega_cr1
        sigma_l = sigma_wg;
        else
        sigma_l = sigma_og;
        end
    end
end
```

fluid_viscosity

```
function [mu_w  , mu_l] =fluid_viscosity(zone  , P_vh  , T_vh  , P_res  , Tf
, G  , Hf  , tetta  , D_ann  , K  , kappa  , P_l  , Ql_SC  , D_tub  , Pnas  ,
go_nas  , ro_gSC  , y_azot  , ro_oSC  , beta_wSC  , ro_wSC  , alpha_g  , m_g
, n_g  , m_b  , n_b  , m_ro  , n_ro  , m_mu  , n_mu  , gruppa  , P_mtr ,
Qg_inj_SC )

[beta_w_l]= volume_share(P_vh, beta_wSC, m_b, n_b, Pnas)
[omega_n, omega_w, omega_priv_g, omega_mix, omega_cr1, omega_cr2]=
flow_rate(zone, P_vh, T_vh,P_res, Tf, G, Hf, tetta, D_ann, K, kappa, P_l,
Ql_SC, D_tub, Pnas, go_nas, ro_gSC, y_azot, ro_oSC, beta_wSC, ro_wSC,
alpha_g, m_g, n_g, m_b, n_b, m_ro, n_ro, m_mu, n_mu, gruppa, P_mtr,
Qg_inj_SC);
[mu_n]= oil_viscosity(P_vh, T_vh, m_mu, n_mu, Pnas, Tf);

mu_w = (0.0014 + 38 * 10 ^ -7 * (ro_wSC - 1000)) / 10 ^ (0.0065 * (T_vh -
273));
%for zone: annulus=1, tubing=0

    if zone > 1
    D = D_ann;
    elseif zone <= 0
    D = D_tub;
    else
    D = 12345;
    end

a = (1 + 20 * beta_w_l ^ 2) / (8 * omega_mix / D) ^ (0.48 * beta_w_l);

    if beta_w_l > 0.5
        if omega_mix < omega_cr2
        mu_l = mu_w;
        else mu_l = mu_w * 10 ^ (3.2 * (1 - beta_w_l));
        end
    else
        if omega_mix < omega_cr1
        mu_l = mu_w;
        elseif and((omega_mix > omega_cr1) , (omega_mix < omega_cr2))
        mu_l = mu_n;
        else
            if a <= 1
            mu_l = mu_n * (1 + 2.9 * beta_w_l) / (1 - beta_w_l);
            else
            mu_l = a * mu_n * (1 + 2.9 * beta_w_l) / (1 - beta_w_l);
            end
        end
    end
end
```

type_and_structure

```
function [structura  , tip ]= type_and_structure(zone  , P_vh  , T_vh  ,
P_res  , Tf  , G  , Hf  , tetta  , D_ann  , K  , kappa  , P_l  , Ql_SC  ,
D_tub  , Pnas  , go_nas  , ro_gSC  , y_azot  , ro_oSC  , beta_wSC  , ro_wSC
, alpha_g  , m_g  , n_g  , m_b  , n_b  , m_ro  , n_ro  , m_mu  , n_mu  ,
gruppa  , P_mtr, Qg_inj_SC    )

[beta_w_l]= volume_share(P_vh, beta_wSC, m_b, n_b, Pnas );
```

```
[omega_n, omega_w, omega_priv_g, omega_mix, omega_cr1, omega_cr2]=
flow_rate(zone, P_vh, T_vh, P_res, Tf, G, Hf, tetta, D_ann, K, kappa, P_l,
Ql_SC, D_tub, Pnas, go_nas, ro_gSC, y_azot, ro_oSC, beta_wSC, ro_wSC,
alpha_g, m_g, n_g, m_b, n_b, m_ro, n_ro, m_mu, n_mu, gruppa, P_mtr,
Qg_inj_SC);
[Qo, Qw, Qg]= production_in_situ_condition(zone, P_vh, T_vh, P_res, Tf, G,
Hf, tetta, D_ann, K, kappa, P_l, Ql_SC, D_tub, Pnas, go_nas, ro_gSC, y_azot,
ro_oSC, beta_wSC, ro_wSC, alpha_g, m_g, n_g, m_b, n_b, m_ro, n_ro, m_mu,
n_mu, gruppa, P_mtr, Qg_inj_SC);

[sigma_ow, sigma_l]= surface_tension(zone, P_vh, T_vh, P_res, Tf, G, Hf,
tetta, D_ann, K, kappa, P_l, Ql_SC, D_tub, Pnas, go_nas, ro_gSC, y_azot,
ro_oSC, beta_wSC, ro_wSC, alpha_g, m_g,n_g, m_b, n_b, m_ro, n_ro, m_mu, n_mu,
gruppa, P_mtr, Qg_inj_SC );
[mu_w, mu_l]= fluid_viscosity(zone, P_vh, T_vh, P_res, Tf, G, Hf, tetta,
D_ann, K, kappa, P_l, Ql_SC, D_tub, Pnas, go_nas, ro_gSC, y_azot, ro_oSC,
beta_wSC, ro_wSC, alpha_g, m_g, n_g, m_b, n_b, m_ro, n_ro, m_mu, n_mu,
gruppa, P_mtr, Qg_inj_SC );

fi_g1 = omega_priv_g / (omega_mix + 0.23 * (sigma_l / 0.067) ^ 0.83 * (mu_l /
0.0011) ^ 0.44 * exp(-0.01 * mu_l / 0.0011));
fi_g2 = omega_priv_g / (omega_mix + 0.41 * (mu_l / 0.0011) ^ 0.1 * (sigma_l /
0.067 * omega_priv_g ^ 2) ^ (1 / 3));
fi_g = (fi_g1 + fi_g2) / 2;

%flow regimes: (in russian- varies from 1 -bubble flow to 12 - annular
%wavy)
%'capelnaya'=1;
%'emulsionnaya'=2;
%'capelno - puzirkovaya'=3;
%'emulsionno - puzirkovaya'=4;
%'emulsionno - snoryadnaya'=5;
%'error1'=6;
%'error2'=7;
%'error3'=8;
%'error4'=9;
%'puzirkovo-snoryadnaya'=10;
%'puzirkovaya'=11;
%'snoryadnaya'=12;

%type:
%'n / w'=1;
%'(n + g) / w'=2;
%'w / n'=3;
%'(w + g) / n'=4;
%'g / n'=5;

%zone:
%'_ann'=1;
%'_tub'=0;
    if and((beta_w_l > 0.5) , (Qg == 0) )
        if omega_mix < omega_cr2
        structura = 1;
        tip = 1;
        else
        structura = 2;
        tip = 1;
        end
    elseif and((beta_w_l > 0.5) , (Qg > 0)  )
        if and(omega_mix < omega_cr2 , or (fi_g <= 0.65 , P_vh > 0.7) )
```

```
        structura = 3;
        tip = 2;
        elseif and(omega_mix >= omega_cr2 , or (fi_g <= 0.65 , P_vh > 0.7))
        structura = 4;
        tip = 2;
        elseif and(omega_mix >= omega_cr2 , or(fi_g > 0.65 , P_vh <= 0.7))
        structura = 5;
        tip = 2;
        else
        structura = 6;
        tip = 6;
        end
    elseif and(beta_w_l <= 0.5 , Qg == 0)
        if omega_mix < omega_cr1
        structura = 1;
        tip = 1;
        elseif and(omega_cr1 < omega_mix , omega_mix < omega_cr2)
        structura = 1;
        tip = 3;
        else
        structura = 2;
        tip = 3;
        end
    elseif and(beta_w_l <= 0.5 , Qg > 0)
        if and(omega_mix < omega_cr1 , or(fi_g <= 0.65, P_vh > 0.7))
        structura = 3;
        tip = 2;
        elseif and(and(omega_cr1 < omega_mix , omega_mix < omega_cr2) ,
or(fi_g <= 0.65 , P_vh > 0.7) )
        structura = 3;
        tip = 4;
        elseif and(omega_mix >= omega_cr2 , or(fi_g <= 0.65, P_vh > 0.7))
        structura = 4;
        tip = 4;
        elseif and(omega_mix >= omega_cr2 , or (fi_g > 0.65, P_vh <= 0.7))
        structura = 5;
        tip = 4;
        else
        structura = 7;
        tip = 7;
        end
    elseif and(beta_w_l == 0 , Qg > 0)
        if or(fi_g <= 0.65 , P_vh > 0.7)
        structura = 10;
        tip = 5;
        elseif or(fi_g > 0.65 , P_vh <= 0.7)
        structura = 10;
        tip = 5;
        else
        structura = 8;
        tip = 8;
        end
    else
    structura = 9;
    tip = 9;
    end
end
```

fraction_share

```
function [fi_g  , fi_n  , fi_w]=fraction_share(zone  , P_vh  , T_vh  , P_res
, Tf  , G  , Hf  , tetta  , D_ann  , K  , kappa  , P_l  , Ql_SC  , D_tub  ,
Pnas  , go_nas  , ro_gSC  , y_azot  , ro_oSC  , beta_wSC  , ro_wSC  , alpha_g
, m_g  , n_g  , m_b  , n_b  , m_ro  , n_ro  , m_mu  , n_mu  , gruppa  ,
P_mtr, Qg_inj_SC  )

[sigma_ow, sigma_l]= surface_tension(zone, P_vh, T_vh,P_res, Tf, G, Hf,
tetta, D_ann, K, kappa, P_l, Ql_SC, D_tub, Pnas, go_nas, ro_gSC, y_azot,
ro_oSC, beta_wSC, ro_wSC, alpha_g, m_g, n_g, m_b, n_b, m_ro, n_ro, m_mu,
n_mu, gruppa, P_mtr, Qg_inj_SC);
[beta_w_l]= volume_share(P_vh, beta_wSC, m_b, n_b, Pnas );
[omega_n, omega_w, omega_priv_g, omega_mix, omega_cr1, omega_cr2]=
flow_rate(zone, P_vh, T_vh, P_res, Tf, G, Hf, tetta, D_ann, K, kappa, P_l,
Ql_SC, D_tub, Pnas, go_nas, ro_gSC, y_azot, ro_oSC, beta_wSC, ro_wSC,
alpha_g, m_g, n_g, m_b, n_b, m_ro, n_ro, m_mu, n_mu, gruppa, P_mtr,
Qg_inj_SC);
[ ro_n]= oil_density(P_vh, m_ro, n_ro, Pnas);
[structura, tip]= type_and_structure(zone, P_vh, T_vh, P_res, Tf, G, Hf,
tetta, D_ann, K, kappa, P_l, Ql_SC, D_tub, Pnas, go_nas, ro_gSC, y_azot,
ro_oSC, beta_wSC, ro_wSC, alpha_g, m_g, n_g, m_b, n_b, m_ro, n_ro, m_mu,
n_mu, gruppa, P_mtr, Qg_inj_SC);
[mu_w, mu_l]= fluid_viscosity(zone, P_vh, T_vh, P_res, Tf, G, Hf, tetta,
D_ann, K, kappa, P_l, Ql_SC, D_tub, Pnas, go_nas, ro_gSC, y_azot, ro_oSC,
beta_wSC, ro_wSC, alpha_g, m_g, n_g, m_b, n_b, m_ro, n_ro, m_mu, n_mu,
gruppa, P_mtr, Qg_inj_SC);

%flow regimes: (in russian- varies from 1 -bubble flow to 12 - annular
%wavy)
%'capelnaya'=1;
%'emulsionnaya'=2;
%'capelno - puzirkovaya'=3;
%'emulsionno - puzirkovaya'=4;
%'emulsionno - snoryadnaya'=5;
%'error1'=6;
%'error2'=7;
%'error3'=8;
%'error4'=9;
%'puzirkovo-snoryadnaya'=10;
%'puzirkovaya'=11;
%'snoryadnaya'=12;

%type:
%'n / w'=1;
%'(n + g) / w'=2;
%'w / n'=3;
%'(w + g) / n'=4;
%'g / n'=5;

%zone:
%'_ann'=1;
%'_tub'=0;

    if zone  == 1
    D = D_ann;
    elseif zone == 0
    D = D_tub;
    else
    D = 12345;
    end
```

```
    if or( or(structura == 11 , structura == 3) , (structura == 4))
    fi_g = omega_priv_g / (omega_mix + 0.23 * (sigma_l / 0.067) ^ 0.83 *
(mu_l / 0.0011) ^ 0.44 * exp(-0.01 * mu_l / 0.0011));
    elseif or(structura == 12 , structura == 5)
    fi_g = omega_priv_g / (omega_mix + 0.41 * (mu_l / 0.0011) ^ 0.1 *
(sigma_l / 0.067 * omega_priv_g ^ 2) ^ (1 / 3));
    elseif or(structura == 1 , structura == 2)
    fi_g = 0;
    else
    fi_g = 0;
    end
    if or(tip== 1 , tip == 2)
        if or(structura == 1, structura == 3)
        fi_ol = omega_n / (omega_mix + (0.54 * (0.01 + beta_w_l ^ 0.152) -
omega_mix / (9.81 * D) ^ 0.5) * (4 * 9.81 * sigma_ow * abs(ro_wSC - ro_n) /
ro_wSC ^ 2) ^ 0.25)   ;
        fi_w_l = 1 - fi_ol;
        elseif or(or(structura == 2,structura == 4) , (structura == 5))
        fi_ol = omega_n / omega_mix;
        fi_w_l = 1 - fi_ol;
        else
        fi_ol = 1234;
        fi_w_l = 1234;
        end
    elseif or(tip == 3, tip == 4)
        if or(structura == 1, structura == 3)
        fi_w_l = omega_w / (omega_mix - (0.425 - 0.827 * omega_mix / (9.81 *
D) ^ 0.5) * (4 * 9.81 * sigma_ow * abs(ro_wSC - ro_n) / ro_n ^ 2) ^ 0.25);
        fi_ol = 1 - fi_w_l;
        elseif or(or(structura == 2,structura == 4) , (structura == 5))
        fi_w_l = omega_w / omega_mix;
        fi_ol = 1 - fi_w_l;
        else
        end
    else
    fi_ol = 7;
    fi_w_l = 7;
    end
fi_n = fi_ol * (1 - fi_g);
fi_w = fi_w_l * (1 - fi_g);
end
```

pressure_gradient

```
function [dP_dL]=pressure_gradient(zone  , P_vh  , T_vh  , P_res  , Tf  , G
, Hf  , tetta  , D_ann  , K  , kappa  , P_l  , Ql_SC  , D_tub  , Pnas  ,
go_nas  , ro_gSC  , y_azot  , ro_oSC  , beta_wSC  , ro_wSC  , alpha_g  , m_g
,n_g  , m_b  , n_b  , m_ro  , n_ro  , m_mu  , n_mu  , gruppa  , P_mtr,
Qg_inj_SC  )

[omega_n, omega_w, omega_priv_g, omega_mix, omega_cr1, omega_cr2]=
flow_rate(zone, P_vh, T_vh, P_res, Tf, G, Hf, tetta, D_ann, K, kappa, P_l,
Ql_SC, D_tub, Pnas, go_nas, ro_gSC, y_azot, ro_oSC, beta_wSC, ro_wSC,
alpha_g, m_g, n_g, m_b, n_b, m_ro, n_ro, m_mu, n_mu, gruppa, P_mtr,
Qg_inj_SC);
[ro_n]= oil_density(P_vh, m_ro, n_ro, Pnas );
[ro_g]= gas_density(P_vh, T_vh, ro_gSC, y_azot, Pnas );
```

```
[mu_w, mu_l]= fluid_viscosity(zone, P_vh, T_vh, P_res, Tf, G, Hf, tetta,
D_ann, K, kappa, P_l, Ql_SC, D_tub, Pnas, go_nas, ro_gSC, y_azot, ro_oSC,
beta_wSC, ro_wSC, alpha_g, m_g, n_g, m_b, n_b, m_ro, n_ro, m_mu, n_mu,
gruppa, P_mtr, Qg_inj_SC);
[fi_g, fi_n, fi_w]= fraction_share(zone, P_vh, T_vh, P_res, Tf, G, Hf, tetta,
D_ann, K, kappa, P_l, Ql_SC, D_tub, Pnas, go_nas, ro_gSC, y_azot, ro_oSC,
beta_wSC, ro_wSC, alpha_g, m_g, n_g, m_b, n_b, m_ro, n_ro, m_mu, n_mu,
gruppa, P_mtr, Qg_inj_SC);

%flow regimes: (in russian- varies from 1 -bubble flow to 12 - annular
%wavy)
%'capelnaya'=1;
%'emulsionnaya'=2;
%'capelno - puzirkovaya'=3;
%'emulsionno - puzirkovaya'=4;
%'emulsionno - snoryadnaya'=5;
%'error1'=6;
%'error2'=7;
%'error3'=8;
%'error4'=9;
%'puzirkovo-snoryadnaya'=10;
%'puzirkovaya'=11;
%'snoryadnaya'=12;

%type:
%'n / w'=1;
%'(n + g) / w'=2;
%'w / n'=3;
%'(w + g) / n'=4;
%'g / n'=5;

%zone:
%'_ann'=1;
%'_tub'=0;

    if zone == 1
    D = D_ann;
    elseif zone == 0
    D = D_tub;
    else
    D = 12345;
    end

    Re = D / mu_l * (ro_n * omega_n + ro_wSC * omega_w + ro_g *
omega_priv_g);
    if Re <= 2000
    lambda = 64 / Re;
    else
    lambda = 0.11 * (68 / Re + 15 * 10 ^ -6 / D);
    end
    if fi_g < 0.03
    dP_dL = (9.81 * cos(tetta / 180 * pi) * (fi_n * ro_n + fi_w * ro_wSC +
fi_g * ro_g)+ lambda / 2 / D * (ro_n / fi_n * omega_n ^ 2 + ro_wSC / fi_w *
omega_w ^ 2)) / 10 ^ 6;
    else
    dP_dL = (9.81 * cos(tetta / 180 * pi) * (fi_n * ro_n + fi_w * ro_wSC +
fi_g * ro_g)+ lambda / 2 / D * (ro_n / fi_n * omega_n ^ 2 + ro_wSC / fi_w *
omega_w ^ 2 + ro_g / fi_g * omega_priv_g ^ 2)) / 10 ^ 6;
    end
end
```

temperature_gradient

```
function [dT_dL ]=temperature_gradient(zone , G , Ql_SC , D_ann , D_tub )
%zone:
%'_ann'=1;
%'_tub'=0;
    if zone == 1
    D = D_ann;
    elseif zone == 0
    D = D_tub;
    else
    D = 12345;
    end
dT_dL = (0.0034 + 0.79 * G) / 10 ^ (Ql_SC / (20 * D ^ 2.67));
end
```

P_and_T

```
function [P_outl  , T_outl]= P_and_T(zone  , P_vh  , T_vh  , P_res  , Tf  , G
, Hf  , tetta  , D_ann  , K  , kappa  , P_l  , Ql_SC  , D_tub  , Pnas  ,
go_nas  , ro_gSC  , y_azot  , ro_oSC  , beta_wSC  , ro_wSC  , alpha_g  , m_g
,n_g  , m_b  , n_b  , m_ro  , n_ro  , m_mu  , n_mu  , gruppa  , P_mtr ,
Qg_inj_SC ,H_tub  )

deltaL = Hf /100;
[dP_dL]= pressure_gradient(zone, P_vh, T_vh, P_res, Tf, G, Hf, tetta, D_ann,
K, kappa, P_l, Ql_SC, D_tub, Pnas, go_nas, ro_gSC, y_azot, ro_oSC, beta_wSC,
ro_wSC, alpha_g, m_g, n_g, m_b, n_b, m_ro, n_ro, m_mu, n_mu, gruppa, P_mtr,
Qg_inj_SC);
[dT_dL]= temperature_gradient(zone, G, Ql_SC, D_ann, D_tub );

%zone:
%'_ann'=1;
%'_tub'=0;

    if zone == 1
    P_outl = (P_vh - dP_dL * deltaL);
    T_outl = T_vh - dT_dL * deltaL;
    elseif zone == 0
    deltaL=(H_tub) / 100;%!
    P_outl = (P_vh - dP_dL * deltaL);
    T_outl = T_vh - dT_dL * deltaL;
    else
    P_outl = 12345;
    T_outl = 12345;
    end
end
```

bottomhole_pressure

```
function [Pbh]=bottomhole_pressure(P_res  , Ql_SC  , K    )
Pbh = P_res - 86400 * Ql_SC / K;
end
```

PDC_casing

```
function [PDC]=PDC_casing(P_res  , Tf  , G  , Hf  , tetta  , D_ann  , K  ,
kappa  , P_l  , Ql_SC  , D_tub  , Pnas  , go_nas  , ro_gSC  , y_azot  ,
ro_oSC  , beta_wSC  , ro_wSC  , alpha_g  , m_g  , n_g  , m_b  , n_b  , m_ro
, n_ro  , m_mu  , n_mu  , gruppa , P_mtr  )

[Pbh]=bottomhole_pressure(P_res  , Ql_SC  , K    );

L_ann(1) = Hf / cos(tetta / 180 * pi);
deltaL = Hf / 100;

%zone:
%'_ann'=1;
%'_tub'=0;

zone = 1;
P_ann(1) = Pbh;
T_ann(1) = Tf;

    for i=2:n
    P = P_ann(i - 1);
    T = T_ann(i - 1);
    L_ann(i) = L_ann(i - 1) - deltaL;

    [P_outl  , T_outl]= P_and_T(zone  , P_vh  , T_vh  , P_res  , Tf  , G  ,
Hf  , tetta  , D_ann  , K  , kappa  , P_l  , Ql_SC  , D_tub  , Pnas  , go_nas
, ro_gSC  , y_azot  , ro_oSC  , beta_wSC  , ro_wSC  , alpha_g  , m_g  ,n_g  ,
m_b  , n_b  , m_ro  , n_ro  , m_mu  , n_mu  , gruppa  , P_mtr    )  ;

    T_ann(i) = T_outl;
    P_ann(i) = P_outl;
    end
end
```

PVT

```
function [ b_n_t  , ro_og_t  , g_om_t]=PVT(P_vh  , P_res  , Tf  , Pnas  ,
go_nas  , ro_gSC  , ro_oSC  , ro_wSC    )
%coefficients parameter calculation (for PVT prorepties) part 1
    if P_vh >= Pnas  ;
    P_vh = Pnas;
    end
R = log(P_vh / Pnas) / log(10 * Pnas);
D = ro_oSC / ro_wSC * ro_gSC / 1.29 * (4.5 - 0.00305 * (Tf - 293)) - 4.785;
SH_t = 1 + 0.029 * (Tf - 293) * (ro_oSC / ro_wSC * ro_gSC / 1.29 - 0.7966);
SH_g_t = 1 + 0.0054 * (Tf - 293);
g_om = 10 ^ 3 * go_nas / (ro_oSC * 293.15 / 273);
U = ro_oSC / ro_wSC * g_om - 186;
    if ro_oSC / ro_wSC <= 0.86
    alpha_n = 10 ^ -3 * 2.683 * (1.169 - ro_oSC / ro_wSC);
    else
    alpha_n = 10 ^ -3 * 1.975 * (1.272 - ro_oSC / ro_wSC);
    end
g_om_t = g_om * SH_t * R * (D * (1 + R) - 1);
ro_g_t_otn = SH_g_t * (ro_gSC / 1.29 - 0.0036 * (1 + R) * (105.7 + U * R));
g_om_t = g_om * SH_t - g_om_t;
```

```
    if g_om_t > go_nas
    g_om_t = go_nas;
    end
ro_gr_t = g_om / g_om_t * (ro_gSC / 1.29 * SH_t * SH_g_t - ro_g_t_otn *
g_om_t / g_om);
lambda_t = 3.54 * (1.2147 - ro_oSC / ro_wSC) + 1.0337 / SH_g_t * ro_gr_t +
5.581 * (1 - 1.61 * ro_oSC / ro_wSC / 1000 * g_om_t) * 10 ^ -3 * g_om_t;
b_n_t = 1 + 1.0733 / SH_t * ro_oSC / ro_wSC * lambda_t * 10 ^ -3 * g_om_t +
alpha_n * (Tf - 293) - 6.5 * 10 ^ -4 * P_res;
ro_og_t_otn = ro_oSC / ro_wSC / b_n_t * (1 + 1.293 / SH_t / SH_g_t * ro_gr_t
/ 1000 * g_om_t);
ro_og_t = ro_og_t_otn * ro_wSC;
end
```

reaga

```
function [b_n_t_lin  , ro_og_lin  , g_om_t_lin  , b_n_t_nas  , ro_og_t_nas  ,
g_om_t_nas]=reaga(P_res  , P_l  , Tf  , Pnas  , go_nas  , ro_gSC  , ro_oSC  ,
ro_wSC  )
%coefficients parameter calculation (for PVT prorepties) part 2
[ b_n_t  , ro_og_t  , g_om_t]= PVT(P_l, P_res, Tf, Pnas, go_nas, ro_gSC,
ro_oSC, ro_wSC);
b_n_t_lin = b_n_t;
ro_og_lin = ro_og_t;
g_om_t_lin = g_om_t;

[ b_n_t  , ro_og_t  , g_om_t]= PVT(Pnas, P_res, Tf, Pnas, go_nas, ro_gSC,
ro_oSC, ro_wSC);
b_n_t_nas = b_n_t;
ro_og_t_nas = ro_og_t;
g_om_t_nas = g_om_t;

end
```

constPVT

```
function [ny,my,ny2,my2]=constPVT(Ylin  , Ynas  , P_l  , Pnas  )
%coefficients parameter calculation (for PVT prorepties) part 2
ny = (log(Ylin) / log(10) - log(Ynas) / log(10)) / (log(P_l) / log(10) -
log(Pnas) / log(10));
my = Ylin / (P_l ^ ny);
ny2 = (-log(Ylin) / log(10) + log(Ynas) / log(10)) / (log(P_l) / log(10) -
log(Pnas) / log(10));
my2 = Ylin * (P_l ^ ny2);
end
```

Appendix B

Experimental setup pictures

Figure 39- Alicat gas flowmeter, mounted on top of the loop

Figure 40- Atmospheric pressure gauge

Figure 41- Valve 2 directing gas towards model

Figure 42- Switch directing gas towards open atmosphere; gas regulator, and inlet pressure Crystal Digital test; Gauge XP2i manometer

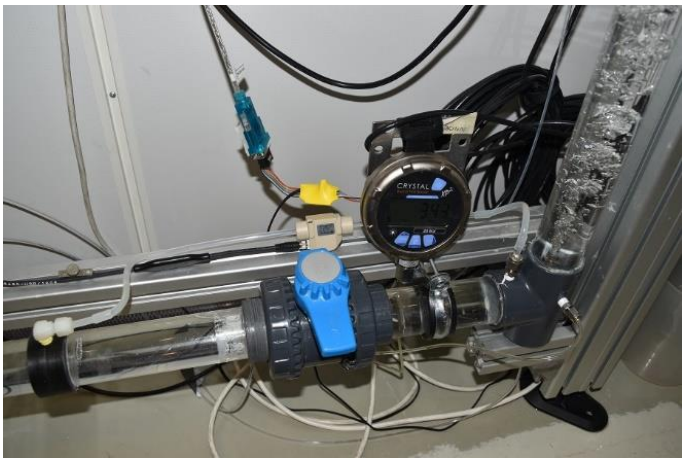

Figure 43- Bottomhole Crystal Digital test Gauge XP2i manometer and the point of pressure measuring and Sensirion SLQ-QT500 liquid flow meter

Figure 44- Rosemount 3051C pressure gauge differential pressure measurer

Figure 45- Open position of Valve 1

Figure 46- A Norgren gas drier

Figure 47-Operator's workplace

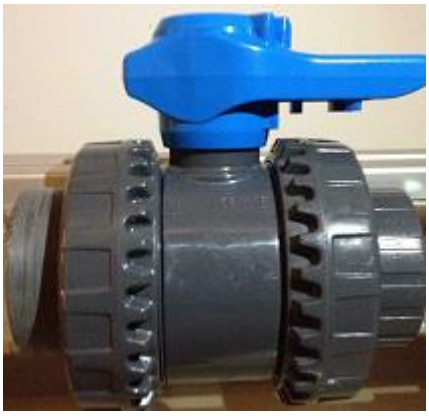

Figure 48- Ball valve on the lower horizontal pipe

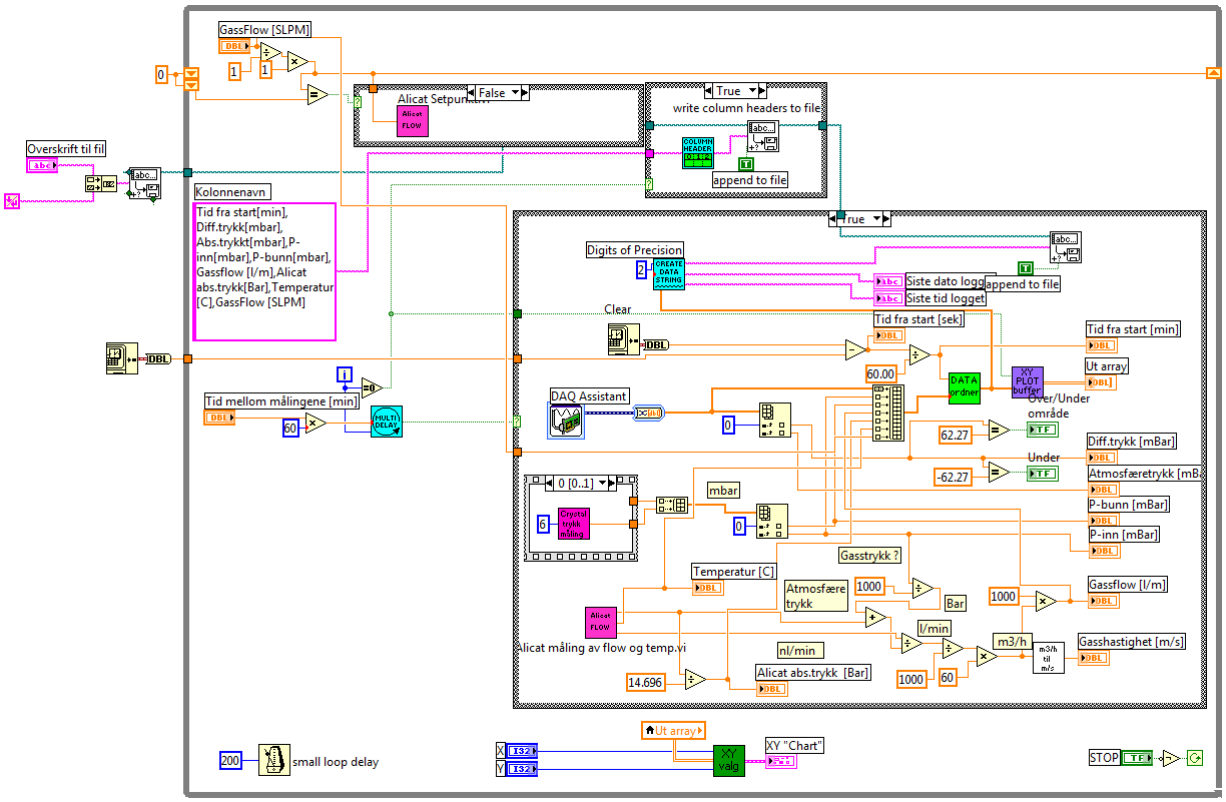

Figure 49- LabVIEW working scheme

Appendix C

Table 58- Liquid flow summary measurements for experiment 1

SLPM	Amount of readings n	Flow [ml/s]			Reliability	Mean dev. from average Savg	Stud. Coeff. (5%, n-1) t	Confidence interval CI	Rel. error sigma, %	Answer
		Average Xavg	Standard deviation S	degree of freedom N						
0,8	239	2448,09	54,40	10	0,95	17,20	2,26	38,91	1,59	Q_liq=(2448,09+-38,92) ml/min; eps=1,59%; alpha=0,95.
0,7	190	2377,10	72,88	10	0,95	23,05	2,26	52,13	2,19	Q_liq=(2377,1+-52,14) ml/min; eps=2,2%; alpha=0,95.
0,6	170	2202,49	77,77	10	0,95	24,59	2,26	55,63	2,53	Q_liq=(2202,5+-55,64) ml/min; eps=2,53%; alpha=0,95.
0,5	202	2041,53	69,64	10	0,95	22,02	2,26	49,81	2,44	Q_liq=(2041,54+-49,82) ml/min; eps=2,45%; alpha=0,95.
0,4	231	1694,21	54,59	10	0,95	17,26	2,26	39,05	2,30	Q_liq=(1694,22+-39,05) ml/min; eps=2,31%; alpha=0,95.
0,3	138	1414,76	37,64	10	0,95	11,90	2,26	26,93	1,90	Q_liq=(1414,76+-26,93) ml/min; eps=1,91%; alpha=0,95.
0,2	177	1138,49	44,39	10	0,95	14,04	2,26	31,76	2,79	Q_liq=(1138,5+-31,76) ml/min; eps=2,79%; alpha=0,95.
0,15	241	970,88	31,32	10	0,95	9,90	2,26	22,41	2,31	Q_liq=(970,89+-22,41) ml/min; eps=2,31%; alpha=0,95.
0,1	183	736,66	50,74	10	0,95	16,05	2,26	36,30	4,93	Q_liq=(736,67+-36,3) ml/min; eps=4,93%; alpha=0,95.
0,05	168	497,74	48,09	10	0,95	15,21	2,26	34,40	6,91	Q_liq=(497,74+-34,41) ml/min; eps=6,92%; alpha=0,95.
0,02	239	246,91	38,47	10	0,95	12,17	2,26	27,52	11,15	Q_liq=(246,92+-27,53) ml/min; eps=11,15%; alpha=0,95.
0,01	163	120,15	18,10	10	0,95	5,72	2,26	12,95	10,78	Q_liq=(120,15+-12,95) ml/min; eps=10,78%; alpha=0,95.

Table 59- Liquid flow summary measurements for experiment 2

SLPM	Amount of readings n	Flow [ml/s]			Reliability	Mean dev. from average Savg	Stud. Coeff. (5%, n-1) t	Confidence interval CI	Rel. error sigma, %	Answer
		Average Xavg	Standard deviation S	degree of freedom N						
0,8	684	2444,03	79,19	10	0,95	25,04	2,26	56,65	2,32	Q_liq=(2444,04+-56,65) ml/min; eps=2,32%; alpha=0,95.
0,7	698	2340,89	124,11	10	0,95	39,25	2,26	88,78	3,79	Q_liq=(2340,89+-88,79) ml/min; eps=3,8%; alpha=0,95.
0,6	630	2201,21	130,50	10	0,95	41,27	2,26	93,36	4,24	Q_liq=(2201,21+-93,36) ml/min; eps=4,25%; alpha=0,95.
0,5	580	2049,38	115,55	10	0,95	36,54	2,26	82,66	4,03	Q_liq=(2049,38+-82,66) ml/min; eps=4,04%; alpha=0,95.
0,4	510	1940,36	78,49	10	0,95	24,82	2,26	56,15	2,89	Q_liq=(1940,37+-56,16) ml/min; eps=2,9%; alpha=0,95.
0,3	579	1622,64	44,49	10	0,95	14,07	2,26	31,83	1,96	Q_liq=(1622,65+-31,83) ml/min; eps=1,97%; alpha=0,95.
0,2	593	1196,31	32,24	10	0,95	10,20	2,26	23,07	1,93	Q_liq=(1196,32+-23,07) ml/min; eps=1,93%; alpha=0,95.
0,15	603	928,79	48,42	10	0,95	15,31	2,26	34,64	3,73	Q_liq=(928,8+-34,64) ml/min; eps=3,73%; alpha=0,95.
0,1	586	732,53	9,06	10	0,95	2,87	2,26	6,48	0,89	Q_liq=(732,54+-6,49) ml/min; eps=0,89%; alpha=0,95.
0,05	398	438,12	44,90	10	0,95	14,20	2,26	32,12	7,33	Q_liq=(438,13+-32,12) ml/min; eps=7,34%; alpha=0,95.
0,02	817	212,13	29,57	10	0,95	9,35	2,26	21,15	9,97	Q_liq=(212,13+-21,16) ml/min; eps=9,98%; alpha=0,95.
0,01	422	72,06	14,57	10	0,95	4,61	2,26	10,42	14,47	Q_liq=(72,07+-10,43) ml/min; eps=14,47%; alpha=0,95.

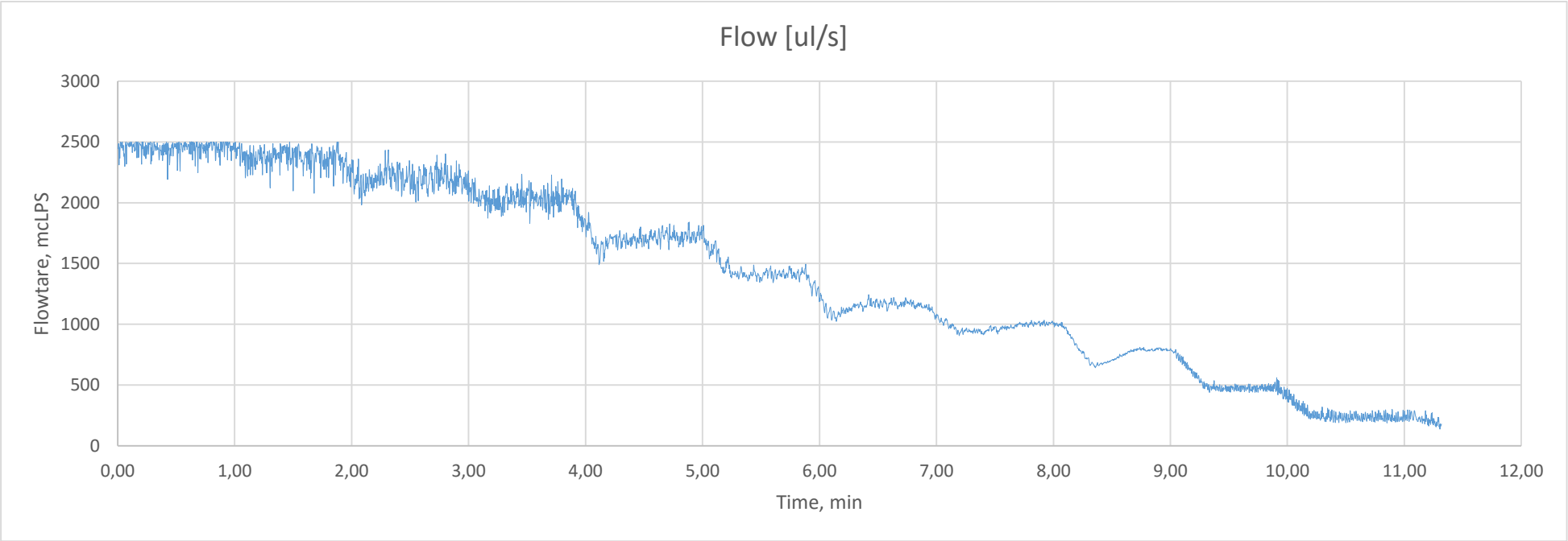

Figure 50- Flow rate values from Sensirion SQL-QT500 liquid flowmeter for experiment 1